RF design

engineering principles and practices

June 1990

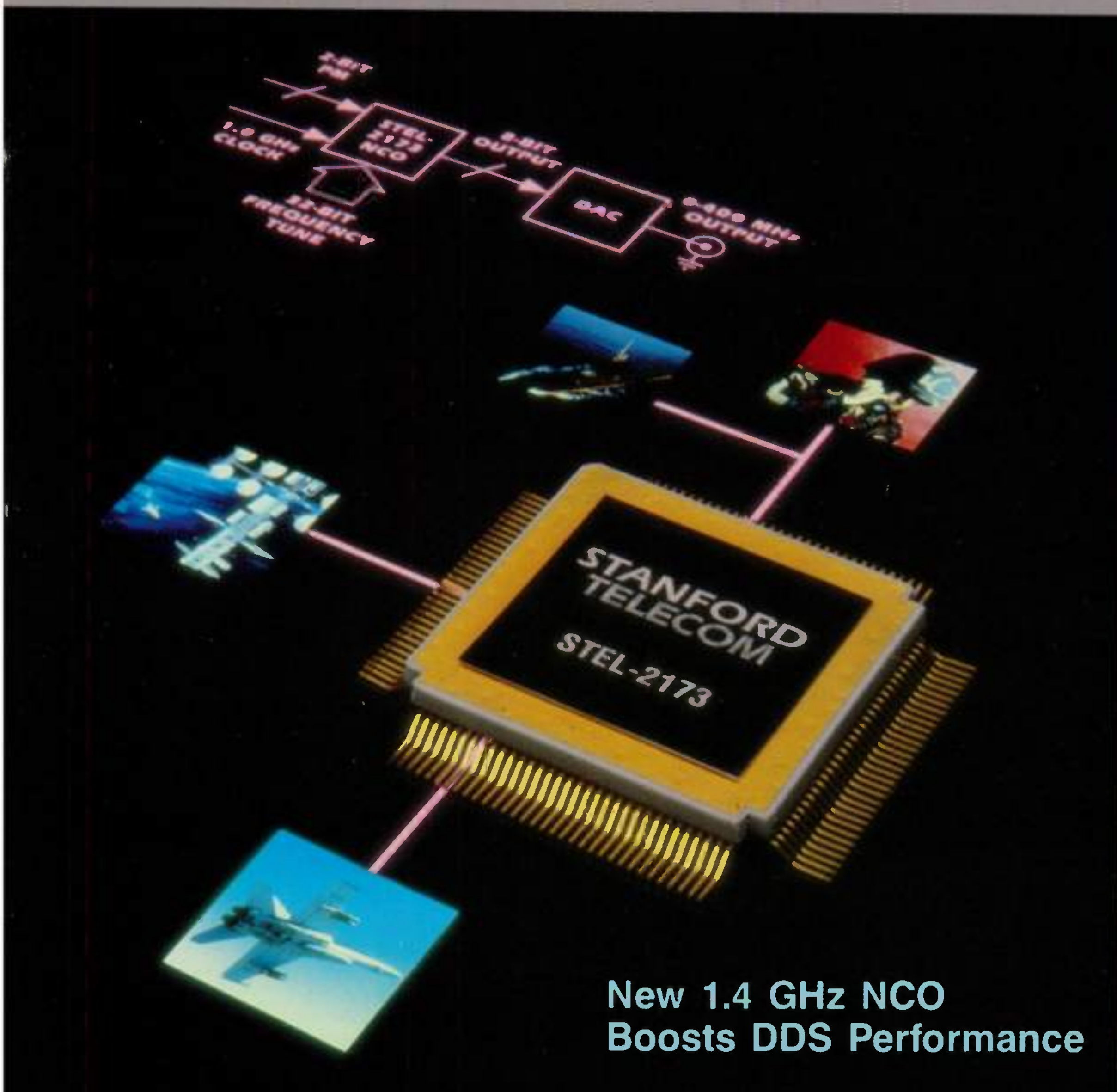

featured technology

Computer Modeling and Analysis

plus

GaAs and Si MMIC Report

Twisted-Wire Lines

Analog CAE Solutions—from picoseconds to GHz

EEsof has the high-frequency analog CAE tools you need today—to build the advanced hardware of tomorrow!

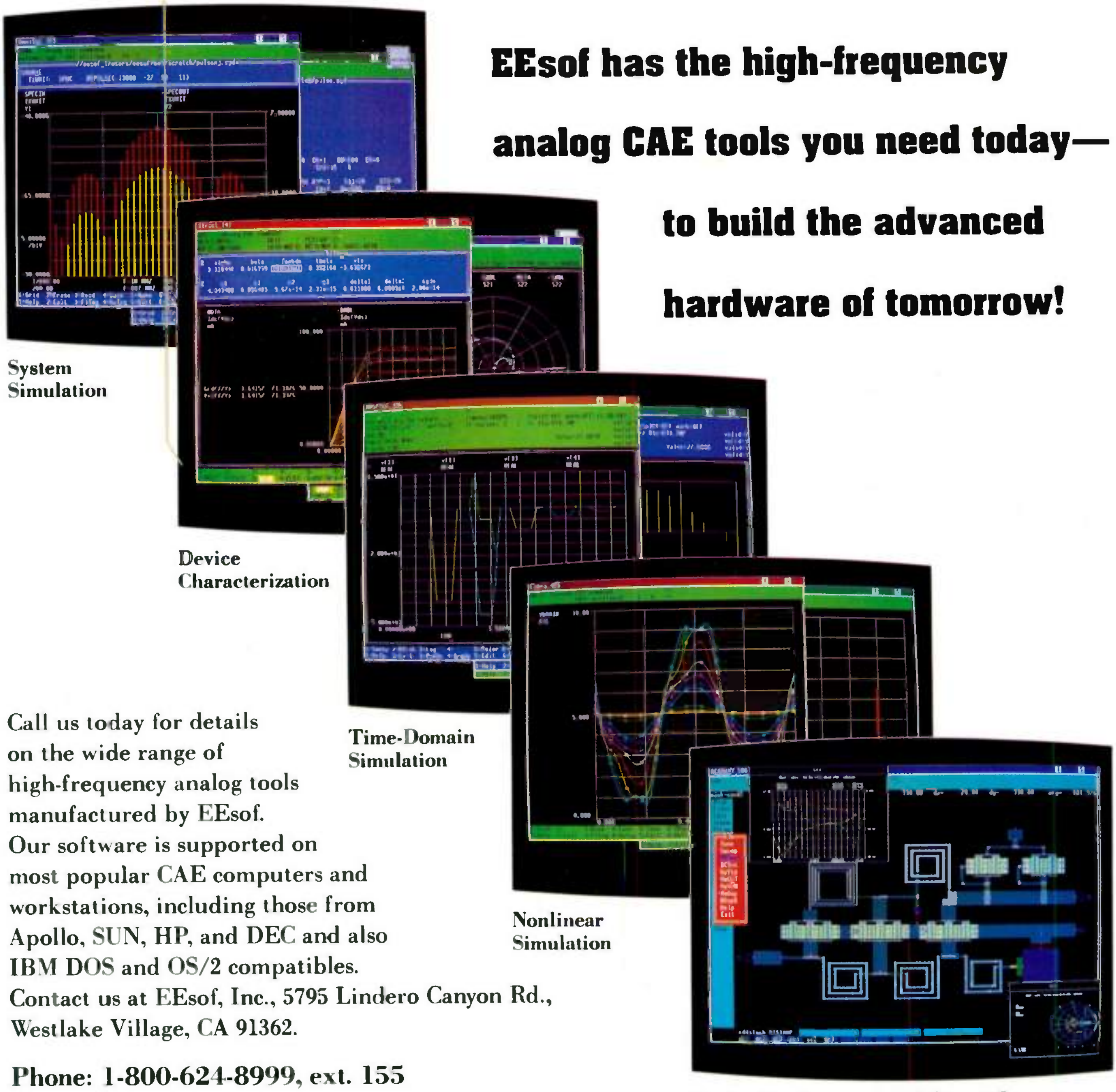

System Simulation

Device Characterization

Time-Domain Simulation

Nonlinear Simulation

Design Environment and Circuit Layout

Call us today for details on the wide range of high-frequency analog tools manufactured by EEsof. Our software is supported on most popular CAE computers and workstations, including those from Apollo, SUN, HP, and DEC and also IBM DOS and OS/2 compatibles.

Contact us at EEsof, Inc., 5795 Lindero Canyon Rd., Westlake Village, CA 91362.

Phone: 1-800-624-8999, ext. 155
FAX: 818-991-7109

EEsof

INFO/CARD 1

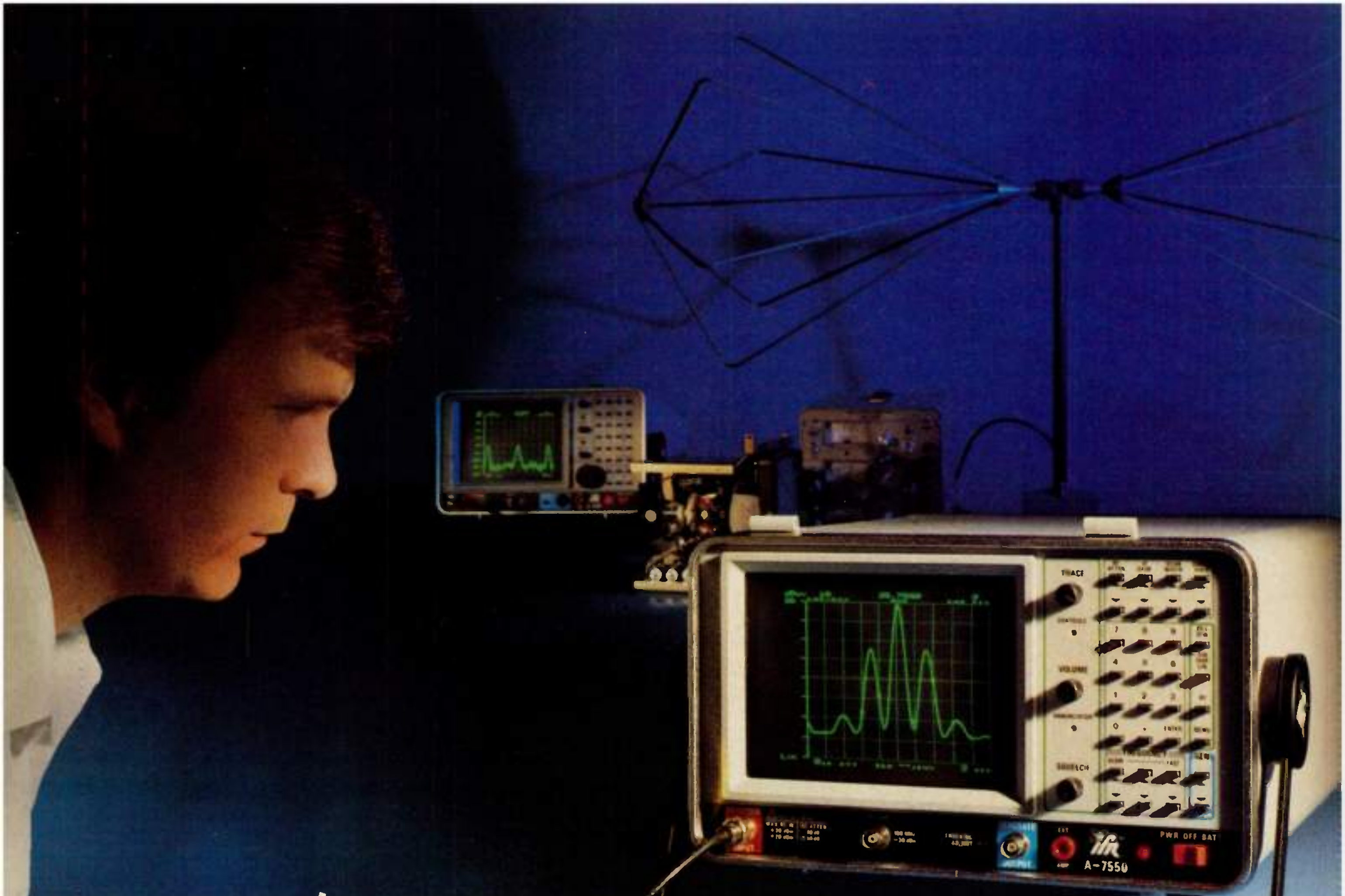

EMI/EMC Testing Made Affordable

A-7550 Spectrum Analyzer with Quasi-Peak Detector

Equally at home in the laboratory, on the manufacturing floor, or in the field, IFR's A-7550 and A-8000 Spectrum Analyzers with optional built-in Quasi-Peak Detectors provide complete EMI/EMC testing capability from 10 KHz to 1000 Mhz. In addition, the extended range of the A-8000 allows the study of interfering signals up to 2600 Mhz in frequency.

Standard features of both the A-7550 and the A-8000 include a synthesized RF system, +30 dBm to −120 dBm amplitude measurement range, frequency spans as small as 1 KHz/division, and resolution bandwidths as narrow as 300 Hz. This gives the A-7550 and the A-8000 a superior frequency and amplitude measurement capability previously unavailable on spectrum analyzers in this price range.

In addition to Quasi-Peak, other available options such as an Internal Rechargeable Battery Pack, Tracking Generator, AM/FM/SSB Receiver, and RS-232 or IEEE-488 Interfaces allow the A-7550 and the A-8000 to be custom configured to solve many other RF testing needs.

For more information or a demonstration contact your local IFR distributor or representative, or contact IFR directly at 316/522-4981.

IFR SYSTEMS, INC.

10200 West York Street / Wichita, Kansas 67215-8935 U.S.A.
Phone 316/522-4981 / TWX 910-741-6952 / FAX 316/524-2623

CRAFTED WITH PRIDE IN USA

INFO/CARD 2

contents

June 1990

featured technology

27 Curve Fitting Made Easy
Linear algebra techniques show that the matrix method of fitting equations to empirical data allows more than just polynomials to be used. An HP9836 program to implement an example is included in this analysis.
— *Brian Miller*

33 MMIC Foundry Models Using Standard CAD Simulators
The accuracy of software models for MMIC design are demonstrated in this comparison of predicted and measured data for GaAs MESFETs, transmission lines, inductors and capacitors. Scaling of known models to new parameters is also addressed.
— *Raymond S. Pengelly and Ulrich L. Rohde*

cover story

42 GaAs NCO Operates up to 1.4 GHz
A new high-speed numerically controlled oscillator (NCO) has been developed, including digital accumulator, phase and amplitude circuitry on one GaAs IC. Maximum clock rate is 1 GHz or greater over 0 to 70C, allowing direct digital synthesis to approximately 450 MHz.
— *Gwyn Edwards*

emc corner

60 Uncertainty in Spectrum Analyzer Based Measurements
This article addresses the accuracy and repeatability performance of spectrum analyzers, with noise figure measurement used for illustration.
— *Dave Massie*

design awards

71 A Bi-Directional Amplifier for SSB Transceivers
Using the near-interchangeability of drain and source in FETs, the author has developed a bi-directional amplifier for use in common transmit-receive circuitry.
— *Mark W. Thompson*

73 Twisted-Wire Transmission Lines
Twisted-wire transmission lines require accurate definition of their characteristic impedances for optimum performance in broadband couplers and transformers. This article presents a method for computating line impedance, based on physical dimensions.
— *John H. Broxon and Douglas K. Linkhart*

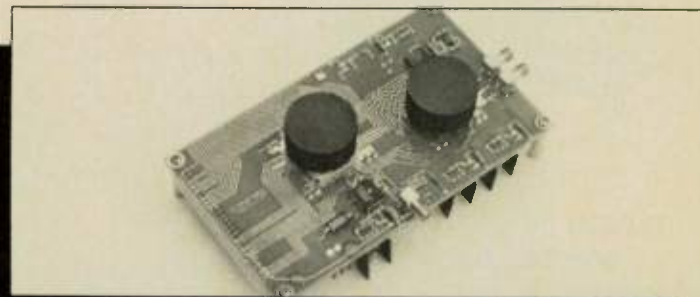

departments

6 Editorial
10 Letters
15 Calendar
16 Courses
17 News
23 Industry Insight
52 Products
59 Software
76 Literature
77 Advertisers Index
79 Info/Card

R.F. DESIGN (ISSN: 0163-321X USPS: 453-490) is published monthly plus one extra issue in September. June 1990, Vol. 13, No. 6. Copyright 1990 by Cardiff Publishing Company, a subsidiary of Argus Press Holdings, Inc., 6300 S. Syracuse Way, Suite 650, Englewood, CO 80111 (303) 220-0600. Contents may not be reproduced in any form without written permission. Second-Class Postage paid at Englewood, CO and at additional mailing offices. Subscription office: 1 East First Street, Duluth, MN 55802. Domestic subscriptions are sent free to qualified individuals responsible for the design and development of communications equipment. Other subscriptions are: $36 per year in the United States; $45 per year in Canada and Mexico; $49 (surface mail) per year for foreign countries. Additional cost for first class mailing. Payment must be made in U.S. funds and accompany request. If available, single copies and back issues are $4.00 each (in the U.S.). This publication is available on microfilm/fiche from University Microfilms International, 300 N. Zeeb Road, Ann Arbor, MI 48106 USA (313) 761-4700.

SUBSCRIPTION INQUIRIES: (218) 723-9355.

POSTMASTER & SUBSCRIBERS: Please send address changes to: R.F. Design, P.O. Box 6317, Duluth, MN 55806.

Our New Look

By Gary A. Breed
Editor

By now, you have certainly noticed some of the changes we have made in the style of *RF Design*. The last design was introduced in January 1985, and although it served us well for five and a half years, we decided it's time for an update.

We want our new design to be practical as well as attractive. All of the layout revisions are intended to make *RF Design* easier to read, as well as looking a little better. Our Table of Contents is a good example. Since 1985, we have continued to grow, and have more articles in every issue. The old design sometimes required small print to fit the information into the allotted space. Our new design has more space to present the articles and large page numbers to make them easy to find.

Products and Software are now included right after our Featured Technology and Cover Story articles, rather than at the back of the magazine. This change wasn't made arbitrarily, it was made because *RF Design* readers have an intense interest in this kind of information. Our INFO/CARD response is terrific!

A number of changes have been made to the layout of the informational columns. Calendar, Courses, Products, Software and Literature all have been "tweaked" to better present their content. Also, we have added some emphasis to our monthly Design Awards feature.

Despite these changes, much of *RF Design* doesn't look much different than it did before. We didn't make changes where they weren't needed. Our articles are presented in the same way (but with extra attention to detail), and the information content of the redesigned sections is no different than before.

Since 1985, we have increased our subscribers by 25 percent, and have seen a dramatic increase in the number of *RF Design* articles used as references in textbooks and other publications. We have continued to grow in advertiser support, despite fluctuations in the RF marketplace. We want our design change to add an exclamation point to that success...!

Introductions

Liane Pomfret joined the *RF Design* editorial staff last December, but hasn't received a formal introduction. With both English Literature and Engineering in her college work, she is well suited for the job. Among her many responsibilities are the News column and communications with our authors.

Charles Howshar is our new Assistant Editor, with a technical emphasis. He has a BSEE from the University of Wyoming and the necessary interest in RF topics. Charles will be handling the Products, Software and Literature sections, as well as technical articles.

In the Sales department, Maryanne Averill has joined Bill Pettit and Kristine Rallis. Maryanne will be handling recruitment and classified advertising, plus bulk reprints of articles. (Individual copies of past articles are still handled by our Circulation department.)

RF design

a Cardiff publication — Established 1978

Main Office:
6300 S. Syracuse Way, Suite 650
Englewood, CO 80111 • (303) 220-0600
Fax: (303) 773-9716

Publisher
Kathryn Walsh

Editor
Gary A. Breed

Assistant Editor
Liane Pomfret

Assistant Editor
Charles Howshar

Consulting Editor
Andy Przedpelski

Account Executive
Bill Pettit
Main Office

Account Executive
Kristine Rallis
Main Office

Recruitment/Classified Sales
Maryanne Averill

Editorial Review Board
Alex Burwasser
Doug DeMaw
Dave Krautheimer
James W. Mize, Jr.
Robert J. Zavrel, Jr.
Ed Oxner
Andy Przedpelski
Jeff Schoenwald
Raymond Sicotte

Advertising Services
Cindy Wieland

Secretary
Theresa Maier

Assistant Circulation Manager
Cindy Zimmer

Convention Manager
Kristin Hohn

Registration Coordinator
Anne Stookesberry

Customer Service Representative
Leann Nowacki

Associate Production Managers
Matt Park
Maurice Lydick

Artists
Kim Austin
Joyce Fields
Brad Fuller
Paul Rivera
Shelley Moore
Sheri Ryder

Composition
Mike C. Moore
Marcie Tichenor

Published by

CARDIFF PUBLISHING COMPANY, INC — BPA

President
Robert A. Searle

Vice President — Production
Cherryl Greenman

Vice President — Convention Management
Kathy Kriner

Circulation Director
Patricia Shapiro

Controller
Jennifer Burger

Credit Manager
Patti McManness

Please address subscription inquiries to:
RF Design, Cardiff Publishing Company,
P.O. Box 6317, Duluth, MN 55806
Postmaster: send form 3579
to the above address.

Constant Gamma 1.5

The steepest slope in the industry.

M/A-COM Semiconductor Products Division announces the addition of a **1.5 gamma GaAs hyperabrupt tuning varactor** to its existing family of 1.0 and 1.25 gamma tuning varactors.

The 1.5 gamma tuning varactor produces the largest tuning sensitivity yet as we continue to upgrade our highly reliable tuning varactor product line.

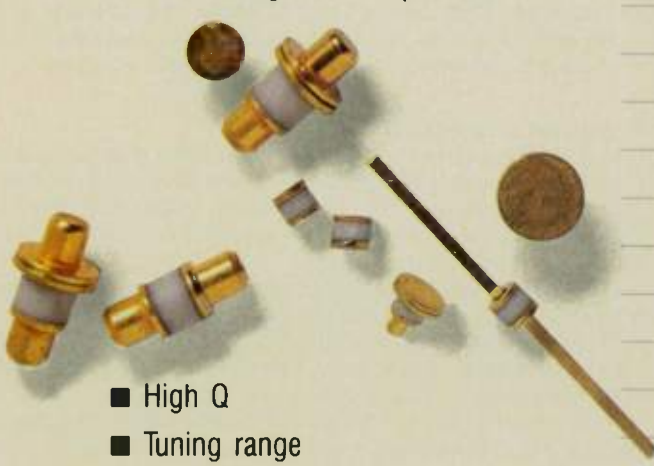

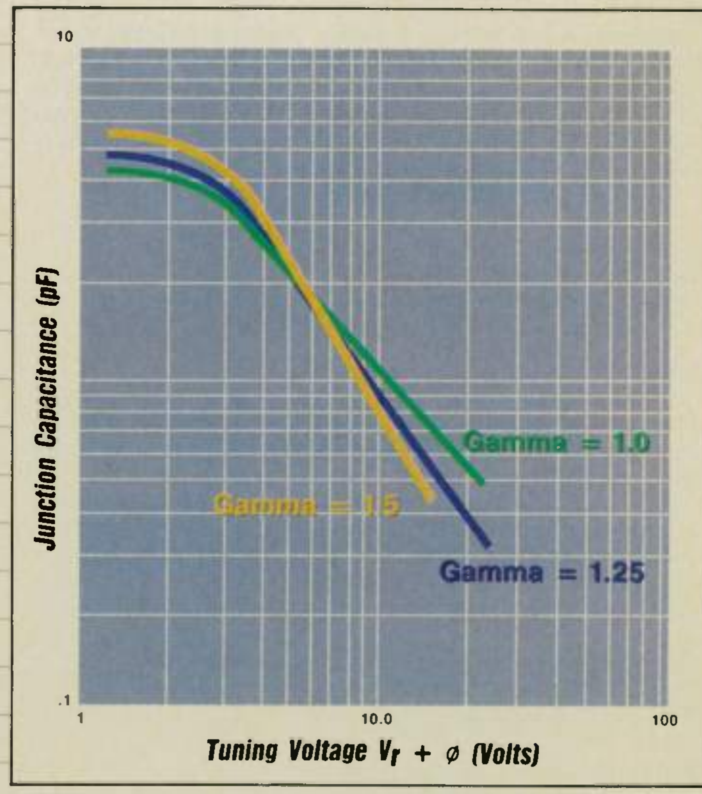

- High Q
- Tuning range
  1.5 gamma 2-12 volts
  1.0 & 1.25 gamma 2-20 volts
- 1.5 gamma available in packages and chips
  1.0 and 1.25 gamma available in beam leads, packages and chips

For technical assistance contact Rick Cory on ext. 1536. For more information, call or write:

M/A-COM Semiconductor Products
South Avenue, Burlington, MA 01803
(617) 272-3000 ext. 3808 ■ FAX (617) 272-8861

M/A-COM

INFO/CARD 7

Letters should be addressed to: Editor, *RF Design*, 6300 S. Syracuse Way, Suite 650, Englewood, CO 80111.

Matching Circuits

Editor:

The article "Design of Transmission Line Matching Circuits" by Stanislaw Rosloniec, which appeared in the February issue, was timely, well done, and quite useful.

However, I would like to set the record straight on one point concerning equations (1) and (2), enabling the determination of Z0 and theta for a single-line match between two arbitrary impedances (and on which Rosloniec's work is essentially based). The equations appear to be attributed, by implication, to an IEEE paper by P.I. Day listed in Reference 3.

To the best of my knowledge, I was the first to derive and publish these two equations. As a young engineer, I was shown a graphical match technique by Joe Owens and Ross Lohr of Hughes Aircraft Co. in Culver City, Calif. Over the next year, I derived the underlying mathematical principles behind that technique and published a paper titled "Microstrip matching networks can be designed fast with a Basic program," which appeared in *Electronics*, December 6, 1973, pp. 127-129.

Thank you for a great magazine!

James J. Lev
Microwave Software
Laguna Hills, CA

Editor:

We wish to thank you for the free subscriptions of *RF Design*. Through this periodical, we have obtained a deeper insight into the world of RF and microwave engineering. It is not only informative but also very useful in the course of our work.

We understand that many hours of hard work are required to produce a good periodical, therefore credit must be given to you and your team of dedicated staff. *RF Design* is undoubtedly the most popular magazine among the engineers in my organisation. I must congratulate you on this very successful periodical.

See Kok Heng
Defence Science Organisation
Republic of Singapore

Antenna Tuner Clarification

The authors of "High-Speed Microprocessor-Controlled Antenna Matching Unit," published in the April 1990 issue, have notified us of a correction to equation (8) in that article. It should have read:

$$e_0 = 0 \rightarrow \alpha = \left(\frac{((\alpha R - \beta)^2 + \alpha^2 X^2)}{R^2 + X^2}\right)^{1/2} \qquad (8)$$

Also, a flow chart is available for the controlling computer program. Interested readers can obtain a copy by sending a self-addressed envelope with 25 cents postage to *RF Design*, at the above address.

Human Plate Antenna Corrections

We also owe David Sullivan an apology. His April article, "A Human Plate Antenna," contained numerous errors that detracted from its unique look at short range RF transmission. On page 52, halfway down the first column, the correct phrase is "...coupling of RF energy to the environment..." In Figure 2 on that page, the tuning capacitor is 3.6 pF, not 36 pF.

Page 55 contained several errors, to be corrected as follows. At the top of the first column, the correct line after "Notes:" is "1) $R_{cp} \leqslant X_p$; $R_{ch} \leqslant X_h$. 2) X_p and X_{h2} are distributed reactances..." Equation (11) should read:

$$R_{ch} = \left[\left(\frac{14.14}{6.36}\right)^2 0.340R_{cp} - 0.174R_{cp}\right]\frac{1}{0.148} \qquad (11)$$

Also, equations (14), (15) and (16) had brackets omitted, and should be:

$$P_T = \left[\left(\frac{1.38}{1.27}\right)^2 + 10.17\left(\frac{1.38}{1.37}\right)^2\right]R_{cp} = 11.50R_{cp}(\mu w) \qquad (14)$$

$$P_p = \left(\frac{2.44}{1.27}\right)^2 R_{cp} = 3.691R_{cp}(\mu w) \qquad (15)$$

$$P_T = \left[\left(\frac{2.12}{1.27}\right)^2 + 10.17\left(\frac{1.12}{1.37}\right)^2\right]R_{cp} = 27.132R_{cp}(\mu w) \qquad (16)$$

The sentence after equation (14) should read "...voltage ratio is $\sqrt{P_t/P_p} = \sqrt{11.50/0.697} = 4.06$." The sentence following equation (16) should be "Here, the predicted ratio $\sqrt{27.132/3.691} = 2.71$."

In the first line of the last paragraph on page 56 the correct information is "...(1/4 in. diameter)..." In the paragraph preceding equation (34) on page 57, the correct statement is "...losses from $k < k_0$ ..." Finally, the author would like to add a reference to the company Data Comm, Inc., for whom this work was done.

We apologize to the readers for these errors, and assure them that we are redoubling our efforts to maintain accuracy.

Prescaler Corrections

In the March cover story, "Designing With High Frequency Prescalers," some of the figure numbers in the text did not match the proper illustrations. With our apologies to Don Apte and Terry Cummings of California Eastern Laboratories, please note the following corrections on page 51:

Near the bottom of the first column, the reference to Figure 9 should instead refer to Figures 6(a) and 7. In the second column, references to Figure 10 and Figure 11 should be for Figure 6(b) and Figure 8, respectively. The Figure 13 reference in the right hand column should instead be for Figure 9.

Also, Figure 5 on page 50 should include a block diagram of the test setup described in the text, included below.

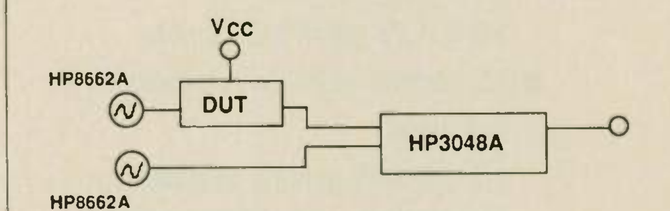

(Ta = 25°C, Vcc = 5 V, fin = 1 GHz, Pin = -10 dBm)

Picture yourself with 500 MHz spectrum, network, and impedance analysis in one instrument.

Picture yourself spending only $25,000.*

Now send for our free video, and get the whole picture.

If your audio, baseband, HF, VHF, and IF designs require spectrum, vector network or impedance analysis, watch this.

Our HP 4195A 500 MHz Network/Spectrum analyzer video shows you how to get the measurement capability you need along with the convenience and flexibility that you want. All in one instrument, for $25,000.*

You'll see how the HP 4195A handles a wide range of applications with balanced specs. Like spectrum analysis performance of −135 dBm sensitivity, 3 Hz to 300 kHz RBW. And >100 dB vector network analysis dynamic range with ±0.05 dB/±0.3 degree accuracy.

So get the picture. Call **1-800-752-0900**. Ask for **Ext. 1151** and receive your free video. It's a picture you'll want to be a part of.

*U.S. list base price.

There is a better way.

HEWLETT PACKARD

INFO/CARD 8

RF calendar

June

18-21 **Seventh International Conference on Testing Computer Software: Putting the Pieces Together**
Fairmont Hotel, San Francisco, CA
Information: USPDI, Testing Computer Software Conference, 1734 Elton Road, Suite 221, Silver Spring, MD 20903-1700. Tel: (301) 445-4400.

July

26-29 **The 1990 International Tesla Symposium**
Hilton Inn, Colorado Springs, CO
Information: International Tesla Society, 330-A West Uintah Street, Suite 215, Colorado Springs, CO 80905-1095.

August

13-17 **Fifth International Conference on Solid Films and Surfaces**
Brown University, Rhode Island
Information: Dr. Joseph J. Loferski, Tel: (401) 863-2652.

21-23 **IEEE EMC 90 Symposium**
Washington Hilton Hotel, Washington, DC
Information: Joe Fisher Tel: (703) 521-6336.

21-23 **Hi-Tech USA '90**
Guadalajara, Jalisco, Mexico
Information: Project Manager, U.S. Trade Center, P.O. Box 3087, Laredo, TX 78044-3087. Tel: (905) or (525) 591-0155; Fax: (905) or (525) 566-1115.

28-30 **Surface Mount '90**
Bayside Exposition Center, Boston, MA
Information: MG Expositions Group, 1050 Commonwealth Ave., Boston, MA 02215. Tel: (800) 223-7126 or (617) 232-3976.

28-5 **XXIII General Assembly of the International Union of Radio Science (URSI)**
Prague, Czechoslovakia
Information: Prof. V. Zima, Institute of Radioengineering and Electronics, Czechoslovak Academy of Sciences, 182 51 Praha 8, Czechoslovakia.

September

9-13 **1990 International Electronics Packaging Conference**
Royal Plaza Hotel, Marlborough, MA
Information: IEPS, 114 N. Hale Street, Wheaton, IL 60187. Tel: (708) 260-1044.

10-13 **20th European Microwave Conference**
The Intercontinental Hotel, Budapest, Hungary
Information: Microwave Exhibitions and Publishers Limited, 90 Calverley Road, Tunbridge Wells, Kent, TN1 2UN, England. Tel: (0892) 544027.

11-13 **Midcon/90**
Dallas Convention Center, Texas
Information: Electronic Conventions Mgmt., P.O. Box 922754, Worldway Postal Center, Los Angeles, CA 90009-2275. Attn: Midcon Sales. Tel: (800) 877-2668.

RF courses

Computer Aided Design of Microstrip Antennas and Arrays
June 26-29, 1990, Boulder, Colorado
Information: University of Colorado, Office of Conference Services. Tel: (303) 492-5151.

New HF Communications Technology: Advanced Techniques
June 18-22, 1990, Washington, DC
ELINT: Analyzing Radar Signals
June 19-21, 1990, Washington, DC
Global Positioning System: Principles and Practice
July 16-18, 1990, Washington, DC
Preparation of Signals for Digital Transmission
August 7-10, 1990, Washington, DC
Antennas: Radiation and Scattering
August 27-28, 1990, Washington, DC
Grounding, Bonding, Shielding and Transient Protection
August 27-30, 1990, Chicago, IL
Information: George Washington University, Continuing Engineering Education, Merrill Ferber. Tel: (800) 424-9773; (202) 994-6106. Fax: (202) 872-0645.

Designing for Surge and Transient Immunity in Electronic and Computer Systems
July 16-19, 1990, Madison, WI
Information: University of Wisconsin-Madison, College of Engineering. Tel: (800) 262-6243; (608) 262-2061. Fax: (608) 263-3160.

Requirements Analysis and Specification
June 18-22, 1990, Los Angeles, CA
Software Project Management: Empirical Success Factors
June 26-28, 1990, Los Angeles, CA
RF and Microwave Circuit Design I
July 9-13, 1990, Los Angeles, CA
RF and Microwave Circuit Design II
July 16-20, 1990, Los Angeles, CA
Fiber Optic Smart Structures and Skins
July 23-27, 1990, Los Angeles, CA
Information: UCLA Extension, Engineering Short Courses. Tel: (213) 825-1047. Fax: (213) 206-2815.

Principles and Applications of Millimeter Wave Radar
July 23-27, 1990, Atlanta, GA
Radar Reflectivity Measurement: Techniques and Applications
July 30-August 2, 1990, Atlanta, GA
Information: Georgia Institute of Technology, Education Extension. Tel: (404) 894-2547.

Electronic Design Techniques and Analysis Required to Meet EMC Requirements
July 12-13, 1990, Novi, MI
Information: JASTECH, Tel: (313) 553-4734

Modern Power Conversion Design Techniques
July 16-20, 1990, Chicago, IL
Information: E/J Bloom Associates, Inc., Mrs. Joy Bloom. Tel: (415) 492-8443

Electronic Packaging Seminar
June 20-21, 1990, Marlborough, MA
Information:International Electronics Packaging Society, Inc. Tel: (708) 260-1044. Fax: (708) 260-0867.

Digital Signal Processing: Techniques and Applications
June 19-22, 1990, San Francisco, CA
June 26-29, 1990, Washington, DC
July 24-27, 1990, Boston, MA
August 14-17, 1990, Washington, DC
Introduction to Datacomm and Networks
June 19-22, 1990, San Francisco, CA
June 19-22, 1990, Washington, DC
July 10-13, 1990, San Diego, CA
July 17-20, 1990, Washington, DC
July 24-27, 1990, Los Angeles, CA
August 14-17, 1990, Washington, DC
Troubleshooting Datacomm and Networks
June 19-22, 1990, Boston, MA
June 19-22, 1990, Los Angeles, CA
July 10-13, 1990, San Diego, CA
July 10-13, 1990, Washington, DC
Introduction to Telecommunications
July 10-13, 1990, Washington, DC
July 17-20, 1990, San Francisco, CA
July 31-August 2, 1990, Ottawa
August 21-24, 1990, San Diego, CA
August 28-31, 1990, Washington, DC
Information: Learning Tree International, John Valenti. Tel: (800) 421-8166; (213) 417-8888. Fax: (213) 410-2952.

Grounding and Shielding
June 19-22, 1990, Las Vegas, NV
Introduction to EMI/RFI/EMC
June 26-28, 1990, Washington, DC
July 17-19, 1990, Chicago, IL
High Speed Digital Design for EMC
June 26-29, 1990, Minneapolis, MN
1992 and the EEC Directive on EMC
July 18-20, 1990, Boston, MA
System Integration and Design for EMC
July 24-27, 1990, Chicago, IL
Information: Interference Control Technologies, Inc., Elizabeth Price. Tel: (703) 347-0030. Fax: (703) 347-5813.

Principles of Analog Oscilloscopes
August 21-22, 1990, Los Angeles, CA
Principles of Digital Oscilloscopes
August 23-24, 1990, Los Angeles, CA
Information: John Fluke Mfg. Co., Inc. Tel: (800) 443-5853 ext. 73. In Canada: (416) 890-7600.

RF and Microwave Circuit Design I: Linear Circuits
June 18-22, 1990, Cambridge, UK
July 9-13, 1990, Los Angeles, CA
RF and Microwave Circuit Design II: Non-Linear Circuits
June 18-22, 1990, Cambridge, UK
July 16-20, 1990, Los Angeles, CA
SAW - Surface Acoustic Wave Devices for Signal Processing
June 18-22, 1990, Cambridge, UK
Information: Mrs. Tina Persson, CEI-Europe/Elsevier, Box 910, S-612 01 Finspong, Sweden. Tel: +46 (0) 122-17570. Fax: +46(0)122-14347.

1990 EMI Training Institute I
August 6-17, 1990, Philadelphia, PA
Information: R&B Enterprises. Tel: (215) 825-1960. Fax: (215) 825-1684.

CRRES to Study Earth's Ionosphere and Magnetosphere

The Combined Release and Radiation Effects Satellite (CRRES), built by Ball Space Systems Division is slated for a mid-June launch aboard the first commercial version of an Atlas-Centaur I expendable launch vehicle. The satellite is a combination of two different projects both conceived in 1979. Originally, there were meant to be two satellites — one to study chemical releases and the other one, called RADSAT, to study the effects of space radiation on microelectronics. In 1983, however, the two projects were combined and CRRES was born. Initially scheduled for launch aboard the space shuttle in June of 1986 the satellite was modified and will be launched this month using General Dynamics' Atlas-Centaur I.

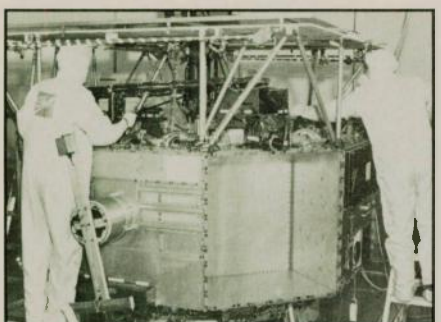

In order to observe phenomena in both the upper ionosphere and the magnetosphere, the satellite is set to follow an elliptical orbit of 22,231 miles by 215 miles. These regions contain charged particles and electrical and magnetic fields that scientists have studied for 30 years for their effects on spacecraft, astronauts, communications and weather. There are five major experiments aboard, two of which are to study the effects of the radiation belts on microelectronics. In particular, a set of solar cells using GaAs rather than silicon will be tested for greater resistance to radiation and temperature. The scientists hope to use this information to study ways of improving performance and counteracting the effects of radiation on space instruments and equipment.

The other three experiments involve mapping and measuring the radiation environment surrounding the earth. Scientists will also examine the radiation environment for changes due to the solar cycles. One of the key experiments is called the Low Altitude Satellite Study of Ionospheric Irregularities (LASSII). This consists of three instruments: a VLF receiver (DC to 5 KHz), a quadrature ion mass spectrometer and a Langmuir probe to measure electron density and temperature. Scientists plan to investigate irregularities in electron density and eventually to use this data to study the effects on communications equipment and transmissions.

Another part of CRRES is to release chemicals such as barium, lithium, strontium and calcium into the atmosphere and study the chemical interactions.

FAST DELIVERY
MANY MODELS ARE IN STOCK

WHEN YOU CONSIDER ...

• Performance • Delivery • Price

AND ADD

• MITEQ's long-term warranty and the long list of custom-selectable options, you will realize that MITEQ's bipolar amplifiers offer unparalleled bargains. Study the data and make your own decision.

OPTIONS

- Integral input limiter
- Bias supplied via the output port
- Low-loss input "bias tee" for photo diodes
- Low frequency operation to below 10 kHz
- Fast recovery from input overloads
- Amplitude and phase matching
- Lower guaranteed noise figure

Model Number	Frequency (MHz)	Gain (Min.) (dB)	Gain Var. (Max.) (±dB)	Noise Figure (Max.) (dB) Low End	Noise Figure (Max.) (dB) Mid Band	Noise Figure (Max.) (dB) High End	VSWR (Max.)	Dynamic Range 1 dB Gain Comp. Output (Min.,dBm)	Nom. DC Power (+15V, mA)
AU-1054	1-500	30	0.5	1.25	1.4	1.5	2:1	+8	55
AU-2A-0150	1-500	30	0.5	1.25	1.4	1.5	2:1	+8	55
AU-3A-0150	1-500	45	0.5	1.25	1.4	1.5	2:1	+10	67
AU-1149	10-180	15	0.5	4.5	5.5	6.5	2:1*	+18	75
AU-1291	.015-500	60	0.75	1.25	1.4	1.5	2:1	+8	90
AM-1300	.01-1000	25	0.75	1.4	1.6	1.8	2:1	+6	50
AM-1052	1-1000	26	0.75	1.4	1.6	1.8	2:1	+6	50
AM-2A-000110	1-1000	27	0.75	1.4	1.6	1.8	2:1	+8	50
AM-1299	1-1000	38	0.75	1.4	1.6	1.8	2:1	+9	75
AM-3A-000110	1-1000	37	0.75	1.4	1.6	1.8	2:1	+9	75

* 75 ohm impedance level

AU-1054 and AU-2A-0150

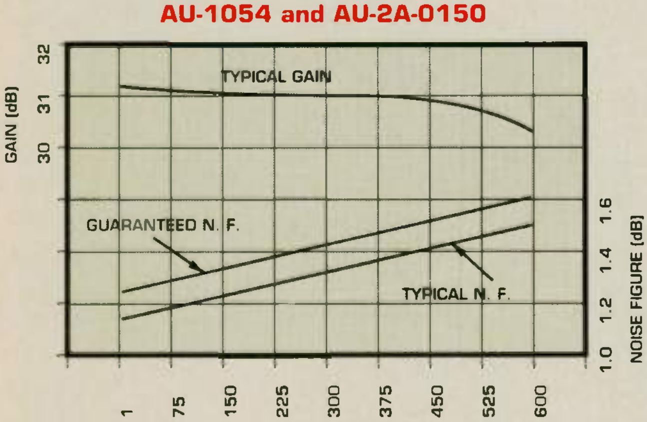

AM-1052 and AM-2A-000110

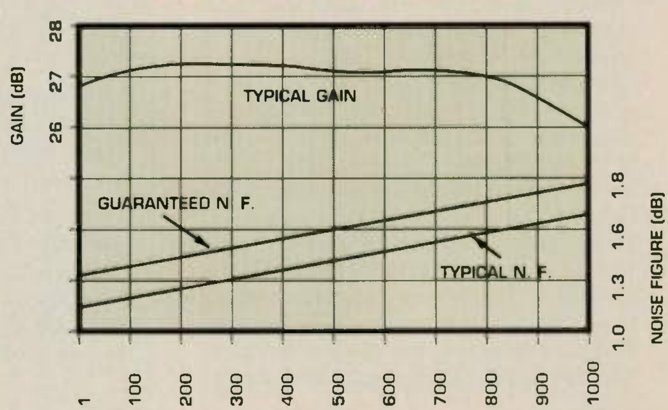

For additional information, please call Bill Pope at (516) 436-7400, on extension 282.

MITEQ

100 Davids Drive, Hauppauge, New York 11788
Tel: (516) 436-7400 • Fax: (516) 436-7430 • Telex:6718148

INFO/CARD 12

Scientists are going to perform one experiment at the satellite's perigee with the hope of finding evidence for their theory that neutral particles can ionize at high speeds without energy derived from a light source. Another experiment, planned for the summer of 1991, will occur over the Caribbean. In this experiment, scientists plan to observe ion behavior both by itself as well as its reactions with other substances. This particular experiment has generated international interest and, as a result, countries such as the Soviet Union and West Germany are participating in the project.

CRRES is a joint project of NASA/Marshall Space Flight Center and the U.S. Air Force Space Test Program, but there are many other contributing groups. For example, Los Alamos, University of Chicago, Aerospace Physics Lab, University of California at Berkeley, Lockheed, University of Alaska, Naval Research Lab, Boston University and Cornell are just a few of the universities and corporations involved with the project.

The satellite will carry the latest generation of spacecraft microelectronics through the radiation regions to correlate their performance and expected failure modes with the measured radiation exposure and investigate ways to improve their operation in the space environment. This is the first in a series of steps to improve the performance of future satellites and communications equipment.

Antenna Data Analysis and Research Using PCs — NIST researchers have developed a new software package that allows scientists, engineers, and programmers to make complex antenna computations on personal computers. The package termed Planar Near Field Codes, has a highly modular structure and can be used to address diverse research problems. The structure of the codes is open so that a user can incorporate a new application into the package relatively easily. Planar Near Field Codes for Personal Computers (NISTIR 89-3929) is available from the National Technical Information Service, Springfield, VA 22161. Order by PB #90-155839 for $17 prepaid. To order the software package, available for $1500, contact Lorant A. Muth, Div. 723.05, NIST, Boulder, CO 80303. Tel: (303) 497-3603.

1990 NVLAP Directory Available — The National Institute of Standards and Technology (NIST) has issued the 1990 Directory of NVLAP Accredited Laboratories. This 1990 Directory of NVLAP Accredited Laboratories provides information on the activities of NIST in administering the National Voluntary Laboratory Accreditation Program (NVLAP) during calendar year 1990. The status of current programs is briefly described and a summary of laboratory participation is provided. Indexes cross reference the laboratories by name, NVLAP Lab Code Number, accreditation program and geographic location. The scope of accreditation of each laboratory, listing the test methods for which it is accredited, is provided. To obtain a copy of the Directory write to: National Technical Information Service (NTIS), Springfield, VA 22161.

Refer to publication number NISTIR 90-4280.

Kearny-National Acquires Coto Corporation — Coto Corporation was purchased by Kearny-National with the intent of combining them with their relay division, Wabash Relay, to create an industry leader in reed relays. The combined Coto-Wabash operation will be directed by CEO Dr. Bruce Campbell, currently president of Coto Corporation.

Balloon to Carry Vital Radio Communications Equipment in Mt. Everest Flight — Racal-Tacticom is supplying vital radio communications equipment for a world record breaking attempt to fly a hot air balloon over the peak of Mt. Everest. The balloon, known as the Star Flyer will be piloted by Per Lindstrand. An HF single sideband transceiver will be fitted in the basket of the balloon and was chosen for its ability to operate in extremely low temperatures. In a manpack configuration it covers the complete HF range of 1.6 to 30 MHz. HF transceivers will be situated in the base camp and at the launch site.

Compact Software Announces Call for Technical Papers — As part of their preparation for the 1990 European User Group Meeting being held at the Military Microwaves Conference and Exhibition in Wembley, London, July 10-13, Compact Software is inviting circuit and sub-system designers to submit short technical articles on the applications of Compact Software CAD tools. 2 to 3 page descriptions should be sent to Dr. Mike Brookbanks, President of the European User Group at Plessey Research and Technology Ltd., Allen Clark Research Center, Caswell, Northampton, United Kingdom. Papers must be received by June 15.

FCC Approves Permanent Air-to-Ground Service — The FCC has allocated four megahertz of the 800-900 MHz reserve spectrum for a terrestrial air-to-ground telephone service to be licensed on an open entry basis. This service will permit airline passengers to place telephone calls from airplanes during flight. In October 1984, GTE Airfone was implemented as an experimental air-to-ground telephone service on a limited number of commercial aircraft. This service has expanded to include several hundred aircraft. With respect to the operation of the new service, the Commission determined that the service should be regulated on a common carrier basis.

AVX and Kyocera Reorganize Sales and Marketing Operations — AVX Corporation has announced the consolidation of its sales and marketing operations with Kyocera Northwest, Inc. Under the AVX Corporation umbrella, Kyocera Northwest will continue to operate its manufacturing facility in Vancouver, Washington, while AVX's manufacturing facilities will continue to manufacture their own product line. Kyocera Northwest's sales force will be incorporated into AVX's existing network of representatives, direct sales personnel and distributors.

Microdyne Purchases Telemetry Business Unit From Acurex — Microdyne recently announced that it has completed the purchase of Acurex Corporation's telemetry business unit, which will operate as Wireless Data Corporation, a wholly-owned Microdyne subsidiary.

Zetex Enters U.S. Semiconductor Components Market — Zetex plc, is forming a U.S. division, Zetex Inc. Zetex plc was formed in July 1989 following a buyout of Plessey Semiconductors' discrete components division. The new U.S. division will be headquartered in Commack, New York.

GTE Continues Communications System Contract — GTE Government Systems announced receipt of a $879.2 million U.S. Army contract for continued work on a tactical communications system known as Mobile subscriber equipment (MSE). This award brings the total value of GTE's contract to $4.2 billion. The MSE system supplies secure voice, data and facsimile capabilities to U.S. Army communicators at corps and division levels. It replaces existing conventional battlefield communications equipment. MSE, a secure, digital system, similar in concept to cellular mobile phones in automobiles, allows military personnel moving through a battlefield to communicate without interruption.

Metelics Opens Philippines Plant — Metelics recently opened Metelics -Philippines, Inc., a new 11,000 square foot facility, to accommodate its recent growth in the commercial diode, component and assembly areas. All engineering, administration, high technology and military products will remain at their Sunnyvale, California headquarters plant.

SILICON POWER MMICS

1 WATT
Broadband Amplifiers

SGS-Thomson Microelectronics introduces the AMP 3020, a +30 dBm, 50 ohm cascadable gain block in the popular 200 mil hermetic, ceramic package.

This unique MMIC amplifier brings a new dimension in power to our silicon MMIC family, a series of broadband amplifiers designed to provide the circuit and system designer with reliable, cost-effective gain-blocks for broadband and narrow-band, commercial and military IF and RF applications.

The "AMP" series cascadable, 50 ohm MMIC amplifiers are manufactured with a proprietary, space-qualified refractory-gold metallization and operate at low junction temperatures for maximum reliability.

A variety of hermetic, surface mount, ceramic package styles are offered to suit individual requirements with chips available for applications demanding the ultimate in miniaturization.

If you are looking for low-cost, reliable solutions to your amplifier needs, come to the Power Source.

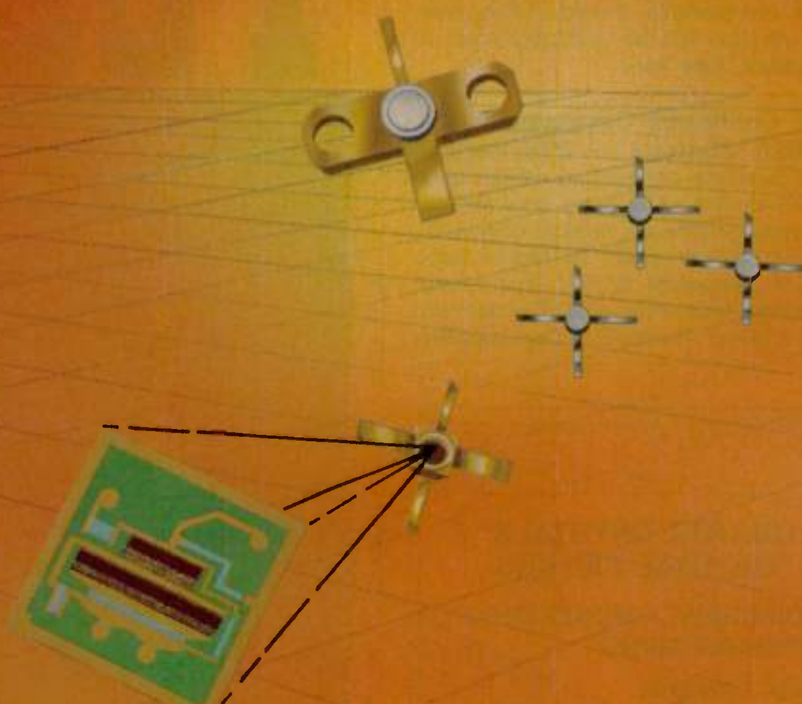

"AMP" SERIES SILICON MMIC AMPLIFIERS

Model #	Freq. GHz	Gain (dB)	Gain* (dB)	Pout (dBm)	N.F. (dB)	Vd/Id (v/ma)
AMP3020	**0.5**	**8.0**	**8.5**	**29.5**	**8.0**	**17/300**
	0.2	**8.2**	**8.5**	**31.0**	**7.0**	**17/300**
AMP0135	1.0	19.0	20.0	3.0	4.5	5/17
AMP0235	1.0	12.5	13.0	5.0	5.5	5/25
AMP0335	1.0	11.5	12.5	10.0	6.0	5/35
AMP0435	1.0	8.5	9.1	11.2	6.0	5.3/50
AMP0420	1.0	10.0	11.5	14.0	6.5	6.3/90
AMP0520	1.0	9.7	9.2	23.0	6.5	12/165
AMP0635	1.0	19.0	20.0	4.5	3.0	3.5/16
AMP0735	1.0	13.0	13.7	5.5	4.5	4/22
AMP0835	1.0	19.0	31.0	14.0	3.0	7.8/36
AMP0910	1.0	8.7	8.0	11.3	5.5	7.8/35
AMP1025♦	1.0	6.3	7.6	27.0	9.0	15/325
AMP1120	1.0	11.5	12.2	17.5	3.5	5.5/60

*Gain @ 0.1 GHz ♦Measured in a 50Ω System

SGS-THOMSON
MICROELECTRONICS

INFO/CARD 20

SGS-THOMSON Microelectronics
211 Commerce Drive
Montgomeryville, PA 18936-1002
(215) 362-8500 • FAX: (215) 362-1293

MMIC Makers See Growth in Communications

By the RF Design Editorial Staff

For manufacturers of microwave monolithic integrated circuits (MMICs), there is plenty of business in military applications, but the future is in commercial and consumer communications products. "We're seeing a big growth in the commercial side — custom chips for hand held global positioning equipment, cellular communications, Korean TV manufacturers," say Louis Pengue, Marketing Manager at TriQuint Semiconductor. But he adds that the military market is in very good shape, "There's a scaling back of weapon systems development, but not in surveillance systems or satellite."

Echoing this general view is Mark Burkett, Associate Vice President of California Eastern Laboratories, who estimates that 50 percent of current shipments are for the defense industry, but that the greatest opportunities are in new applications in the 800 MHz through S-Band frequency range. However, some companies have noticed more of a change in military markets. "I would say the commercial market is the fastest growing just because we are pushing hard — trying to make up for losses in the defense market," observes Dave Strand, Marketing Administrator at the Anzac Division of Adams-Russell.

The development of MMIC technology reflects these market views. "Customers are asking us to combine standard devices with diodes, transistors, hybrids — essentially, higher levels of integration," comments David Salustri, Product Marketing Engineer at Hewlett-Packard Company, Microwave Semiconductor Division. Meeting customer demand for more complex circuits is the aim of SGS-Thomson Microelectronics, also. "Collector isolation processing for silicon MMICs and higher F_T and F_{max} devices will allow for development of circuits other than broadband Darlington amplifiers," says Carl Lump, Manager of Marketing of SGS' RF and Microwave Products Operations.

Examples of highly integrated designs include a Ku-band satellite transceiver developed by Qualcomm, and a 44 GHz downconverter recently announced by TRW (see photo above). The Qualcomm transceiver uses six

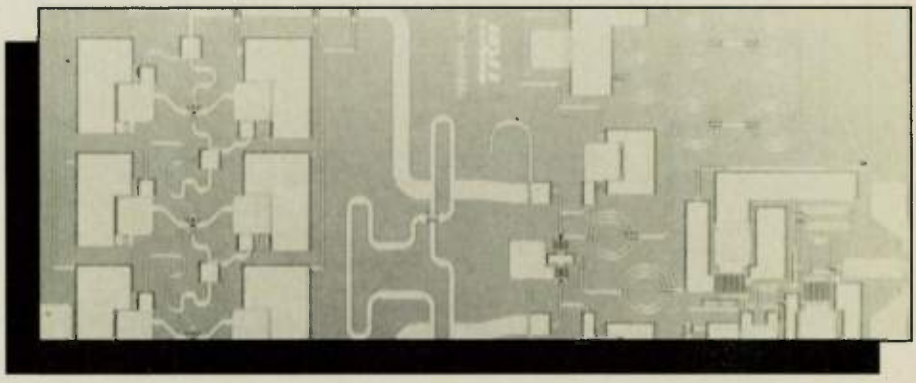

MMICs interconnected on a 2 by 2 inch hybrid substrate. Functions include a low-noise amplifier, medium power transmit amplifier, up and downconverters, switches, IF amplifiers, VCO and multipliers. At least four additional companies were involved in this project. Qualcomm worked with Texas Instruments and Hughes for GaAs foundry work, and with Pacific Monolithics and through them, TriQuint, for additional subsystem development. The TRW device includes a three-stage low-noise amplifier, a single-balanced mixer, and a two-stage IF amplifier on a single MMIC.

These examples were developed using GaAs for higher GHz and mm-wave applications, in a custom manner. New UHF through S-Band applications will have greater use of silicon. According to Gary LaBelle, Avantek's Director of Marketing, Semiconductor Products, that firm will continue to emphasize standard products, but ones which are attractive for more advanced uses, such as digital cellular and spread spectrum. "These systems require more sophisticated receivers, lower power consumption, and lower cost," he notes. The added value of more complex integrated functions will be required by customers.

GaAs Versus Silicon

All the well-known tradeoffs of GaAs and silicon are considered by MMIC customers. GaAs has higher power handling, and operates to higher frequencies, but has greater power consumption and is noisier at lower frequencies. Silicon draws less power, and has good low frequency noise performance, but has some high frequency limitations. While this is generally, true, MMIC makers are quick to point that these are changing. "Silicon MMIC technology will displace some applications currently held by GaAs," predicts California Eastern Laboratories' Burkett, who adds that NEC research labs has demonstrated a silicon process with transistor F_T of 40 GHz. On the other hand, in a paper at RF Technology Expo 90, Pacific Monolithics described a family of GaAs MMICs characterized for operation under 3 GHz, and in some cases, as low as 20 MHz.

While the emphasis at a given MMIC manufacturer may be either GaAs or silicon (or both) the customer sets the performance requirements, and ultimately, the price guidelines. For the minimum cost considerations predominant in commercial applications, silicon will be used when possible, with GaAs dominating applications where its performance is required.

At present, both technologies are booming with only a few exceptions. Early GaAs military programs have moved from development to production, boosting that segment of the MMIC industry. Silicon MMICs are strong in defense applications, but are more strongly driven by growing communications markets. Estimates of MMIC growth range from "the market is flat" to the excitement of 30-50 percent annual growth. The midpoint of this range is still a healthy growth rate, warranting the optimism expressed by a majority of MMIC firms. *RF*

MODEL	POWER OUT	FREQUENCY RANGE	GAIN	WxDxH (CM)	AC LINE	PRICE $
700LC	1.5W CW	003-1000 MHz	33dB	25x28x13	100-240V	1,695.00
102LC	2W CW	25Hz-100 MHz	33dB	19x31x15	100-240V	1,349.00
502LC	2W CW	.01-525 MHz	36dB	19x32x15	100-240V	1,695.00
704FC	4W CW	.5-1000 MHz	33dB	23x18x09	100-240V	2,195.00
505LC	5W CW	.05-400 MHz	37dB	19x32x15	100-240V	1,895.00
505FC	5W CW	.5-525 MHz	40dB	25x28x13	100-240V	1,655.00
706FC	6W CW	.5-1000 MHz	38dB	25x28x13	100-240V	2,695.00
110C	10W CW	2-60 MHz	40dB	19x32x15	100-240V	1,450.00
110LC	10W CW	.01-100 MHz	40dB	25x37x15	100-240V	1,950.00
210LC	10W CW	.008-225 MHz	40dB	25x37x15	100-240V	2,495.00
310FC	10W CW	5-300 MHz	40dB	25x28x13	100-240V	2,250.00
510FC	10W CW	.5-525 MHz	43dB	25x28x13	100-240V	2,595.00
710FC	10W CW	1-1000 MHz	40dB	25x28x13	100-240V	5,995.00
115LC	15W CW	.001-100 MHz	43dB	38x32x13	100-240V	2,255.00
225LC	20W CW	.01-225 MHz	45dB	25x37x15	100-240V	3,295.00
520FC	20W CW	1-525 MHz	45dB	25x28x13	100-240V	3,895.00
720 FC	20W CW	500-1000 MHz	43dB	48x46x13	100-240V	6,650.00
125LC	25W CW	50Hz-100 MHz	40dB	48x40x13	100-240V	3,300.00
125C	25W CW	5-50 MHz	45dB	48x46x13	100-240V	1,495.00
112C	25W CW	1-120 MHz	45dB	25x37x15	100-240V	1,995.00
320FC	25W CW	1-300 MHz	45dB	30x20x13	100-240V	2,895.00
535FC	35W CW	200-512 MHz	45dB	30x20x13	100-240V	3,895.00
150C	50W CW	2-50 MHz	47dB	38x37x15	100-240V	2,595.00
250LC	50W CW	.01-230 MHz	45dB	43x42x19	100-240V	7,550.00
250FC	50W CW	1-200 MHz	45dB	38x37x15	100-240V	4,995.00
550FC	50W CW	200-512 MHz	45dB	30x20x13	100-240V	4,995.00
161C	100W CW	5-90 MHz	45dB	38x37x15	100-240V	5,250.00
190LC	100W CW	.01-100 MHz	50dB	48x43x18	100-240V	8,850.00
162LP	100W CW	20-200 MHz	50dB	38x37x15	100-240V	6,250.00
116C	100W CW	.01-220 MHz	50dB	71x56x76	100-240V	8,995.00
155LCR	100W CW	.006-12 MHz	50dB	48x40x13	100-240V	4,150.00
LA100H	100W CW	.3-100 MHz	50dB	48x48x13	100-240V	5,990.00
LA100F	100W CW	100-250 MHz	50dB	48x48x13	100-240V	6,595.00
LA100U	100W CW	200-400 MHz	50dB	48x48x13	100-240V	6,250.00
LA100UE	100W CW	100-500 MHz	50dB	48x48x13	100-240V	6,995.00
LA200H	200W CW	.5-100 MHz	53dB	48x48x13	100-240V	6,995.00
LA200F	200W CW	100-250 MHz	53dB	48x48x13	100-240V	11,500.00
LA200U	200W CW	200-400 MHz	53dB	48x48x13	100-240V	10,995.00
LA200UE	200W CW	250-500 MHz	53dB	48x48x13	100-240V	12,500.00
162LPS	200W Pulse	10-220 MHz	55dB	48x38x18	100-240V	5,995.00
122C	200W CW	.01-220 MHz	50dB	71x56x76	100-240V	10,850.00
247V	200W Peak	118-138 MHz	10dB	48x46x13	100-240V	5,255.00
247U	200W Peak	200-400 MHz	10dB	48x46x13	100-240V	5,500.00
121CA	250W CW	5-32 MHz	55dB	48x43x18	100-240V	5,950.00
164UP	300W Pulse	200-400 MHz	55dB	48x38x18	100-240V	7,595.00
LP300H	300W Pulse	.3-100 MHz	56dB	48x48x13	100-240V	7,550.00
LA500H	500W CW	5-50 MHz	57dB	71x56x76	100-240V	12,500.00
LA500V	500W CW	10-100 MHz	57dB	71x56x76	100-240V	13,500.00
134C	500W CW	.01-220 MHz	57dB	58x69x127	3 Phase	19,800.00
134CM	500W CW	1-200 MHz	57dB	58x69x127	3 Phase	18,500.00
166UP	500W Pulse	200-400 MHz	57dB	48x51x18	100-240V	9,500.00
LA600U	600W CW	200-400 MHz	57dB	71x56x76	100-240V	23,500.00
166HP	800W Pulse	100-200 MHz	57dB	48x51x18	100-240V	11,500.00
137C	1000W CW	.01-220 MHz	60dB	69x69x127	3 Phase	28,500.00
137CM	1000W CW	1-200 MHz	60dB	69x69x127	3 Phase	27,250.00
LA1000H	1000W CW	2-32 MHz	60dB	71x56x76	100-240V	22,500.00
135CB	1000W Pulse	2-30 MHz	60dB	48x51x46	100-240V	10,990.00
LA1000V	1000W CW	10-100 MHz	60dB	71x56x76	100-240V	26,900.00
166LP	1000W Pulse	8-100 MHz	60dB	48x51x18	100-240V	9,550.00
LP1000	1000W Pulse	10-120 MHz	60dB	48x51x18	100-240V	11,500.00
167HP	1500W Pulse	120-200 MHz	60dB	53x56x46	100-240V	17,950.00
167LP	2000W Pulse	10-100 MHz	63dB	53x65x46	100-240V	17,900.00
140C	2000W CW	.01-220 MHz	60dB	137x69x127	3 Phase	44,990.00
140CM	2000W CW	5-150 MHz	60dB	137x69x127	3 Phase	41,500.00
LA3000H	3000W CW	5-45 MHz	65dB	137x76x127	180-255V	69,500.00
LP4000H	4000W Pulse	2-50 MHz	66dB	71x56x76	100-240V	27,500.00

Made in U.S.A.

THE INDUSTRY'S

MOST WANTED

TCXO

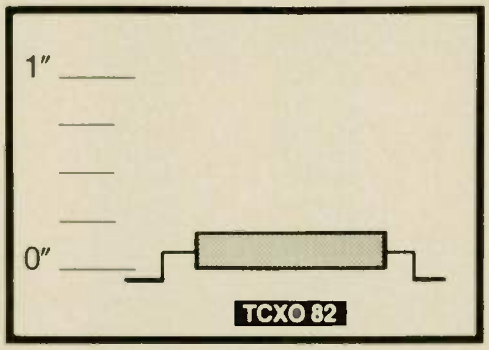

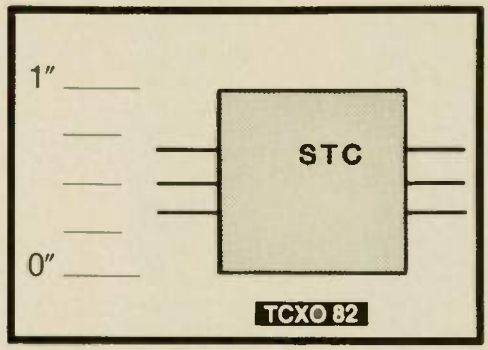

The latest TCXO from STC

DESCRIPTION:

- 0.2 cubic inches
  1″ × 1″ × 0.2″ high
- Mil grade available
- Surface mountable
- Custom configurable
  leads

MODE OF OPERATION:

- Low phase noise
- Frequencies up to 350 mhz
- Low power consumption
- Highly stable, precision
  performance

Analog Chip
Temperature Compensation Technology

Buy one or borrow one.

Call us for technical literature and complete details
on our unique offer.

STC COMPONENTS, INC., 636 REMINGTON ROAD, SCHAUMBURG, IL 60173
1.800.624.6491 • 708.490.7150 • FAX 708.490.9707 • CANADA: 1.800.624.6494
UK: 0279.626626

INFO/CARD 22

Curve Fitting Made Easy

By Brian Miller
Hewlett-Packard

Curve fitting is a powerful tool for the RF design engineer. It allows interpolation between data points for device characterization and correction. It can also assist in the interpretation of device data; e.g., does gain vary linearly with temperature, or is gain dependent on temperature squared? Figures 1, 2 and 3 are simple examples used to illustrate the utility of curve fitting. Figure 1 is a scattergram of the gain drift over temperature of 5 samples of an amplifier. Figure 2 includes the straight line which best fits the data. Figure 3 adds a best fit 2nd order curve to the raw data. It is apparent that the data is best modeled by the 2nd order curve of Figure 3. Most engineers recognize the value of curve fitting but are reluctant to employ it because curve fitting is computationally intense. Fortunately, linear algebra provides a simple method to fit a curve to data which is not only easy to use, but allows curves other than polynomials to be fit to the data.

Let us assume the we have n data points; $(x_1, y_1), (x_2, y_2), \ldots (x_n, y_n)$. We want to find the mth order polynomial, $y=a_0 + a_1x + a_2x^2 + \ldots a_mx^m$, which best fits the n data points. The method of least squares is the traditional, but tedious, approach used to solve for the polynomial coefficients $a_0 \ldots a_m$. The method of least squares calculates the squared error between each data point and the curve which is fit to the data. The total squared error is the sum of all the individual squared errors. The polynomial coefficients are obtained by taking the partial derivative of the total squared error with respect to each coefficient, and forcing the partial derivatives equal to zero.

To fit an mth order polynomial to a set of n data points using the method of least squares, requires the solution of the matrix equation

$$\mathbf{v} = \mathbf{A}^{-1}\mathbf{B} \qquad (1)$$

(bold print denotes a matrix) where:

$$y = a_0 + a_1x + a_2x^2 + \ldots + a_mx^m \qquad (2)$$

$$\mathbf{A} = \begin{bmatrix} n & \sum_{k=1}^{n} x_k & \sum_{k=1}^{n} x^2_k & \cdots & \sum_{k=1}^{n} x^m_k \\ \sum_{k=1}^{n} x_k & \sum_{k=1}^{n} x^2_k & \sum_{k=1}^{n} x^3_k & \cdots & \sum_{k=1}^{n} x^{m+1}_k \\ \vdots & \vdots & \vdots & & \vdots \\ \sum_{k=1}^{n} x^m_k & \sum_{k=1}^{n} x^{m+1}_k & \sum_{k=1}^{n} x^{m+2}_k & \cdots & \sum_{k=1}^{n} x^{2m}_k \end{bmatrix} \qquad (3)$$

Equation 3

$$\mathbf{v} = \begin{pmatrix} a_0 \\ a_1 \\ \cdot \\ \cdot \\ a_m \end{pmatrix} \qquad (4)$$

$$\mathbf{B} = \begin{pmatrix} \sum_{k=1}^{n} y_k \\ \sum_{k=1}^{n} y_kx_k \\ \vdots \\ \sum_{k=1}^{n} y_kx^m_k \end{pmatrix} \qquad (5)$$

Most modern computers solve matrix operations easily, so the equation is not difficult to solve. However, because the matrices **A** and **B** are so tedious to construct, the method of least squares is cumbersome to use.

Fortunately, linear algebra provides a simpler and more powerful method. It is possible to generate an mth order curve fit for a set of n data points by solving

$\mathbf{v} = (\mathbf{M}^t\mathbf{M})^{-1}\mathbf{M}^t\mathbf{y}$ [$\mathbf{M}^t$ denotes the transpose of **M**].

where

$$\mathbf{v} = \begin{pmatrix} a_0 \\ a_1 \\ \cdot \\ \cdot \\ a_m \end{pmatrix} \qquad (7)$$

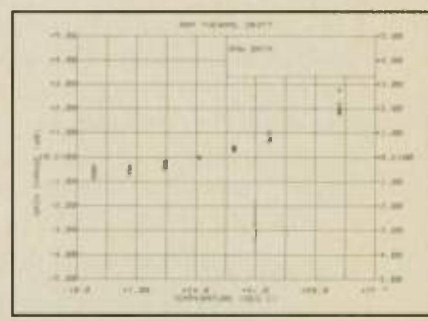

Figure 1. Raw data.

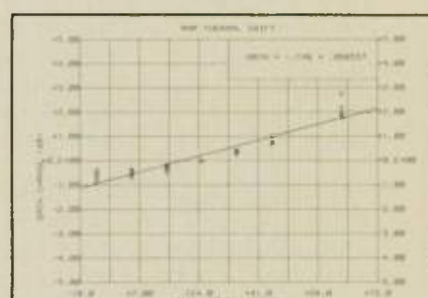

Figure 2. Straight line fit for data.

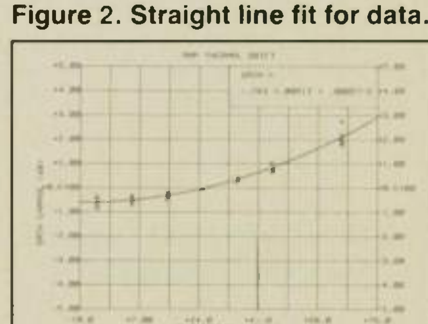

Figure 3. Second order curve fit for data.

american technical ceramics CORP.

News From ATC

Published by ATC June 1990

SPECIAL REPORT

This engineer just discovered ATC STA-TUNE™ - and the solution to his "circuit tuning" problem . . .

He did it with a miniature, (1/8" square) trimmable multilayer porcelain capacitor, available in capacitance values from 1 pF to 68 pF with adjustment ranges of 0.15 pF to 3 pF. This engineer just discovered what American Technical Ceramics' new STA-TUNE™ trimmable capacitor can do. Want to see what ATC's STA-TUNE can do for you?

Call our APPLICATIONS HOTLINE at (516) 547-5708 Today.

ADVANTAGES:

- Rugged
- Stable
- High Q
- Low Noise
- High MTBF
- Surface Mountable
- High current capability
- Reduced need for 1% tolerance parts
- Low Profile

ELECTRICAL CHARACTERISTICS:

- Quality Factor (Q)=greater than 10,000 at 1 MHz
- Temperature Coefficient of Capacitance (TC) = 90 ± 20 PPM/°C (-55°C + 125°C)
- Working Voltage (WVDC) = 500 VDC
- Dielectric Withstanding Voltage (DWV) = 200% WVDC
- Insulation Resistance (IR) = 10^6 Megohms min. @ 25°C and rated WVDC

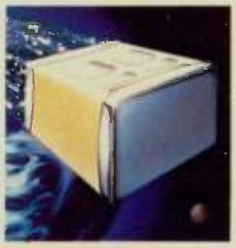

The Leader in RF Capacitor Technology. . See Us For Solutions.

INFO/CARD 76

Now Available From ATC: TS1003 A Case Tuning Stick® Kit

$89.95

For your higher frequency in-test value selection needs.

ATC's *New* A Case Tuning Stick® consists of an ATC 100 Series Superchip® measuring only .055 x .055, permanently attached to a non-conductive holder.

The Stick material is selected so that its effect on the capacitance value and Q is minimal. ATC TS1003 Tuning Stick Kit is available off the shelf. 48 Hour **QUIK-PICK**sm Shipment.

TS1003 Tuning Stick ® Kit contains 27 values:

CAP. VALUE (pF)	TOL.	CAP. VALUE (pF)	TOL.	CAP. VALUE (pF)	TOL.
0.1	B	3.9		22	
0.5		4.7	C	27	
1.0		5.6		33	J
1.2		6.8		39	
1.5	C	8.2		47	
1.8		10	J	56	
2.2		12		68	K
2.7		15		82	
3.3		18		100	

Tolerance Code: B = ±0.1pF; C = ±0.25pF; J = ±5%; K = ±10%

Also available: ATC's B-Case Tuning Stick Kits TS1001 and TS1002

INFO/CARD 23

american technical ceramics CORP.
one norden lane, huntington station, new york 11746-2102 • (516) 547-5700 • fax 516-547-5748 • telex 825707

Please see us at the MMT-S, Booth #909.

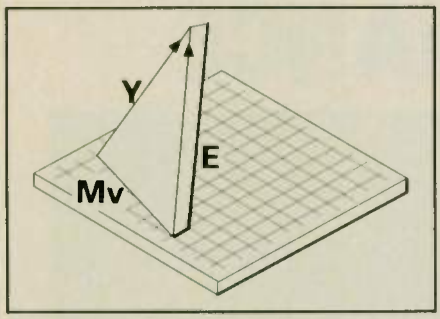

Figure 4. Mv in two dimensional space.

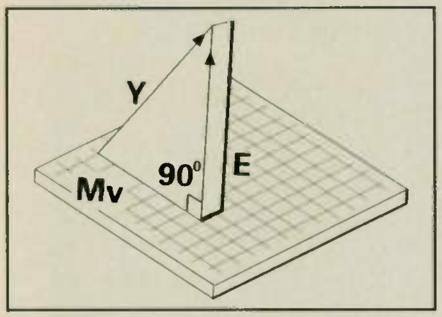

Figure 5. Mv and error (E).

$$\mathbf{M} = \begin{bmatrix} 1 & x_1 & x_1^2 & \ldots & x_1^m \\ 1 & x_2 & x_2^2 & \ldots & x_2^m \\ \cdot & \cdot & \cdot & & \cdot \\ \cdot & \cdot & \cdot & & \cdot \\ 1 & x_n & x_n^2 & \ldots & x_n^m \end{bmatrix} \quad (8)$$

$$\mathbf{y} = \begin{bmatrix} y_1 \\ y_2 \\ \cdot \\ \cdot \\ y_n \end{bmatrix} \quad (9)$$

This is called the matrix method. The matrices **M** and **y** are easy to construct and the matrix equation can be implemented on most computers.

A simple understanding of how the technique works can be obtained geometrically. Consider the case where it is desired to fit a straight line, $y=a_0+a_1x$, through 3 data points; (x_1, y_1), (x_2, y_2), (x_3, y_3). Solve the following system of equations:

$$y_1 = a_0 + a_1x_1 \quad (10)$$

$$y_2 = a_0 + a_1x_2 \quad (11)$$

$$y_3 = a_0 + a_1x_3 \quad (12)$$

Then rewrite equations 10-12 in matrix form as **y** = **Mv** where,

$$\mathbf{y} = \begin{bmatrix} y_1 \\ y_2 \\ y_3 \end{bmatrix} \quad (13)$$

$$\mathbf{M} = \begin{bmatrix} 1 & x_1 \\ 1 & x_2 \\ 1 & x_3 \end{bmatrix} \quad (14)$$

$$\mathbf{v} = \begin{bmatrix} a_0 \\ a_1 \end{bmatrix} \quad (15)$$

There is complete freedom to vary a_0 and a_1, but unless the 3 data points are collinear, **y** will never equal **Mv**. Regard **y** as a vector in 3-dimensional space. **Mv** will create another vector, with coordinates $(a_0+a_1x_1, a_0+a_1x_2, a_0+a_1x_3)$. The task is then to minimize the distance (or error, **E**) between the vectors **y** (y_1, y_2, y_3) and **Mv** $(a_0+a_1x_1, a_0+a_1x_2, a_0+a_1x_3)$ as illustrated in Figure 4. The vector **Mv** can be rewritten as the sum of 2 vectors

$$\mathbf{Mv} = a_0 \begin{bmatrix} 1 \\ 1 \\ 1 \end{bmatrix} + a_1 \begin{bmatrix} x_1 \\ x_2 \\ x_3 \end{bmatrix} \quad (16)$$

Consequently, regardless of the choice of a_0 and a_1, **Mv** will always lie in the plane described by the vectors:

$$\begin{bmatrix} 1 \\ 1 \\ 1 \end{bmatrix} \text{ and } \begin{bmatrix} x_1 \\ x_2 \\ x_3 \end{bmatrix} \quad (17)$$

Therefore, **Mv** is constrained to a 2-dimensional space.

Referring to Figure 4, the error, **E**, is minimized when it is perpendicular to the plane containing **Mv**. Define $\underline{\mathbf{v}}$ as the particular values of a_0 and a_1 which cause **E** to be perpendicular to the plane of **Mv**. Define $\underline{\mathbf{E}}$ to be the error vector under these conditions (Figure 5). Because $\underline{\mathbf{E}}$ is perpendicular to the plane of **Mv**, the dot product of $\underline{\mathbf{E}}$ with any vector **Mv** is zero. Thus,

$$(\mathbf{Mv}) \bullet \underline{\mathbf{E}} = 0 \quad (18)$$

But the dot product of 2 vectors equals the matrix multiplication of the 2 vectors if the transpose of the 1st vector is taken before multiplying; i.e., $A \bullet B = A^tB$. Applying this to Equation 18;

$$(\mathbf{Mv})^t\, \underline{\mathbf{E}} = 0 \quad (19)$$

Substituting $\underline{\mathbf{E}} = (\mathbf{y} - \mathbf{M}\underline{\mathbf{v}})$

$$(\mathbf{Mv})^t(\mathbf{y} - \mathbf{M}\underline{\mathbf{v}}) = 0 \quad (20)$$

$$\mathbf{v}^t\mathbf{M}^t(\mathbf{y} - \mathbf{M}\underline{\mathbf{v}}) = 0 \quad (21)$$

WE'VE REDUCED EVERYTHING BUT THE PERFORMANCE

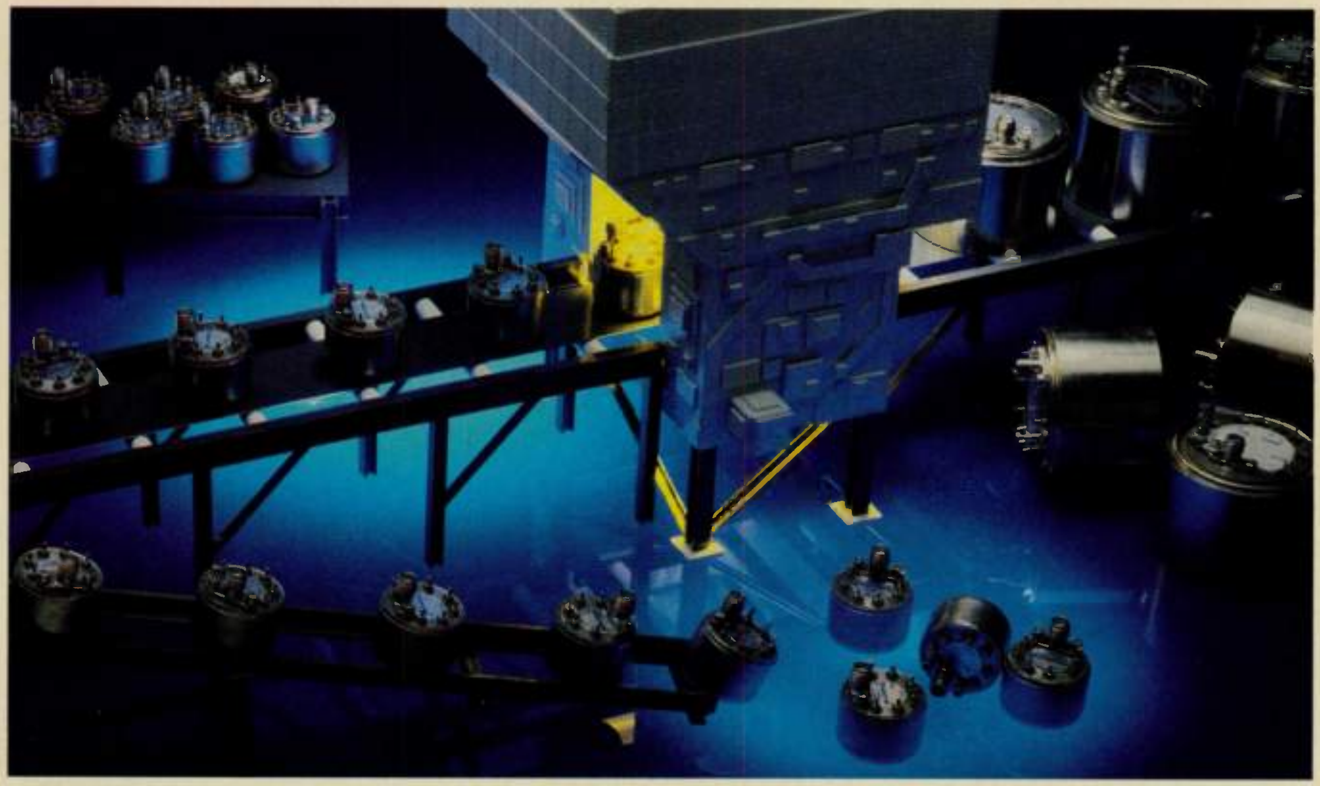

Avantek's New 2 to 8 GHz YIG Oscillators... as Low as $385.00*

Reduce your next-generation system's cost, size and weight at the same time. Avantek's next-generation YIG oscillators cost less, are smaller (0.5 cu. in.) and lighter (1.8 oz.) than other YIG oscillators available today. Ideal for next-generation portable equipment and low cost instrumentation. Fast tuning and phase lockable, these miniature YIGs deliver unmatched performance and unparalleled prices.

High Performance Oscillators... *Designed* for Low Cost

Avantek's revolutionary new approach to YIG oscillator design and manufacturing gives you the competitive edge... can help create new product lines...and open up new market opportunities. These compact, low-cost YIG oscillators offer real performance improvements. Typical tuning speed is an ultra-fast 10 ms (to within 5 MHz of final frequency). They operate with single input bias voltage...and, require no heater power. Two low-cost high-performance miniature YIG oscillators cover the 2.0 to 8.0 GHz frequency range.

AV-7028 2.0 to 8.0 GHz Miniature YIG Oscillator Tuning Speed

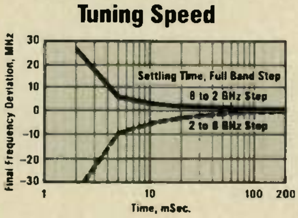

AV-7036 covers the 3.0 to 6.0 GHz range. AV-7028 provides 2.0 to 8.0 GHz frequency coverage. For both models, phase noise is typically −100 dBc/Hz at 20 kHz offset from carrier. And, power output is +13 dBm.

Off-the-Shelf Delivery from Your Local Avantek Distributor...

These low-cost, high-performance, compact YIG oscillators are available now. For the name and address of your local Avantek distributor or literature and applications assistance, contact us today.

*Price for each in 1,000 piece quantity.

Avantek Regional Offices

North America
Eastern: (301) 381-2600
Central: (708) 358-8963
Western: (805) 373-3870
Europe: (44) 276-685753
Asia: (01) (408) 943-5484

AVANTEK

INFO/CARD 44

```
10    'DIMENSION ARRAYS TO ALLOW UP TO 200 RAW DATA POINTS AND UP TO A
20    '9TH ORDER CURVE FIT
30     REAL Err(200),Temp(200),M(200,10),V(10),Y(200)
40     '
50     ' A1, A2, A3 AND A4 ARE ARRAYS CONTAINING INTERMEDIATE RESULTS BECAUSE
60     ' THIS COMPUTER CANNOT PERFORM MULTIPLE MATRIX OPERATIONS ON ONE LINE
80     ' A1 = M TRANSPOSE
90     ' A2 = A1*M
100    ' A3= A2 INVERSE
110    ' A4= A1*A3
120    '
130    REAL A1(10,200),A2(10,10),A3(10,10),A4(10,200)
150    '
160    'TEMP DATA: TEMP (DEG C), ERROR (dBm)
170    DATA 65,1.82,45,.60,35,.29,15,-.48,5,-.65,-5,-.85,25,0    'UNIT #5
180    DATA 65,2.25,45,.83,35,.38,15,-.32,5,-.54,-5,-.61,25,0    'UNIT #4
190    DATA 65,1.9,45,.68,35,.28,15,-.21,5,-.34,-5,-.36,25,0     'UNIT #3
200    DATA 65,2.77,45,1.03,35,.45,15,-.35,5,-.55,-5,-.73,25,0   'UNIT #2
210    DATA 65,2.04,45,.77,35,.44,15,-.16,5,-.4,-5,-.51,25,0     'UNIT #1
220    DATA 999
230    '
240    'READ IN THE RAW DATA
250    No_pts=0
260 Read_data:READ X
270    IF X>100 THEN Process
280    No_pts=No_pts+1
290    Temp(No_pts)=X
300    READ Err(No_pts)
310    GOTO Read_data
320    '
330 Process:INPUT "WHAT ORDER CURVE FIT (1-10) ",Ord
340    '
350    'REDIMENSION ARRAYS TO REFLECT THE ACTUAL # OF DATA POINTS AND THE ORDER
360    'OF CURVE FIT REQUIRED
370    REDIM Err(No_pts),Temp(No_pts),V(Ord+1)
380    REDIM M(No_pts,Ord+1),A1(Ord+1,No_pts),A4(Ord+1,No_pts),Y(No_pts)
390    '
400    'STUFF DATA INTO APPROPRITE ARRAYS
410    FOR I=1 TO No_pts
420       Y(I)=Err(I)
430       M(I,1)=1
440       FOR J=1 TO Ord
450          M(I,J+1)=Temp(I)^(J)
460       NEXT J
470    NEXT I
480    '
490    'CALCULATE BEST FIT STRAIGHT LINE
500    MAT A1= TRN(M)
510    MAT A2= A1*M
520    MAT A3= INV(A2)
530    MAT A4= A3*A1
540    MAT V= A4*Y
550    '
560    '
570    'PRINT RESULTS
580    FOR J=0 TO Ord
590       PRINT USING "K,D,K,SD.3DE";"a",J," = ",V(J+1)
600    NEXT J
610    '
620    END
```

Figure 6. Program to perform a curve fit on the data given in Figure 1.

$$v^t(M^t y - M^t M \underline{v}) = 0 \qquad (22)$$

But equation 22 is true only if $(M^t y - M^t M \underline{v}) = 0$. Thus,

$$M^t M \underline{v} = M^t y \qquad (23)$$

$$\underline{v} = (M^t M)^{-1} M^t y \qquad (24)$$

Figure 6 is a simple program which utilizes this technique to perform a curve fit on the data given in Figure 1. The program runs on an HP9836 computer, using BASIC 5.0. There are no special cautions to using this technique to curve fit. As usual with curve fitting, it is best to use the lowest order curve which provides a reasonable fit. This provides a more intuitive model of the system and a result which is easier to apply. It is possible to exactly fit an (n-1) order curve through n data points, however the resulting curve may not be useful for interpolation between the data points. Figure 7 shows 4 data points fit with a straight line, and with a 3rd order curve. The straight line is a more reasonable approximation to the trend of the data.

Curve fitting can become even more powerful when we recognize that we are not restricted to polynomial functions of x. Equation 6 can be extended to work with any functions and it is possible to approximate any data with a weighted, linear summation of functions of x. Assuming n data points (x_k, y_k) to be approximated by: $y = a_0$ to $a_1 f(x) + a_2 g(x)$, where f(x) and g(x) are any function. The best fit is obtained by:

$$v = (M^t M)^{-1} M^t y \qquad (25)$$

where

$$v = \begin{bmatrix} a_0 \\ a_1 \\ a_2 \end{bmatrix} \qquad (26)$$

$$M = \begin{bmatrix} 1 & f(x_1) & g(x_1) \\ 1 & f(x_2) & g(x_2) \\ \cdot & \cdot & \cdot \\ \cdot & \cdot & \cdot \\ 1 & f(x_n) & g(x_n) \end{bmatrix} \quad (27)$$

$$y = \begin{bmatrix} y_1 \\ y_2 \\ \cdot \\ \cdot \\ y_n \end{bmatrix} \quad (28)$$

Figure 8 illustrates how to use equation 25 to fit a sine wave to noisy data. For this problem:

$$f(x) = \sin(x) \quad (29)$$

$$g(x) = \cos(x) \quad (30)$$

The raw data is a sine wave immersed in noise and the curve fit is very accurate. In this case the curve fit equations are actually calculating the 1st terms of the Fourier series for this data.

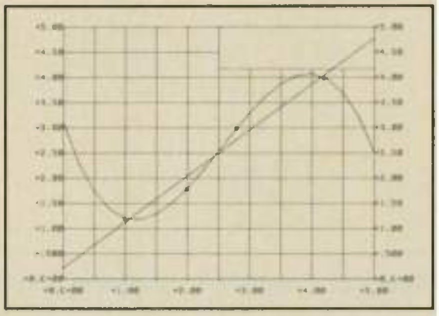

Figure 7. Example of straight line and 3rd order curve fit.

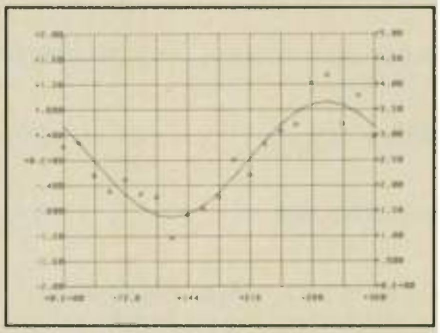

Figure 8. Sine wave fit to noisy data.

It can be shown that for polynomial curves, the method of least squares and the matrix method are equivalent. They both minimize squared error between the actual data and the curve which is to approximate the data. However, the matrix method is easier to implement. It also allows data to be approximated by a linear sum of non-polynomial functions and is therefore the preferred method to fit empirically derived data. ***RF***

References

1. H. Anton, C. Rorres, *Elementary Linear Algebra with Applications*, John Wiley and Sons, Inc., 1987.
2. L. Pipes, L. Harvill, *Applied Mathematics for Engineers and Physicists*, McGraw-Hill, Inc., 1970, pp. 561-567.

About the Author

Brian Miller received his BSEE from the University of Colorado in 1979 and is a research and development engineer at Hewlett Packard, TAFC-34, Spokane, WA 99220. His phone number is (509) 921-3288.

MMIC Foundry Models Using Standard CAD Simulators

By Raymond S. Pengelly
and Ulrich L. Rohde
Compact Software

GaAs MMIC foundries generally provide considerable amounts of data regarding their technologies, design rules and device models. However, there is usually a significant lack of information regarding the way in which the performance of various components can be predicted, and how those components can be used as the basis for "scaling" of similar structures having differing values and performances.

This paper attempts to display various ways in which industry standard linear/nonlinear simulators, such as Microwave Harmonica™, can be used to predict successfully the performance of a number of standard MMIC features, including transmission lines, discontinuities, inductors, capacitors, resistors and MESFETs. The simulated results are compared to measured data supplied by a number of GaAs MMIC foundries and further examples show how the models can be used to provide additional information to that provided by foundry design manuals.

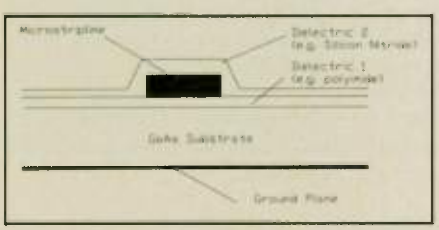

Figure 1. Typical MMIC microstripline structure.

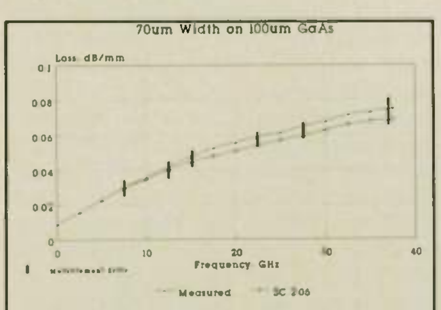

Figure 2. Losses in GaAs microstripline.

Transmission Lines and Discontinuities

One of the basic elements in many MMICs is the microstrip transmission line. These lines will almost always be configured within the IC such that they have mitred bends, tees, and other discontinuities associated with them. It is, therefore, necessary to be able to predict accurately the impedance and loss of such lines and discontinuities over wide frequency ranges. Even though many MMICs only operate up to 10 GHz or so, it is often necessary to have accurate models up to 60 GHz so that the harmonic responses of the circuit can be predicted successfully in a nonlinear simulator.

In a general way, MMIC microstrip line simulation needs to be able to accommodate more than one dielectric above and below the line metallization and include multi-metallization schemes, as shown in Figure 1. Figure 2 compares the measured loss of 50 ohm microstriplines on 100 micron thick GaAs with simulated results using the TRL routine in SuperCompact™ 2.0 as:

```
TRL 1 2 W=70UM P=1MM GAAS
.
.
.
DATA
GAAS: MS H=100UM ER=12.95
MET1=0.4  UM  +  MET2=AU3.5UM
TAND=0.001
END
```

In many cases, microstriplines are meandered with mitred bends to contain electrically long lines within small areas. These lines are modeled as coupled lines using the SuperCompact CPL statements together with the ABEND statements for the mitred bends. Work by Raytheon Research on such structures (1) has resulted in very good agreement between the predictions and results for the magnitude and phase of the S-parameters (Figure 3). This figure also shows the large differences that exist if the meanderline is only considered as a straight section of microstripline.

Many MMICs contain other discontinuities, such as microstrip tees and crossovers. For example, the simple GaAs IC filter structure of Figure 4(a), designed by Texas Instruments, contains 2 microstrip tees (MTEE) and open end effects in the open circuit stubs (OPEN). Again the agreement between

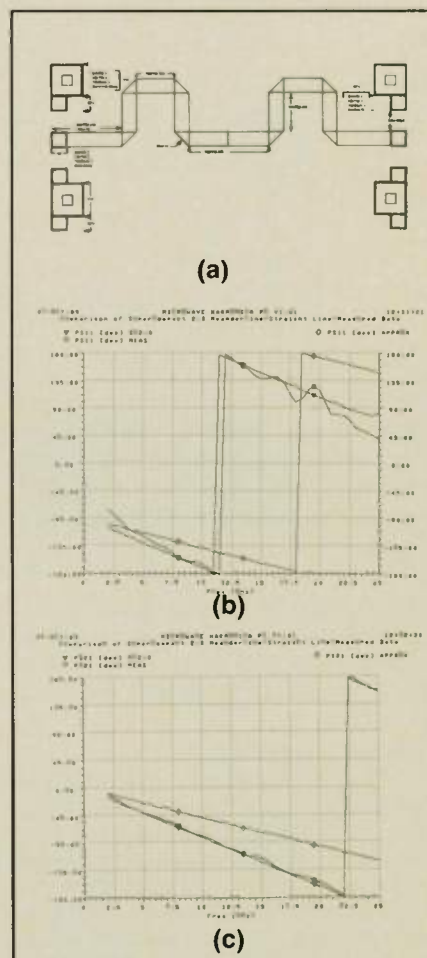

Figure 3. (a) Meanderline test structure on GaAs; comparison of measured results and straight-line approximations for (b) phase of S11, (c) phase of S21.

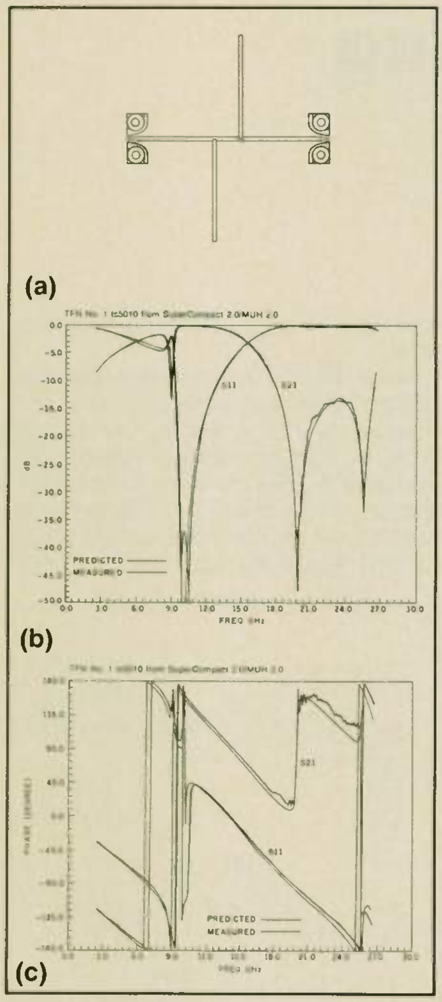

Figure 4. (a) "Simple" GaAs filter structure; predicted versus actual response for (b) S11 and S21 magnitude, and (c) S11 and S21 phase.

measurement and prediction is excellent to frequencies of at least 26.5 GHz for magnitude and phase of S11 and S21, as shown in Figures 4(b) and 4(c).

Lumped Elements

The use of lumped elements in MMICs has been a popular technique for many years. Such elements allow the required component values to be contained within small areas, leading to the efficient use of GaAs, reducing overall IC area and, therefore, cost. Lumped element inductors, such as spirals, and capacitors, such as indigitated types, have been simulated using a variety of techniques (2,3,4). The latest version of SuperCompact incorporates such techniques to accurately predict the S-parameters of new structures over wide ranges of frequency. Figure 5(a) shows a 4 turn spiral inductor on GaAs having 12 micron track and 12 micron gap widths with multiple air-bridging to allow the convenient connection of the center of the spiral to other circuitry. Figure 5(b) shows the good agreement between the measured results for this spiral and the simulated results using the RECI model in SuperCompact 2.0 as:

```
RECI 1 2 L1=88UM A1=100UM
B1=100UM N=4 W=12UM+
S=12UM T=3UM G GAAS
.
.
.
DATA
GAAS: MS H=200UM ER=12.95
MET1=TI 0.4UM
+ MET2=AU 3.5UM TAND=0.001
```

The phase of S11, for example, is accurate to within 5 degrees up to 18 GHz, the limit of the measured data.

Similarly, we have compared the results of RF-on-Wafer probed interdigitated and overlay capacitors with SuperCompact simulations up to 18 GHz on 200 micron thick GaAs. Figure 6(a) and (b) show the results for 0.25 pF interdigitated (ICAP) and 20 pF overlay (MIM) capacitors, respectively.

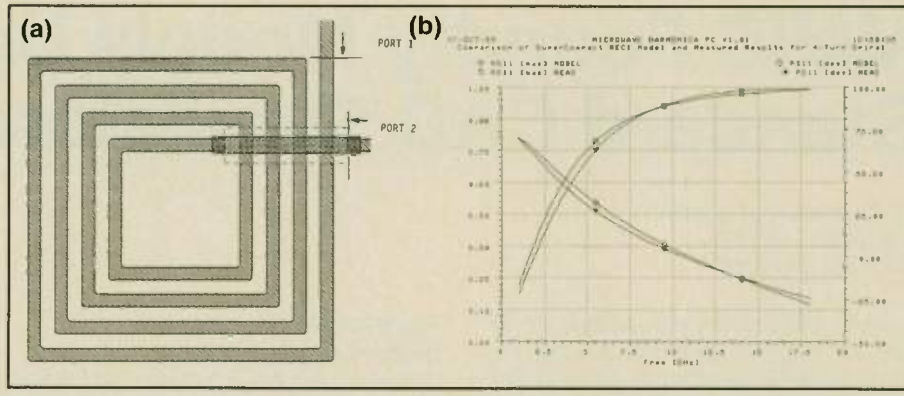

Figure 5. (a) 4-turn spiral inductor typical in MMICs; (b) its simulated and measured S11 magnitude and phase.

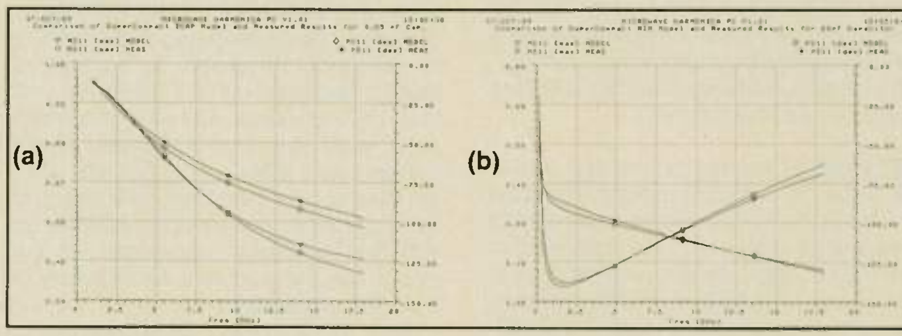

Figure 6. Simulated and measured S11 magnitude and phase of (a) 0.25 pF interdigitated capacitor, and (b) 20 pF overlay capacitor.

Thin film and ion-implanted resistors have basically the same equivalent circuit and can be modeled effectively by using a parallel combination of a TFR (thin film resistor statement), two microstriplines (which can have differing widths), and the microstrip gap statement GAP to model the parasitic capacitance that exists between the ends of the gold metallizations.

MESFETs

The linear simulator SuperCompact (contained within Microwave Harmonica) has unique temperature and bias dependent field-effect and bipolar transistor models for both S-parameters and noise-parameters. In addition to the usual pi-equivalent circuit for the small signal S-parameters of the MESFET, for example, activated by the FET statement in the netlist, the simulator has the ability to predict the complete noise parameters of the device by invoking the NFAC label within the FET listing. This, together with the TJ and TEMPC labels, allow the noise parameters of the device to be simulated as functions of channel temperature (TJ) using temperature co-

STANDARD CATALOG AMPLIFIERS, KHz TO GHz FREQUENCIES

WE OFFER THE AMPLIFIER USER A UNIQUE COMBINATION OF ADVANTAGES FROM A SINGLE SOURCE:

- ULTRA BROAD BAND FREQUENCY RESPONSE
- SUPERIOR PERFORMANCE SPECS AND WORKMANSHIP
- IMMEDIATE OFF-THE-SHELF DELIVERY
- VERY COMPETITIVE PRICING

...and now a simple way to get a price quotation fast! Simply check (✓) the appropriate box(s) below and mail or FAX this ad back to us.

CUT HERE

✓	Model No.	Frequency Response	SS Gain (dB) Min.	Flatness (dB) Max.	Noise Figure (dB)	PO@ 1dB C (dBm) Min.	VSWR In/Out	VDC	Current (mA)	Case/ Connector
Wide Band / Low Noise Amplifiers										
	W40C	1MHz—40MHz	42	±.5	1.0 Typ 1.2 Max	+5	2:1	+15	20	C/SMA
	W50ETC	10KHz—50MHz	24	±.5	5.3 Typ 6.0 Max	+23	2:1	+15	125	E-75/BNC
	W50ATC	10KHz—50MHz	50	±.5	1.3 Typ 1.5 Max	+5	2:1	+15	25	C-75/BNC
	W110F	5MHz—110Mhz	55	±.5	1.1 Typ 1.2 Max	+15	2:1	+15	80	C/SMA
	W110H	5MHz—110MHz	30	±.5	1.2 Typ 1.4 Max	+5	2:1	+15	30	C/SMA
	W500K	1KHz—500MHz	30	±1	1.7 Typ 2.2 Max	+3	2:1	+15	25	C-75/BNC
	W500C	5MHz—500MHz	40	±.5	1.4 Typ 1.6 Max	+10	2:1	+15	50	C/SMA
	W500EF	5MHz—500MHz	60	±.5	1.3 Typ 1.4 Max	+20	2:1	+15	190	A/SMA
	W500H	5MHz—500MHz	33	±.5	1.2 Typ 1.4 Max	+5	2:1	+15	25	C/SMA
	W1G2M	10KHz—1000MHz	30	±1	2.0 Typ 3.0 Max	+5	2:1	+15	35	C-75/SMA
	W1G2H	5MHz—1000MHz	30	±.5	1.3 Typ 1.5 Max	+5	2:1	+15	40	C/SMA
	W2GH	500MHz—2000MHz	22	±1	4.0 Typ 4.5 Max	+5	2:1	+15	30	C/SMA
	WFR1-4GA-14	100MHz—4000MHz	28	±1	3.5 Typ 4.0 Max	+14	2:1	+15	100	A-75/SMA
Medium Power Amplifiers										
	P150D	35KHz—150MHz	27	±.5	5.0 Typ	+30	2:1	+24	400	H/SMA
	P150M	500KHz—150MHz	26	±.5	5.0 Typ	+30	2:1	+24	600	H/BNC
	P150ML	400KHz—150MHz	24	±1	11 Typ	+29.5	2:1	±24	600	H/BNC
	P500A	2MHz—500MHz	37	±.5	4.5 Typ	+30	2:1	+24	500	H/SMA
	P500L	5MHz—500MHz	17	±.7	10 Typ	+30	2:1	+24	420	H/BNC
	P500ML	2MHz—500MHz	16	±1	11 Typ	+28	2:1	+24	600	H/BNC
	P1GB	50MHz—1000MHz	30	±1	5.5 Typ	+30	2:1	+20	800	A-S/SMA
	P1000M	5MHz—1000MHz	20	±.5	6 Typ	+21	2:1	+20	200	H/SMA
	P2GF-2	10MHz—2000MHz	32	±1	7.5 Typ	+30	2:1	+15	1000	F-1S/SMA
	P42GA-29	.5GHz—4.2GHz	30	±1.5	6.5 Typ	+29	2:1	+20	1200	F-1S/SMA

Name ______________________ Company ______________________

Title ______________________ Address ______________________

Tel. No. ______________________ City/State/Zip ______________________

TRONTECH INC

63 Shark River Road, Neptune, New Jersey 07753 U.S.A. ▪ (201)922-8585 ▪ TELEX 13 2445 ▪ FAX (201)922-3903

Represented in: Switzerland, Italy, Holland, West Germany, India, England, Japan, Canada, Israel, France, Sweden

INFO/CARD 27

HP's new alternative for stringent RF testing

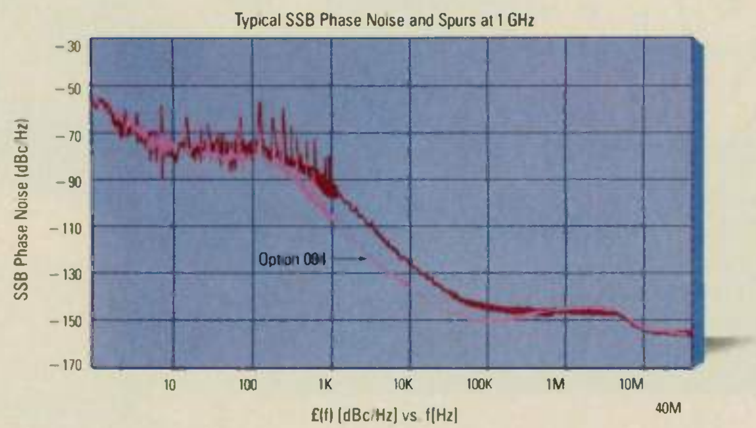

unsurpassed at 1-2 GHz

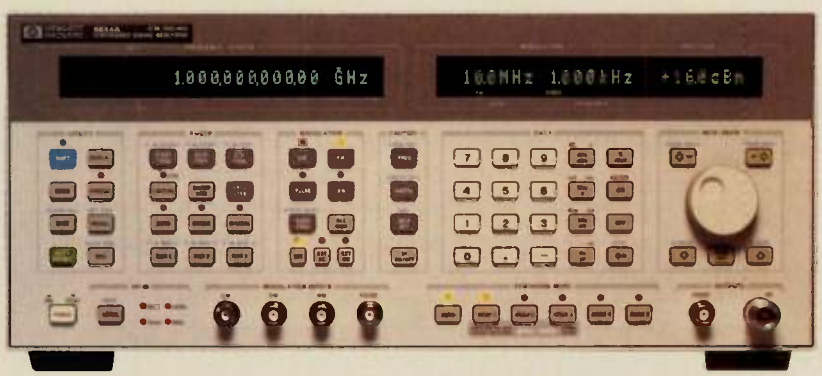

unexpected at $17K.*

Now, rigorous RF testing at 1 and 2 GHz costs much less. That's because the new HP 8644A Synthesized Signal Generator gives you the best possible signal purity. With prices that start at just $17,000.*

The HP 8644A has no substitute for demanding in-channel and out-of-channel testing. At 1 GHz, SSB phase noise is −128 dBc/Hz (20 kHz offset) standard. Optionally −136 dBc/Hz. Spurious is less than −100 dBc. And residual FM is less than 1 Hz. You also get AM, FM, pulse, and other modulations to create complex signals.

That means absolute confidence in two-way radio tests. Trusted IF/LO substitution in telemetry and radar. And real-world signal simulation in VOR/ILS testing.

For all the details, call 1-800-752-0900 today. Ask for Ext. 740P and we'll send a FREE selection guide to help you get the best purity... at the right price.

*U.S. list price.

There is a better way.

HEWLETT PACKARD

INFO/CARD 28

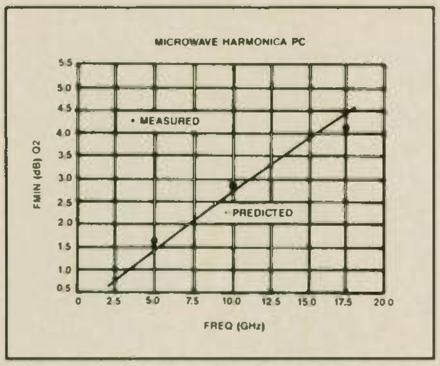

Figure 7. Measured vs. predicted noise figure for a Texas Instruments 0.5 micrometer gate FET.

efficients for the transistor parameters (activated by the TEMPC label in the DATA statements). A fuller description of this model is given in references 5 and 6. A typical FET statement is:

FET 1 2 0 G=40MS CGS=0.3PF GDS=(1/250) CDS=0.05PF
+RG=3 RS=3 RD=2 RI=6 CDG=0.04PF
+CDC=0.01PF LG=0.1NH LD=0.1NH LS=0.05NH TJ=25CEL
+TEMPC NFAC=0.5 NRG=0.1 NCG=0.2 FC=100MHZ

NFAC is coded such that its value equals the gate length of the FET when IPS=15 percent IDSS (usual low-noise bias). NFAC activates the noise model; NRG and NCG are related to the correlation coefficients that exist between the gate and drain noise sources in the FET. FC defines the corner frequency of the 1/f noise in the transistor.

By measuring the noise and S-parameters of a particular foundry FET of one gate length and width at different bias points, fitting the measured data to the model for FMIN, ZOPT and RN and (by using optimization within SuperCompact) obtaining the factors NFAC, NCG, NRG and FC, one can then scale the FET in gate length and width to obtain S- and noise-parameters for other FET sizes that use the same technology. Figure 7 shows the result of doing this for a Texas Instruments 0.5 micron gate

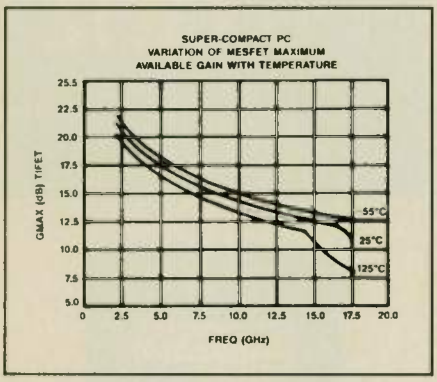

Figure 8. SuperCompact's simulated performance of G_{max} for the 0.5 micrometer gate FET versus frequency, for three temperatures over the military specified range.

length, 300 micron gate width MESFET over the 1 to 18 GHz frequency range for FMIN. Since both the intrinsic and extrinsic (parasitic) noise sources are dependent directly on the transistor chip temperature, the temperature dependence of the noise figure and S-parameters can also be calculated. Figure 8 shows the simulation for maximum available gain MAG for the same Texas Instruments MESFET as a function of temperature over −55 to +125 degrees C. Temperature coefficients can also be associated with inductors, resistors, capacitors and transmission lines within Microwave Harmonica.

Scaling of Elements

Foundries can only give electrical details on a limited number of passive and active elements because the amount of fabrication and measurements required to cover complete ranges of such elements would be very time consuming and expensive. The ability of a CAD program to accurately simulate components of similar geometry and layout to those within foundry manuals but having different dimensions and, therefore, parameter values is undoubtedly important to allowing the design engineer to "fill in the gaps" in the design library of the foundry. Two examples of this are:

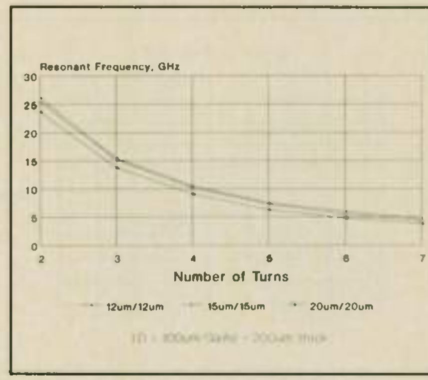

Figure 9. Resonant frequency of spiral inductors as function of track/gap width.

1. To show, through the RECI model in SuperCompact, variations in the resonant frequency of a spiral inductor as a function of the number of turns and track and gap dimensions.

Figure 9 shows the result of scaling of multiturn square spiral inductors as a function of first resonant frequency. The number of turns of the spiral were

INFO/CARD 31

"We came to TRW with our Model 1000 Digital Lincompex, a rack-mounted unit used to suppress noise in strateg c voice communication systems. It weighed 22 pounds and drew 115 watts of power. TRW's engineers helped us redesign the unit using just a few off-the-shelf digital signal processing ICs and software-programmable memory chips.

"We ended up with our Model 2200 LINK-PLUS, an all-digital, software-driven module that far exceeds the capabilities of traditional Lincompex units. It weighs less than 3 ounces, draws only 0.5 watts of power, and is small enough to fit in the handset of the world's most powerful tactical radio communication systems.

"And thanks to TRW's value engineering, the LINK-PLUS is affordable. TRW's manufacturing specialists showed us the smartest, most cost-effective way to produce the unit, in volumes from 10 to 10,000.

"If you'd like to know more reasons why TRW engineering makes our LINK-PLUS the best value in the radio communications market today, call us."

AMAF®

AMAF Industries, Inc.
Columbia, MD 21045
301.982.1585
FAX: 301.997.3485

TRW

TRW Electronic Systems Group

213.814.1842
INFO/CARD 32

GaAs NCO Operates up to 1.4 GHz

Gwyn Edwards
Stanford Telecommunications, Inc.

Stanford Telecom Inc.'s STEL-2173 Gallium Arsenide Numerically Controlled Oscillator has been successfully simulated to operate at an unprecedented 1.4 GHz at room temperature, and up to 1 GHz over the full commercial temperature range of 0 to 70C, giving an output bandwidth of more than 450 MHz with a frequency resolution of 0.23 Hz. The STEL-2173 is based on a newly developed architecture (patent pending) proprietary to Stanford Telecom, and features phase accumulation, PSK modulation and phase to amplitude conversion on one chip. Previous GaAs implementations of NCOs have required external modulators and ROM lookup tables, greatly complicating the system design at microwave clock frequencies. When combined with an 8-bit DAC, the STEL-2173 makes up a complete two chip DDS system.

Designed by Stanford Telecom's ASIC and Custom Products Group in Santa Clara, Calif., the device is fabricated by TriQuint Semiconductor. Using TriQuint's modeling tools the device has been successfully simulated to operate at a 720 psec. cycle time, resulting in the already mentioned 1.4 GHz clock frequency. The STEL-2173 was designed for optimum performance using the TriQuint TQ6112, an 8-bit, 1 GHz GaAs DAC, the de-facto standard for such applications.

The requirements of modern communication systems have created much interest in the use of digital techniques for frequency synthesis. Examples of this are spread-spectrum and frequency hopping systems, which push system requirements beyond the limits of analog synthesis techniques, especially in terms of frequency resolution and switching speeds. The basic unit of DDS is the Numerically Controlled Oscillator (NCO), a device which can generate digitized sinusoidal signals with very high frequency resolution and virtually instantaneous switching speed. These signals can then be converted to analog form with a digital to analog converter (DAC). The capabilities of such techniques have up until now permitted the generation of signals with bandwidths of more than 20 MHz with microhertz resolution and more than 70 dB of spectral purity; and with lower purity and resolution with bandwidths of more than 250 MHz. The latest development in this area is the STEL-2173 GaAs NCO.

The STEL-2173 GaAs NCO

This device is the latest in a wide variety of NCO devices designed by Stanford Telecom. With it, the company continues a long-standing history of generating new noise reduction and information compression techniques, as well as new architectures. It expands the capabilities of direct digital synthesizers by combining the capabilities and features of devices previously only available in CMOS with the high speed of GaAs. Prototype devices have been tested at over 1 GHz and are currently available from Stanford Telecom. When combined with the TriQuint TQ6112 GaAs DAC the characteristics of the resulting synthesizer rival those of systems able to operate at less than one tenth of this speed. Spurious signal levels reach a new low for systems operating in this frequency band, and in addition the device boasts the fastest frequency switching capability available today. Combined with the built in phase modulator, this device makes possible system performance that exceeds that previously possible by a large margin, and where phase modulation is not required, this capability can be utilized to provide quadrature outputs from a pair of devices. The block diagram of the STEL-2173 is shown in Figure 1.

At the input interface, the Δ-Phase Buffer Register is used to temporarily store the Δ-Phase data written into the

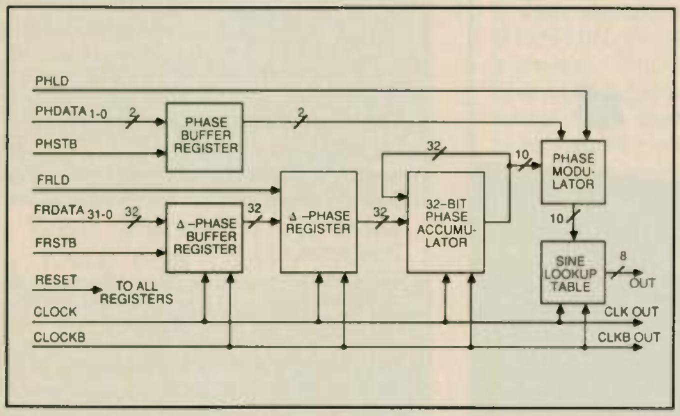

Figure 1. Block diagram of the STEL-2173 GaAs NCO, featuring a 32-bit phase accumulator, BPSK/QPSK phase modulator, and an on-chip sine lookup table.

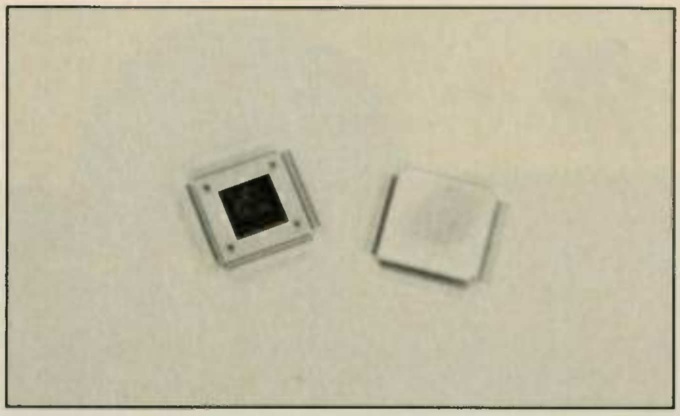

Figure 2. The STEL-2173 is packaged in a 132-pin flatpack. The package is designed with 50 ohm I/O lines for optimum speed, with one ground pin for every two signal pins.

Buying MIL-qualified connectors doesn't guarantee that the parts you need will arrive on time, or that they'll work when you get them. And with MIL specs changing so much, it's often hard to know what you're going to get.

Freedom of choice.
We offer MIL-qualified SMA connectors in all the popular configurations, and 100 types of SMB and SMC QPL connectors . . .twice as many as anyone else.

What you see is what you get.
Call or write for our QPL brochure. It's the only literature currently available which shows the important changes mandated by Amendment 2 of MIL-C-39012, including economical silver-plated SMB and SMC connectors.

Connectors that work.
Our production standards exceed MIL-C-39012 requirements. 11% of our workforce is in quality control to make sure these standards are met. Need proof? We have shipped over 150,000 cable assemblies with AEP SMB connectors for the ARC-164 military radio -- no rejections. We've also shipped over 200,000 SMA and SMB connectors to a major radio manufacturer -- no rejections.

Connectors when you need them.
All of our QPL connectors are available through our network of stocking distributors. If they're out of stock or you need large quantities, we can deliver most QPL items within six weeks from the factory.

The rest of the story.
If you need a connector that isn't covered by MIL-C-39012, we've still got you covered.

Call or write for our latest catalogue which shows our:

- **SMA connectors**, including hermetic-seal MIC launchers.
- **SMB, SMC and SLB** (Slide-on mating) connectors in thousands of varieties.
- **7000 series connectors**, with unequalled performance in microminiature size.
- **75 ohm connectors** with matched impedance for critical applications.
- **Cable terminations**, adapters, cable assemblies, and more.

But don't take our word for it . . . try us once and see what it's like to get parts that perform, shipped when promised, and at a price that will probably save you some money, too.

AEP . . .*Performance*, not promises.

APPLIED ENGINEERING PRODUCTS
P.O. Box 510
New Haven, CT 06513
Tel: 203/776-2813
Fax: 203/776-8294

INFO/CARD 34

device. This allows the data to be written asynchronously on the rising edge of the frequency write strobe. The data is written as a single 32-bit parallel word to facilitate high-speed frequency change using ECL signal levels. External logic can be used to interface the device to a microprocessor. The data is transferred from the Buffer Register into the Δ-Phase Register after a falling edge on the frequency load input. Similarly, the Phase Buffer Register is used to temporarily store the Phase data written into the device. This allows the data to be written asynchronously on the rising edge of phase write strobe. The data is transferred from this register into the Phase ALU after a falling edge on the phase load input. At each clock cycle the number stored in the 32-bit Δ-Phase Register is added to the previous value of the Phase Accumulator. The number in the Phase Accumulator represents the current phase of the synthesized sine and cosine functions. The number in the Δ-Phase Register represents the phase change for each cycle of the clock, i.e., $\Delta\phi/\Delta t$, where $\Delta t = 1/f_{clk}$. This number is directly related to the output frequency by the following equation:

$$f_{out} = (f_{clk} \times \Delta\text{-Phase})/2^{32}$$

where, f_{out} is the frequency of the output signal, and f_{clk} is the clock frequency.

The NCO achieves its high operating frequency by making extensive use of pipelining in its architecture. The pipeline delays within the NCO represent a total of 24 clock cycles for frequency changes. The Δ-Phase Register controls the updating of the Δ-Phase word in such a way that the pipelining becomes transparent to the user, so that when a frequency change occurs at the output the change is instantaneous, i.e., it occurs in one clock cycle, with complete phase coherence. Similarly, the desired phase changes also occur instantaneously, with no undershoot or overshoot. The pipeline limits the maximum frequency switching rate of the device to 1/16th of the clock frequency, but phase switching can occur at the clock rate itself.

The Phase Accumulator performs an important function within the NCO architecture. It is a high-speed, pipelined, 32-bit parallel accumulator, generating a new sum in every clock cycle. The overflow bit is discarded, since the required output is the modulo(2^{32}) sum, which represents all the possible values

SIEMENS

New! A high-performance, low cost GaAs MMIC amplifier!

Our latest GaAs MMIC amplifier in a plastic SOT 143 package delivers more power at lower cost than ever before.

Performance unmatched by silicon...
Use Siemens CGY 50 broadband amplifier as a cascadable 50 ohm gain block for broad- and narrow-band applications from 100 MHz to 3 GHz. You'll get low noise, more power, and excellent linearity that silicon parts can't deliver. (For example, at 4.5 volts supply voltage and 50 mA current, typical power output is 16 dBm from 200 to 1800 MHz with a noise figure of 3 dB and a gain of 9 dB.)

...at a new low cost for GaAs!
Siemens new plastic CGY 50 is about half the cost of ceramic GaAs MMIC amplifiers, making it affordable for your commercial avionics, communications, and other RF applications.

So why settle for silicon when you can have the power of GaAs at an affordable price?
Call **1 (800) 888-7730** today for samples, design assistance, or our new data sheet.

Special Products Division,
Siemens Components Inc.,
186 Wood Avenue South,
Iselin, New Jersey 08830

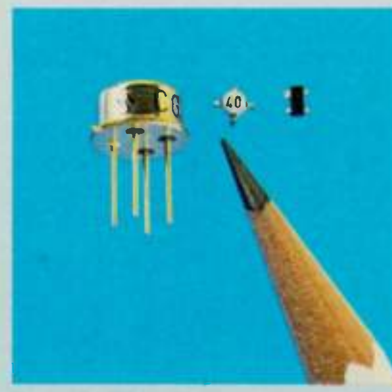

Specify Siemens for the latest in SMT.

CGY 50–The Latest Evolution in the Siemens Series

PERFORMANCE DATA								
	Package	P_{1dB} (dBm)	Gain (dB)	Noise Figure (dB)	Gain Flatness (dB)	IP_3 (dBm)	Gain Control Dynamic Range (dB)	Frequency Range
 CGY 50	SOT 143	16	9	3.0	1.4	31	20	100 MHz–1.8(3) GHz
 CGY 40	Micro-X	17.5	10	2.9	1.4	32.5	20	100 MHz–1.8(4) GHz
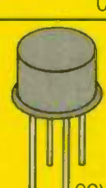 CGY 31/21	TO-12	19	19	3.8	1.5	34.5	30	40 MHz–1.8(3) GHz

SCI-1001

of the modulo(2π) phase angle. In the accumulator, the carry output of each 2-bit adder cell is pipelined to the next most significant cell. In this way the length of the accumulator does not reduce the maximum operating speed. The Phase ALU performs the addition of the phase modulation data to the Phase Accumulator output, giving the device the capability of generating BPSK and QPSK signals, as well as making possible to use two devices synchronously to generate quadrature output signals. The phase modulation data word is 2 bits wide, and this is added to the 2 most significant bits of the Phase Accumulator output to form the modulated phase used to address the look-up table. The pipeline delay associated with the phase modulator is only 8 clock cycles, since the phase modulating function is at the output of the accumulator.

The output of the Phase ALU is used to address the sine lookup table memory. The sine functions are generated from the ten most significant bits of the Phase accumulator, giving this device the capability of generating signals of such purity that are only matched by much lower speed CMOS devices. The output of the lookup table is an 8-bit word, and in the absence of phase modulation it maps the phase angle generated by the Phase Accumulator according to the equation:

$$OUT_{7\text{-}0} = 127 \times \sin(360 \times (\text{phase} + 0.5)/1024)\text{degrees} + 128$$

The result is accurate to within 1 LSB. When the phase accumulator is zero, e.g., after a reset, the decimal value of the output is 129 (81Hex). A photograph of the STEL-2173 NCO chip is shown in Figure 2.

Quantization Effects

A consideration which is extremely important in practice is the effect of quantization on the output signal. There are two sources of quantization distortion in a practical NCO, amplitude quantization and phase angle quantization. The first occurs since the output is always quantized to a finite number of bits; in the case of the STEL-2173, eight bits. Quantization of the phase angle is inevitably necessary to reduce the size of the look-up table to a reasonable size. For example, the phase accumulator of the STEL-2173 has 32 bits of resolution, and this would result in a very large look-up table (4 GigaBytes!) without quantization, and quantizing the phase accuracy to ten bits results in a significant saving in the size of the lookup table without reducing the basic frequency resolution of the device. Both of these quantizing effects result in spurious components which are dependent on the output frequency selected. These spurious components are the results of the distortion of the output waveform relative to the ideal. In general, many of these distortion components will occur at frequencies above half the clock frequency (the Nyquist frequency). Once again, since this is a sampled data system, these will fold back into the frequency interval 0 to $f_{clk}/2$ and will then not be harmonically related to the signal. They will inevitably appear in the frequency range being used, and conse-

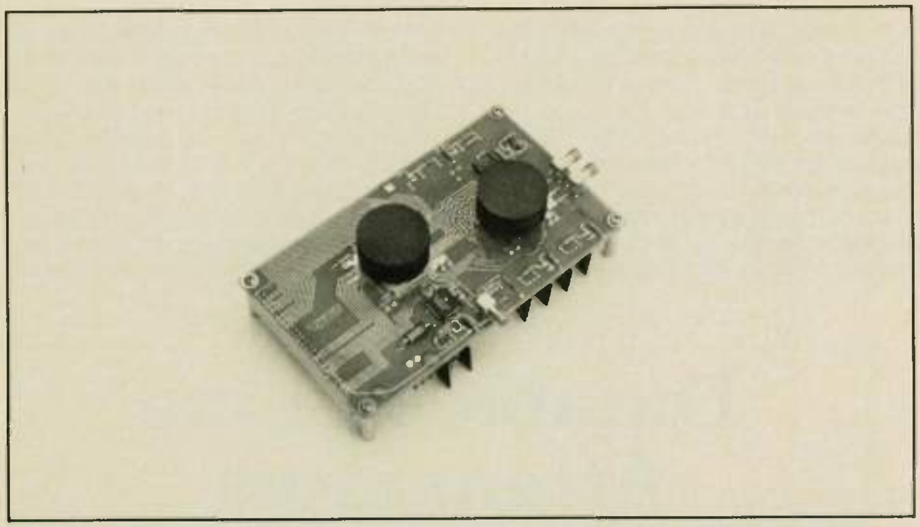

Figure 4. The STEL-2273 DDS board, showing the STEL-2173 NCO chip and the TQ6112 DAC.

quently cannot be removed by filtering.

Since this is a doubly quantized system the prediction of the frequencies and magnitudes of these spurious signals is fairly complicated. As a rule of thumb the quantized magnitude of the largest spurs can be predicted by assuming a signal-to-spurious ratio of approximately 7.8 dB per bit for the amplitude quantization. For example, if the amplitude is quantized to 8 bits, the worst case spurs will be at about −62 dBc. To reduce the effect of phase quantization so that not more than 1 or 2 dB of spur degradation occurs, the device needs 10 bits of phase resolution, or a 1024 point look-up table as is used in the STEL-2173. The size of the lookup table is further reduced in the STEL-2173 by taking advantage of certain features of the sine function. This is only possible when the lookup table is incorporated on chip, because this technique requires further processing of the output of the lookup table. This is an exclusive feature of the STEL-2173 relative to other GaAs NCOs. Thus the STEL-2173 provides a signal with all spurious signals below about −59 dBc, as shown in the FFT in Figure 3. This is approximately 10 dB better than the performance of previously available systems using an 8-bit address (total, for all four quadrants) lookup table.

In a practical DDS system the result will usually fall short of this by a margin that can range from a few dB to tens of dB due to imperfections in the DAC, including non-linearities, both static and dynamic, and glitch energy. The last two factors will cause the performance to degrade as both the clock frequency and output frequency increases. As in any system where digital and analog circuits are intermixed, getting the performance to approach the theoretical limits gets much more difficult as the frequencies increase.

Frequency Switching Speed

Since NCOs generate sinewaves from a continuously incrementing phase angle they are theoretically capable of switching frequencies from one clock cycle to the next simply by changing the value stored in the Δ-Phase Register every clock cycle. In practice the accumulator adder circuit cannot complete the multi-bit addition in a single clock period because of the delay caused by the carry bits rippling through the adder. However, the devices are designed to start a new addition every clock cycle by pipelining the adder circuit. This results in a processing delay from the time a new value is loaded into the Δ-Phase Register to the time when the frequency of the output signal actually

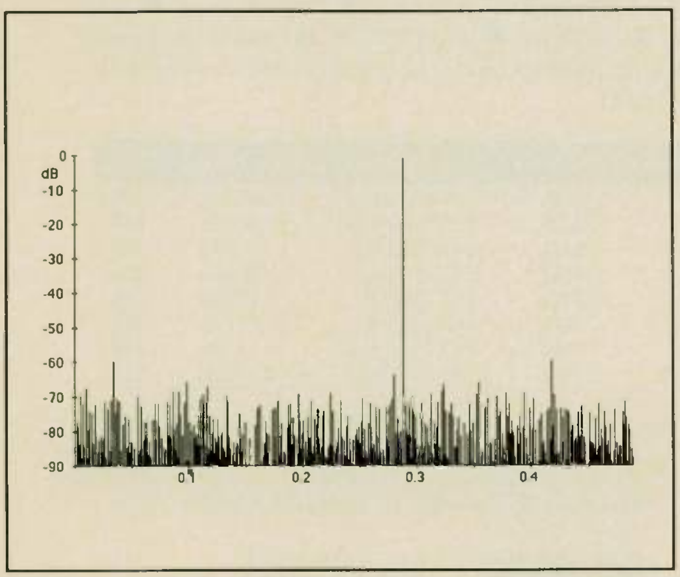

Figure 3. FFT of typical output of STEL-2173, with 10-bit address lookup table.

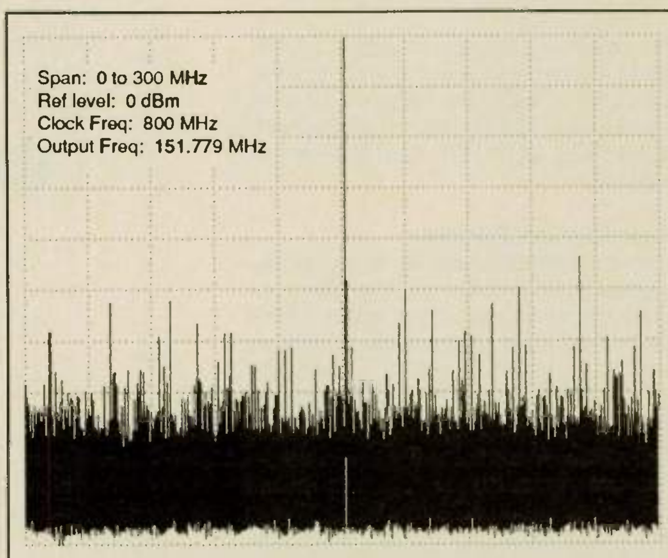

Figure 5. Spectrum plot of typical output of the STEL-2273 board, showing the exceptionally clean output signal for this class of DDS.

changes, and further new values should not be loaded until this has occurred. The consequence of this is a limitation on the maximum frequency update rate, which is a function of the frequency resolution of the device. The 32-bit STEL-2173 has a maximum update rate of 62.5 MHz (every 16 clock cycles). The accumulator works on 2 bits of data in each clock cycle, and consequently the data stored in the Δ-Phase Register should not be disturbed until the current value has propagated through the 16 cycle pipeline. Despite this limitation on the rate at which the Δ-Phase Register can be updated, the NCO output does actually switch frequencies from one clock cycle to the next, with complete phase coherence. The continuous-time relationship between frequency and phase is:

$$f = d\phi/dt$$

i.e. frequency is the rate of change of the phase of the sinewave. The discrete-time equivalent is:

$$f = \Delta \phi / \Delta t$$

where Δ t is the clock period, so that the frequency becomes:

$$= \Delta\phi/(2^R t_{clk}) = \Delta\text{-Phase} \times f_{clk}/2^R$$

where R is the resolution of the device, in this case 32 bits. Thus, simply by changing Δ-Phase, the instantaneous frequency can be changed from one clock cycle to the next. This frequency change capability is unparalleled in analog synthesizers.

The STEL-2273 DDSA complete Direct Digital Frequency Synthesizer using the STEL-2173 GaAs NCO chip has been built and evaluated. The board is shown in Figure 4.

The board measures 6 by 3.5 in. and operates from a single −15 volt supply. Regulators for the different voltages required on the board are built in. The board will shortly be available as the STEL-2273, and uses the TriQuint TQ6112 DAC to generate output signals from 0 to 450 MHz. Because of the limitations of the DAC, the performance of the DDS falls short of the theoretical performance of the STEL-2173 NCO chip by a substantial margin at its maximum operating frequency of 1 GHz. A spectral plot of the performance of the system operating at a clock frequency of 750 MHz is shown in Figure 5.

Applications

DDS systems are finding applications in many diverse areas, ranging from spread spectrum data and telecommunication systems, automatic test equipment, instrumentation and factory automation equipment to radar. They are particularly useful where their special features, such as high frequency precision and switching speed are useful. For example, in spread spectrum applications, the phase coherent high speed frequency switching can be utilized for hopped frequency carrier generation. Similarly, in radar systems the same feature can be utilized to generate a high precision and highly repeatable chirp signal, used in ranging applications. In instrumentation and automatic test equipment applications the ease of programming by digital sources is the primary feature. The STEL-2173 extends the range of such applications as a result of its extremely high operating frequency. *RF*

About the Author

Gwyn Edwards is a Member of Technical Staff at Stanford Telecommunications, Inc., 2421 Mission College Blvd., Santa Clara, CA 95054-1298, tel. (408) 980-5666.

Synthesized Signal Generator Introduced by Leader Instruments

The model 3220 AM/FM synthesized RF signal generator produced by Leader Instruments has a frequency range from 100 kHz to 1.3 GHz with ± 1ppm accuracy, and a resolution of 10 Hz below 650 MHz and 20 Hz up to 1.3 GHz. RF output units are selectable between dBu or dBm with a range of +13 to −133 dBm and 0.1 dB resolution. A continuous variable mode setting key enables the output level to be varied within ± 5 dB in 0.1 dB steps starting at any output level. Four convenient preset levels can be set for commonly used test levels. Reverse power protection to 50 W is standard.

The 3220 has a residual FM signal-to-noise ratio of 60 dB or better. At 500 MHz, the specified single-sideband phase noise is −120 dBc/Hz with a 20 kHz offset from the carrier. EMI/RFI leakage is less than 1 microvolt. Modulation modes are AM (0-90.0 percent), FM (0-99.9 kHz), AM/FM simultaneous, and DC-FM (0-5 kHz). FM deviation resolution is extended to 10 Hz for DC-FM mode and also for FM less than 9.99 kHz. There are four internal modulation frequencies to chose from.

A program/data entry keypad facilitates programming for semi-automatic operation. 100 address locations are provided in internal RAM which are battery backed in the event of AC line interrupt. Convenient edit features enable

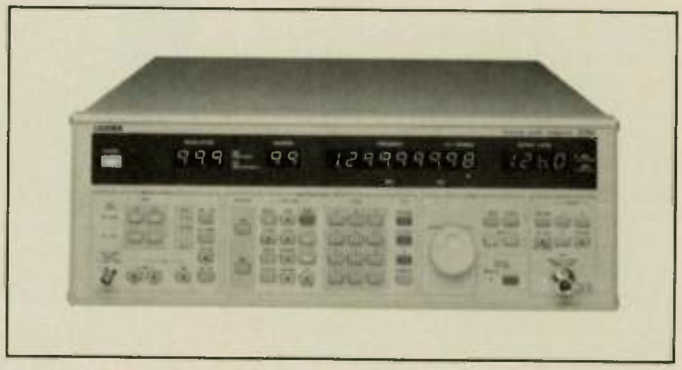

rapid variation of all front panel generator parameters recalled without distributing RAM contents. A GPIB listener interface option is available for applications that require high throughput testing. The 3220 is priced at $5995.

Leader Instruments Corp.
INFO/CARD #198.

Surface-Mounted Radiation Monitor

Loral Microwave-Narda, has released a new monitor for stationary requirements. The model 8820 SMARTS ™ provides manufacturers and users of high power microwave systems or satellite uplink shelters an inexpensive solution for full time safety monitoring. The SMARTS features 2 to 18 GHz frequency coverage, field-replaceable thermocouple-based true RMS detection elements, and operation that is similar to a smoke detector. Factory set to a 1 mW/cm^2 alarm threshold, the SMARTS LED flashes once every 40 seconds during normal operation and generates audible, visual and TTL alarms when the threshold is exceeded. The unit can operate over a one year period with no operator intervention or control.

Loral Microwave-Narda
INFO/CARD #197.

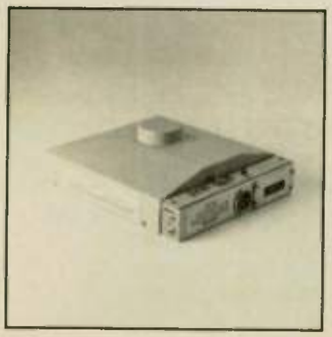

Modular Microcircuit Package

The modular HP 83040 series microcircuit package from Hewlett-Packard Company offers microwave designers a design and

test package that minimizes the delays and expense of custom-package solutions. The package is designed for circuit designs up to 26.5 GHz, and insertion loss is typically less than 1 dB. Expandable to accommodate additional circuit modules, it also allows users to test their designs and evaluate stand-alone building blocks for characterization and integration into higher-level systems.

This series is available in 0.254 mm (to 26.5 GHz) and 0.635 mm (to 18 GHz) substrate thicknesses, with center sections and through-line circuits available in 1-,2-,5-,10-, and 20-mm lengths.

Hewlett-Packard Company.
INFO/CARD #196.

EMI/RFI Filter Kit

Murata Erie is offering a design engineering sample kit of EMI/RFI filters in a multitude of configurations and values. Included in the kit are a variety of two and three lead filters with and without ferrite beads, ferrites beads, chip filters, signal line filters, etc., numbering almost 1,000 individual components. Also with this kit there are feed-thru low pass filters, with both eyelet and coaxial mounts.

This new sample kit is packaged with an EMI/RFI suppression manual that provides detailed information on widely accepted techniques and design considerations appropriate to minimize EMI and RFI. Specifications, attenuation characteristics and circuit configurations for each filter are also supplied.

Murata Erie North America
INFO/CARD #195.

5 MHz 12-Bit A/D Converter

The ADC604 is a 5 MHz, 12-bit A/D converter designed for high dynamic range spectrum analysis applications. Packaged in a 46-pin hermetic DIP, this hybrid's linearity allows near 14-bit performance with harmonic and two-tone IMD products at −83 dBc typically and guaranteed to be at least −80 dBc. ADC604 is a two-step subranging ADC subsystem containing ADC, sample/hold amplifier, voltage reference, tim-

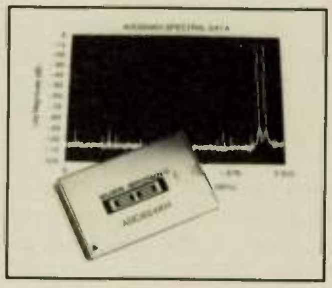

ing, and error-correction circuitry. This device dissipates 6 W and is available in a ceramic/metal package. Other specifications include ± 1.25 V input range, 40 MHz analog input bandwidth, 68.6 dB SNR, and ± 1/2 LSB differential linearity error. The specific operating temperature range is 0 to +70 degrees Celsius, and logic is TTL.

Burr-Brown Corp.
INFO/CARD #194.

Tacan Band Amplifier

Microwave Solutions' tacan band amplifier, MSH-254401 operates over the frequency range of 960 to 1210 MHz. The input/output gain is 32 ± 2 dB over this frequency range and delivers power output of +10 dBm minimum. The maximum noise figure is 5.0 dB at a power consumption of +15 VDC and 150 mA in a "flat-pak" outline. Input/output VSWR is 1.5/1.5. Lower noise figure, higher output power and different gain options are available.
Microwave Solutions, Inc.
INFO/CARD #193.

Broadband HF Antenna

The DPA-232A/A is a broadband, high-frequency antenna intended for use in a polarization-diversity receiving system requiring two signals corresponding to the orthogonal components of an incident wave. The antenna consists of two orthogonal balanced dipoles oriented in a vertical plane. It operates in the 2 to 32 MHz frequency range and has a nominal impedance of 50 ohms.
Antenna Research Associates
INFO/CARD #192.

Microstrip Probe

Design Technique announces the availability of its microstrip probe which provides an effective tool for testing MIC circuits. The probe works over the full 18 GHz range and has a typical return loss of 20 dB and insertion loss of 0.5 dB. The microstrip probe utilizes x, y, and z positioners for probe placement and is made up

of a probe head (MH350110F), priced at $750, and a probe tip (MSP10-01), priced at $750.
Design Technique International, Inc.
INFO/CARD #191.

Microwave Test Cable Assemblies

The FB series of microwave test cable assemblies from W.L. Gore are metrology-grade products that provide performance to 26.5 GHz. The FB series cable assemblies are designed for use as port return cables for vector automatic network analyzers and other microwave test equipment. The cable assemblies are available with test connectors including 3.5 mm and 7 mm for mode-free operation through 18 GHz or 26.5 GHz.
W.L. Gore & Associates, Inc.
INFO/CARD #190.

Microwave Power GaAs FET

Model D-6872 GaAs FET operates from 1 to 26.5 GHz with a typical output power of 24 dBm at 18 GHz and an associated gain of 6 dB. The device size is 350 μm x 500 μm x 75 μm and is available in packaged form. It is produced using Molecular Beam Epitaxy (MBE).
Litton Electron Devices
INFO/CARD #189.

2-Way Power Dividers

TRM, Inc. has released model DL 5205 and model DL 216 2-way power dividers. Model DL 5205 operates over the 1-100 MHz frequency range. Its maximum insertion loss is 0.50 dB; minimum isolation is 30 dB, amplitude balance is 0.10 dB; phase balance is 1 degree. DL 216 operates over the 5-725 MHz frequency range. Its maximum insertion loss is 1.00 dB, typical insertion loss is 0.70 dB; minimum isolation is 20 dB; amplitude balance is 0.20 dB; phase balance is 1 degree.
TRM, Inc.
INFO/CARD #188.

High Performance 1.6 GHz PLL

The QUALCOMM Q3036 1.6 GHz PLL is a high performance fully integrated PLL on one chip. The Q3036 has low phase noise, high phase detector gain, high frequency at the VCO, and high frequency at the reference point. It is fully integrated and includes the pulse swallow counters, phase/frequency detector, and dual modulus prescalar on a single chip. The price is $49.00.
Qualcomm Inc.
INFO/CARD #187.

RF Switch/Attenuator PIN Diodes

Metelics' MPN-7360, -7370, and -7380 PIN diodes offer up to 800 volts breakdown and utilize a moisture resistant glass passivated mesa construction. They offer up to 5 microseconds lifetime and series resistance as low as 0.27 ohms typical at 100 mA bias.
Metelics, Corp.
INFO/CARD #186.

Probe Positioner

The model PS201 provides smooth precision operation in manual probing of wafers, hybrids, and MIC's. The positioner achieves zero stick-slip, zero hysteresis motion in the x-axis, the x-y plane, and the z-axis. Gold plated arms provide signal extraction/insertion from DC to 1 GHz, as well as high impedance (500 ohms), coplanar 50 ohms, low capacitance and DC probing.
Orion Alpha Corp.
INFO/CARD #185.

RNet Series Telemetry Radios

Motorola introduces the RNet 150 and 450 Series of Telemetry Radios operational on the UHF and VHF frequency bands (403-430 MHz, 450-470 MHz and 136-174 MHz). The models are available on two-channel operation and measure 3.3" x 1.52" x 2.70". They weigh 10.2 ounces. Key features include low current drain, voice and data transmission capability, and variable

power levels.
Motorola, Inc.
INFO/CARD #184.

21-Decade Amplifiers

Models VMA 3K8-208 through −232 offer +23 dBm output levels in ultra high speed pulse and baseband applications; the entire 3 kHz to 8 GHz band is covered. Housed in a 1.0" x 0.5" x 1.0" x

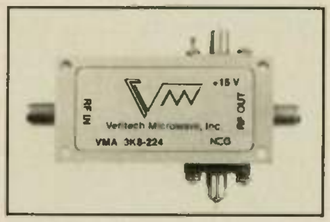

3.1" frame with SMA connectors, these units operate from +15 V at 270 to 840 mA and −15 V at 50 to 100 mA. Internal regulation and over/reverse voltage protection are included. Typical rise times for pulses are 45-60 picoseconds.
Veritech Microwave, Inc.
INFO/CARD #183.

Power MOSFET

DEI has released its DE-375 and DE-375L Series FAST POWER ™ MOSFETs in the E-M Symmetry package. With less than 1 nH insertion inductance, both the DE-375 and the DE-375L feature less than 7 nanoseconds switching times, multi-megahertz frequencies, and very low profile and weight. Total power dissipation of the DE-375 is 200 W ant the DE-375L is 100 W. N-channel devices are available in voltages from 300 V to 1000 V and current ratings from 11 A to 40 A. The price for 500 pieces for DE-375 is $128 and for DE-375L is $69.
Directed Energy, Inc.
INFO/CARD #182.

GaAs FET MMIC SPDT Switch

The model AS018M2-00 non-reflective GaAs FET MMIC SPDT Switch from Alpha Industries works from DC to 18 GHz. It is designed with two series and three shunt 0.25 μm E-beam written gate FET's. Characteristics are typical isolation of 53 dB, typical insertion loss of 2.5 dB, and typical switching speed of 2-3 nanoseconds at 18 GHz. Bias requirements are 0 and −5 volts with currents typically less than 100 μA at −5 volts.
Alpha Industries, Inc.
INFO/CARD #181.

Non-Woven Laminates

Isoclad[R] Types GR and 900 Series PTFE non-woven composite laminates provide x-y plane dimensional stability and reliable dielectric consistency to improve production and yields. Both meet MIL-P-13949 standards for types GR and GP materials. Type GR Series is designed for frequency dependent applications and the Type 900 Series has characteristics of both woven and non-woven laminates. The materials are offered in a wide variety of dielectric constants from 2.17 through 6.0.
ARLON
INFO/CARD #180.

Silicon Monolithic Amplifiers

The HPMA-02XX/03XX/04XX/20XX/21XX series silicon monolithic Darlington amplifiers introduced by Hewlett-Packard come in two types of microplastic packages: the 85 with straight microstrip leads, and the 86 with bent leads for surface mounting. The

gain, bandwidth and power-output capabilities vary, depending on the device. The HPMA-2185/86 offers the highest gain with 18 dB typical at 1 GHz. The HPMA-0485/86 is the top power handler with 12.5 dBm typical output power at 1 dB gain compression. For under 500 pieces, the price range is $2.15 for HPMA-02XX to $3.40 for HPMA-2111. For over 500 pieces, the price range is $2.05 for HPMA-02XX to $2.95 for HPMA-2111.
Hewlett-Packard Company.
INFO/CARD #179.

Quartz Crystal Temperature Sensors

The TELE QUARZ GROUP announces its latest product,

quartz crystal temperature sensors. The advantage of this type of sensor is that its frequency is temperature dependent. They are available in the 8 to 45 MHz frequency range. Other specifications are less than 7 pF shunt capacitance, a thermal time constant typically 3 seconds, and a temperature stability of typically 90 ppm/K.
TELE QUARZ GROUP.
INFO/CARD #178.

Developmental Absorber

The ECCOSORB[R] FJA series is a high temperature, lightweight, line of developmental absorbers from Emerson and Cuming. This line can withstand continuous temperatures to 550 degrees F (288 degrees C) without burning, melting, or emitting toxic fumes. ECCOSORB FJA 9-18 9-18 has a weight of 0.3 lbs/ft^2 and a thickness of 0.30". ECCOSORB FJA 6-18 has a wight of 0.4 lbs/ft^2 and a thickness of 0.40". Both broadband absorbers have an expected performance of 20 dB in the operating range of 9-18 GHz and 6-18 GHz respectively.
Emerson & Cuming, Inc.
INFO/CARD #177.

Extended Range NMR Amplifier

ENI announces the model NMR-300L/50M, an RF amplifier for high-resolution NMR analytical spectroscopy systems with magnet strengths between 4.7 and 14.1 Tesla. This amplifier produces 300 W of pulse power over the frequency range of 5-220 MHz, reducing to 150 W up to 250 MHz, and 50 W from 200-600 MHz. Full output power is achieved with a 20 percent duty cycle and pulse widths of up to 20 milliseconds. RF rise times are less than 1 microsecond and RF fall times are less than 150 nanoseconds. The unit is available for 90-day delivery at a cost of $12,500.
ENI
INFO/CARD #176.

Crystal Clock Oscillators

Hybrids International, Ltd. has introduced a complete line of crystal clock oscillators from 1 Hz to 500 MHz. These are supplied in PID, HALF DIP, and surface mount packages.
Hybrids International, Ltd.
INFO/CARD #175.

Low-Noise Front Ends

MITEQ has released a series of moderate bandwidth low-noise front ends. The front end consists of a miniature low-noise RF preamplifier, an image reject mixer, and an optional IF preamplifier. These are available in the frequency range from 0.6 to 10 GHz with noise figures as low as 1 dB at 0.6 GHz to 2.6 dB at 10 GHz. Image rejection is typically 20 dB. The IF frequency range covers 2-400 MHz in octave bands.

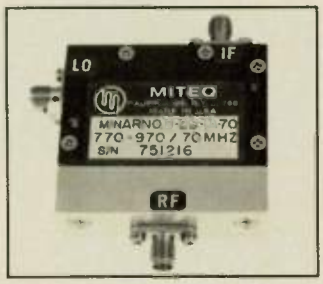

MITEQ
INFO/CARD #174.

Conical Monopole Antenna

Model PCM-213/A is a broadband passive conical monopole antenna primarily designed for receive applications over the frequency range from 20 MHz to 1300 MHz. The conical monopole antenna is linearly polarized and produces an omnidirectional radiation pattern with a nominal gain of 4.0 dBi in broadband mode. The antenna is comprised of 16 removable rods and a base plate/head assembly.
Antenna Design & Mfg. Corp.
INFO/CARD #173.

Limiting Amplifier

Armatek's model MH359301 limiting amplifier family operates at 5-500 MHz and features a typical ±0.5 dB output variation over a 40 dB input power range. Biased at 15 V and 70 mA, the unit has 36 dB gain and limits at a nominal output power of 0 dBm. Typical even harmonic suppression is −25 dB with phase shifts of 0.0025 degrees per MHz per dB of compression. The family is available in Dual In-Line packages.
Armatek, Inc.
INFO/CARD #172.

Software

Eagleware

Formerly Circuit Busters

Personal RF and microwave simulation software. Enjoy the freedom of using a powerful program on your own IBM personal computer.

NEW! =SUPERSTAR= V3.3

=SuperStar= version 3.3 has just been released with:

- Over 1000 S-parameter device files
- More output data formats
- Optimizer improvements
- New element models
- Tunable markers
- Only $695

=PROFESSIONAL EXTENSION=

New! =SuperStar= Professional Extension has all =Superstar= V3.3 features plus:

- Monte Carlo and yield analysis
- Models for microstrip, stripline, waveguide, and coax
- Components defined by user via equations
- Only $995

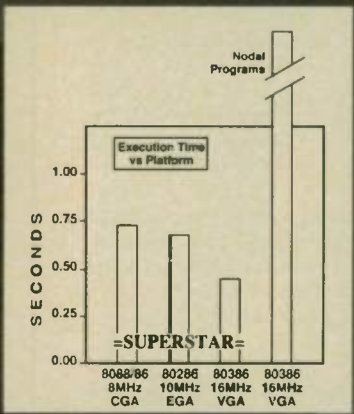

=SuperStar= V3.3 and Professional Extension are fast!
Experience real-time bench-like circuit tuning with =SuperStar=.
Graph shows times for a typical broadband amplifier.
Tuning and optimization are blindingly fast because =SuperStar=:

- Preprocesses the circuit file
- Generates inline code for equation definitions
- Uses routines written in assembly
- Uses unique graphic display techniques
- Provides chain-matrix connections

Other Eagleware PC programs:

=FILTER= L-C filter synthesis
=EQUALIZE= group delay equalization
=OSCILLATOR= oscillator synthesis
=TLINE= transmission line and synthesis

Programs run on standard IBM PCs and compatibles, include a 30 day money-back guarantee, free support and no annual maintenance fees. For further information telephone Eagleware. Immediate shipment arranged with COD, VISA or Mastercard.

Eagleware

1750 Mountain Glen
Stone Mountain, GA 30087 USA
Tel (404) 923-9999 FAX (404) 925-7524

VISA MasterCard

INFO/CARD 50

Signal Design/ Analysis Package

Signal Design and Analysis Environment™ SDA-™ allows users to design infinite and finite duration impulse-response (IIR and FIR) filters. It calculates coefficients in polynomial or second order-section formats and displays frequency and impulse response and pole-zero plots. Using the designed filters, the signal editor can perform both linear and nonlinear filtering operations and can display up to 40 signals simultaneously.
Comdisco Systems, Inc.
INFO/CARD #210.

Spice Models for SFC's

Intusoft introduces switched capacitor filter models for use with Spice. The Spice models include Linear Technology LTC 1059, LTC 1060 and 1064 series and National Semiconductor's MF5 and MF10. Modeling techniques used to develop these models include switch, Z transform, and Laplace domain elements. It is available on floppy disk for $20.
Intusoft.
INFO/CARD #209.

Amplifier Simulation Program

SW.I.F.T. Enterprises introduces A.S.P. 2.0. This amplifier simulation program provides the user with menu driven options in designing narrow band amplifiers without the need for S-parameter design knowledge. Included are automatic or user interactive design routines, performance data, matching circuits, a help menu auto 'Q', and a utility to optimize the noise figure. A screen plotting utility has been added for gain, NF and VSWR. A.S.P. 2.0 sells for $75 and is designed to run on IBM compatibles with DOS 2.11 or later and least 360K memory. EGA and a math co-processor are required.
SoftWare Innovations For Technology Enterprises.
INFO/CARD # 208.

Circuit Analysis for the 386

COMTRAN Integrated Software introduces AC-CAP ™ that runs on 2 megabyte 386 platforms. The package is comprised of AC-CAP, S-WAVE, and PLOTFT. It simulates and optimizes active and passive analog circuits, calculates gain, phase, and impedance vs. frequency. PLOTFT provides frequency domain graphics from S-WAVE data in a format that can be combined with AC-CAP's graphics. S-WAVE is a FFT/IFT tool that handles data files up to 32K points with over 300dB of dynamic range. Some features include smoothing, convolution, de-convolution and correlation.
COMTRAN, A Division of Jensen Transformers, Inc.
INFO/CARD #207.

W.A.V.E. Upgrade

Vespine Software Division of Electronic Decisions Inc. introduces version 1.1 of W.A.V.E.™ integrated data analysis and acquisition software, with improved basic arithmetic functions. For complex applications, W.A.V.E. 1.1 uses a macro library facility where user-created macros can be stored to simplify the management of elaborate macro groups. W.A.V.E. 1.1 is priced at $749 and is designed for use on the IBM-PC/XT/AT and IBM PS/2.
Electronic Decisions, Inc.
INFO/CARD #206.

Transmitter Intermodulation Software

B.T. Chomycz introduces F-INTERMOD and O-INTERMOD, software that calculate RF intermodulation products resulting when 2 to 50 radio transmitters are located nearby. The software is priced at $400 and can run on an IBM PC or compatible computer with 640K RAM and a 360K floppy disk drive.
B.T. Chomycz.
INFO/CARD #205.

INFO/CARD 51

INFO/CARD 52

Uncertainty in Spectrum Analyzer Based Measurements

By Dave Massie
Hewlett-Packard Co.
Signal Analysis Division

This article presents a technique for using a spectrum analyzer in noise figure measurements. Even though a spectrum analyzer has a higher uncertainty factor than a noise figure meter, it is still capable of providing acceptable results for many applications. Although the application described is noise figure measurement, the performance considerations are applicable to EMC measurements, as well.

Two techniques exist for making a noise figure measurement with a spectrum analyzer. The first is to directly measure the noise level of the device under test (DUT) with the spectrum analyzer. Unfortunately, this technique depends on the absolute amplitude and bandwidth accuracy of the spectrum analyzer. The other technique is the same as that used in automatic noise figure meters.

This technique uses a calibrated noise source which can be turned on and off. The ratio of the measured noise level between the on and off states of the noise source, commonly known as the Y factor, is used to calculate noise figure. The measurement-system noise figure, NF_{sys}, is measured first during a calibration step. Then, the DUT is connected to the measurement system and the DUT/system noise figure, NF_{tot}, is measured along with the DUT gain, G_{dut}. The DUT noise figure, NF_{dut}, can then be extracted from the cascaded noise figure equation:

$$nf_{tot} = nf_{dut} + \frac{nf_{sys} - 1}{g_{dut}} \quad (1)$$

The latter technique has the advantage of making relative, not absolute noise power measurements. However, several error mechanisms translate to noise figure error when measuring relative noise power levels. The magnitude of noise figure error depends not only on the magnitude of the noise power measurement error, but also on the noise figure of the measurement system, the amount of noise available from a calibrated source, and the DUT's gain and noise figure.

Since noise figure and gain are typically expressed in dB, and many of the equations involved in this discussion require linear values, it is appropriate to describe the naming convention used to distinguish between the logarithmic values and their linear counterparts. Logarithmic values will be expressed in uppercase letters and their corresponding linear values will be lowercase. Thus, NF will be noise figure in dB and nf will refer to the linear equivalent commonly known as noise factor.

Noise Figure Calculations

Using the DUT in the measurement system shown in Figure 1, the system has a certain noise figure and gain attributed to it. NF_{sys}, G_{sys}, and the noise source have a particular excess noise ratio (ENR) of N_s dB and the system bandwidth (B) is constant along with the temperature (T).

During calibration, with the noise source on and connected to the measurement system, the noise power, n_{con}, (in watts) detected by the spectrum analyzer is:

$$\begin{aligned} n_{con} &= (g_{sys})[KTB + KTB(n_s - 1)] + (g_{sys})KTB(nf_{sys}) \\ &= (g_{sys})KTB(nf_{sys} + n_s) \end{aligned} \quad (2)$$

With the noise source off, the noise power, n_{coff}, is:

$$n_{coff} = (g_{sys})KTB(nf_{sys}) \quad (3)$$

Which makes the Y factor for the calibration:

$$y_{cal} = \frac{n_{con}}{n_{coff}} = \frac{nf_{sys} + n_s}{nf_{sys}} \quad (4)$$

Rearranging the previous equation, the system noise factor can be calculated in terms of the Y factor:

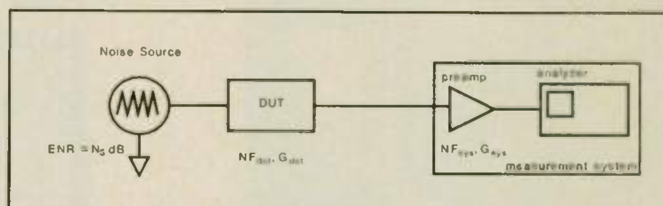

Figure 1. Noise figure test setup.

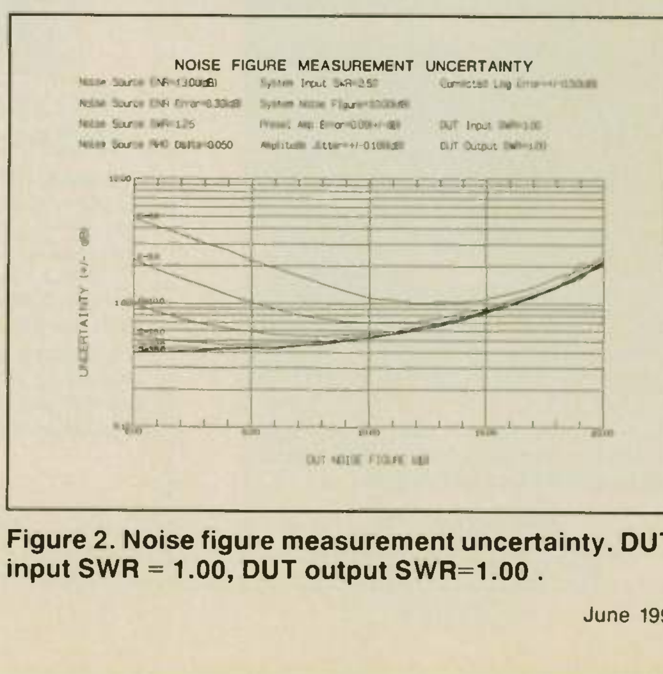

Figure 2. Noise figure measurement uncertainty. DUT input SWR = 1.00, DUT output SWR=1.00 .

Model 3115 Double Ridge Guide
1–18 GHz
Model 3116 Double Ridge Guide
18–40 GHz

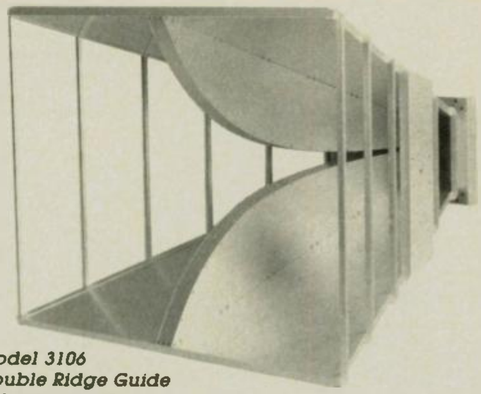

Model 3106
Double Ridge Guide
200 MHz–2 GHz

Model TR3 Non-Metallic Tripod
22.68 kg capacity
two other models available

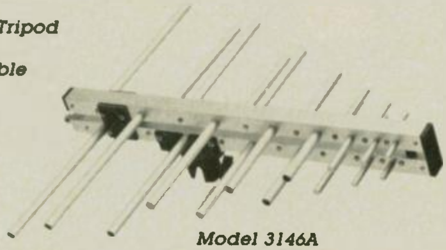

Model 3146A
Log Periodic
300 MHz–1 GHz
four other models available

Model 1060 Turntable
with controller and IEEE-488 bus option
1-7.6 meter diameter available
three other models available

Model 6502
Active Loop
10 kHz–30 MHz
four other models available

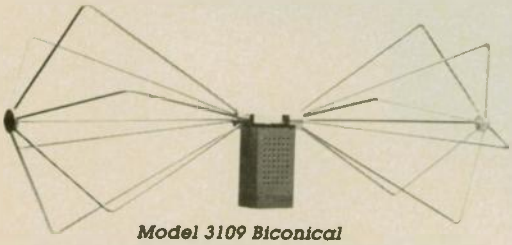

Model 3109 Biconical
20–300 MHz
three other models available

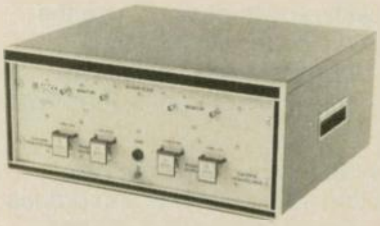

Model 3925 PLISN
5 kHz–1 GHz
five other models available

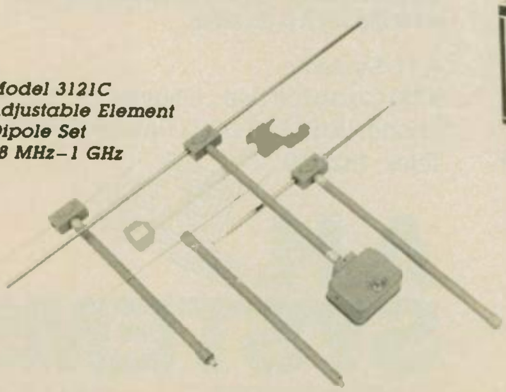

Model 3121C
Adjustable Element
Dipole Set
28 MHz–1 GHz

TEST WITH CONFIDENCE.

ENGINEERED TO PERFORM

If compliance testing is your primary responsibility, you need top-of-the-line products you can count on. Like EMCO antennas, designed for repeatable FCC/VDE testing. Manufactured for the stringent requirements of MIL-STD testing. With high sensitivity for TEMPEST testing. Most have VSWR ratios of less than 2:1. And all exhibit exceptional dynamic range and linearity.

CALIBRATED INDIVIDUALLY

Every EMCO antenna is individually calibrated using both C63.4 and ARP 958 standards, then shipped to you with a signed Certificate of Compliance—a claim no other manufacturer of test antennas can make.

MANUFACTURED WITH CARE

We choose only the best and most durable materials for EMCO products. Then we pay close attention to details—machined tolerances are often less than one one-thousandth of an inch. And while we've automated for efficiency, we still take the time to hand-assemble and inspect each one of our products.

TWO-YEAR WARRANTY, SERVICE WORLD-WIDE

Because we know how well every EMCO product is engineered and built, we can back each one with a two-year warranty—twice the industry standard. And EMCO has more than 30 representatives worldwide to help you—wherever you are. Call our 800 number for more information and the name of your EMCO representative. Ask for your free catalog of EMCO products, too!

1-800-253-3761

EMCO™
The Electro-Mechanics Company

Call toll-free between 7:30 AM and 4:30 PM Central Time
800-253-3761 in USA or 512-835-4684 in Texas
Telex 797627 Fax 512-835-4729
P.O. Box 1546 Austin, Texas 78767

08151/89161 Fax 08151/16610
Munchner Str. 2 D-8137 Berg 1 West Germany

INFO/CARD 54

$$nf_{sys} = \frac{n_s}{y_{cal} - 1} \tag{5}$$

and the gain of the system can be determined from the difference between n_{con} and n_{coff}:

$$g_{sys} = \frac{n_{con} - n_{coff}}{KTB(n_s)} \tag{6}$$

Inserting the DUT with gain, G_{dut}, and noise figure, NF_{dut}, the detected noise powers can be expressed by the total gain, G_{tot}, and noise figure, NF_{tot}, of the system/DUT combination. When the noise source is on, the noise power, n_{don}, (in watts) detected by the spectrum analyzer is:

$$\begin{aligned} n_{don} &= [(g_{tot})(KTB + KTB(n_s - 1))] + (g_{tot})KTB(nf_{tot}) \\ &= (g_{tot})KTB(nf_{tot} + n_s) \end{aligned} \tag{7}$$

With the noise source off, the noise power, n_{doff}, detected is:

$$n_{doff} = (g_{tot})(KTB)(nf_{tot}) \tag{8}$$

Subsequently, the Y factor for the measurement is

$$y_{meas} = \frac{n_{don}}{n_{doff}} = \frac{nf_{tot} + n_s}{nf_{tot}} \tag{9}$$

Rearranging the previous equation, the noise factor can be calculated in terms of the Y factor:

$$nf_{tot} = \frac{n_s}{y_{meas} - 1} \tag{10}$$

The total gain can be determined from the difference between n_{don} and n_{doff}:

$$g_{tot} = \frac{n_{don} - n_{doff}}{KTB(n_s)} \tag{11}$$

Since g_{tot} and g_{sys} are known, the gain of the DUT, g_{dut}, can be calculated as:

$$g_{dut} = \frac{g_{tot}}{g_{sys}} = \frac{n_{don} - n_{doff}}{n_{con} - n_{coff}} \tag{12}$$

Knowing g_{dut}, nf_{tot}, and nf_{sys}, nf_{dut} can be determined by rearranging the cascade noise figure equation:

$$nf_{dut} = nf_{tot} - \frac{nf_{sys} - 1}{g_{dut}}$$

$$nf_{dut} = \frac{n_s}{y_{meas} - 1} - \frac{\left(\frac{n_s}{y_{cal} - 1}\right) - 1}{g_{dut}} \tag{13}$$

$$nf_{dut} = \frac{(n_s)(g_{dut})(y_{cal} - 1) - (y_{meas} - 1)(y_{cal} - 1 - n_s)}{(g_{dut})(y_{meas} - 1)(y_{cal} - 1)}$$

Substituting and rearranging terms allows nf_{dut} to be seen in terms of the measured noise power levels and the ENR of the noise source:

$$nf_{dut} = \frac{(n_s)\left(\frac{n_{don} - n_{doff}}{n_{con} - n_{coff}}\right)\left(\frac{n_{con}}{n_{coff}} - 1\right) + \left(\frac{n_{don}}{n_{doff}} - 1\right)\left(\frac{n_{con}}{n_{coff}} - 1 - n_s\right)}{\left(\frac{n_{don} - n_{doff}}{n_{con} - n_{coff}}\right)\left(\frac{n_{don}}{n_{doff}} - 1\right)\left(\frac{n_{con}}{n_{coff}} - 1\right)} \tag{14}$$

$$NF_{dut} = 10 \log (nf_{dut}) \tag{15}$$

Developing The Error Model

Any amplitude error incurred when measuring the relative noise power levels or any inaccuracy in the noise source ENR will create an error in the noise figure measurement. Measuring the relative noise powers with a spectrum analyzer introduces several error mechanisms such as mismatch, log fidelity, and repeatability. In addition, errors are associated with impedance, impedance change from on to off, and amplitude inaccuracy of the noise source.

To determine the measurement uncertainty, a computer simulation of the noise figure measurement, including the error mechanisms involved, is used. The error mechanisms are randomized, and a large number of simulated measurements are computed. The distribution, variance, and standard deviation of the DUT noise figure are calculated from this large sample. The uncertainty shown on the graphs in Figures 2-5 represents a point that is two standard deviations on the noise figure distribution curve. Therefore, approximately 97 percent of the measurements simulated are within this range.

Two errors will not be accounted for here due to the particular spectrum analyzer used. First the spectrum analyzer is assumed to be preselected so that both noise at the image frequency and harmonic down-converted noise are eliminated. The other error concerns analyzer tuning repeatability between calibration and measurement sweeps. The analyzer is assumed to have a synthesized LO, and therefore, tuning error is not considered.

Mismatch Errors

During calibration, the mismatch error between the noise source and measurement system would be constant for a given frequency if it were not for the change in the output impedance of the noise source between on and off states. Assume a noise source and measurement system which, in the absence of any errors, would measure ideal noise power levels of n_{coni} and n_{coffi}. When mismatch errors are introduced, the mismatch error equation describes the noise power variation:

$$n_{conmm} = \frac{n_{coni}}{|1 - (\Gamma_{ns})(\Gamma_{sys})|^2} \tag{16}$$

where Γ_{ns} is the complex reflection coefficient of the noise source in the on state, and Γ_{sys} is the input reflection coefficient of the measurement system.

When the noise source is off, its output impedance changes slightly. The change in output impedance can be taken into account by adding a term $\Gamma_{ns\Delta}$ to Γ_{ns}. The variation in noise power level, with the noise source off, may then be written as:

$$n_{coffmm} = \frac{n_{coffi}}{|1 - (\Gamma_{ns} + \Gamma_{ns\Delta})(\Gamma_{sys})|^2} \tag{17}$$

A similar mismatch error analysis applies when the DUT is measured except there are two mismatch errors. If the ideal power level with the noise source on is n_{doni}, then the noise power variation will be:

$$n_{donmm} = \frac{n_{doni}}{[|1 - (\Gamma_{ns})(\Gamma_{din})|^2][|1 - (\Gamma_{sys})(\Gamma_{dout})|^2]} \tag{18}$$

where Γ_{din} and Γ_{dout} are the input and output reflection coefficients of the DUT. Likewise, the variation in noise power with the noise source off is:

$$n_{doffmm} = \frac{n_{doffi}}{[|1 - (\Gamma_{ns} + \Gamma_{ns\Delta})(\Gamma_{din})|^2][|1 - (\Gamma_{sys})(\Gamma_{dout})|^2]} \tag{19}$$

Log Fidelity Errors

In most spectrum analyzers, log fidelity is a periodic function of amplitude. Periodic log-fidelity errors are usually expressed as a log-fidelity increment error, $\log_{inc}$, bounded by a maximum value, $\log_{max}$. Some analyzers are capable of correcting their log error in real time, therefore removing the periodicity of the log-fidelity function. In these analyzers, the log-fidelity error is a random function and is expressed as a maximum $\pm E_{logcor}$ dB. In either case, the log-fidelity errors are taken into account in the following manner.

The noise figure equation shows that any log-fidelity error between the noise power level pairs used to calculate y_{cal}, y_{meas} and the DUT gain term (Eq. 20) is important.

$$\frac{n_{don} - n_{doff}}{n_{con} - n_{coff}} \tag{20}$$

E_{logdut} represents the log-fidelity error between N_{don} and N_{doff}. E_{logcal} represents the log-fidelity error between N_{con} and N_{coff}. Finally, $E_{logdutcal}$ represents the log-fidelity error between the numerator and denominator of the DUT gain term.

The highest noise level occurs with the DUT inserted and the noise source turned on. This noise level, N_{donmm}, will be the reference level for the other noise power levels. Therefore, N_{doffmm} relative to N_{donmm} has a log-fidelity error of $\pm E_{logdut}$ dB. The noise level N_{conmm} relative to N_{donmm} has an error $\pm E_{logdutcal}$ dB, and N_{coffmm} relative to N_{conmm} has an error of $\pm E_{logcal}$ dB. The noise power levels including the log fidelity error terms are:

$$N_{don} = N_{donmm} \tag{21}$$

$$N_{doff} = N_{doffmm} + E_{logdut} \tag{22}$$

$$N_{con} = N_{conmm} + E_{logdutcal} \tag{23}$$

$$N_{coff} = N_{coffmm} + E_{logdutcal} + E_{logcal} \tag{24}$$

The magnitude of the error terms for analyzers that specify log error as a log increment error may be calculated using the noise-power levels previously calculated in the mismatch-error analysis. Therefore, the magnitude of the log-fidelity error terms may expressed as:

$$E_{logdut} = (N_{donmm} - N_{doffmm})\log_{inc} \tag{25}$$

$$E_{logdutcal} = (N_{donmm} - N_{conmm})\log_{inc} \tag{26}$$

$$E_{logcal} = (N_{conmm} - N_{coffmm})\log_{inc} \tag{27}$$

If E_{logdut}, $E_{logdutcal}$, or E_{logcal} exceed the value $\log_{max}$, then they take on the value of $\log_{max}$.

For analyzers that specify corrected log fidelity, the magnitude of the log error terms is simply E_{logcor},

$$E_{logdut} = E_{logdutcal} = E_{logcal} = E_{logcor} \tag{28}$$

Amplitude Repeatability Errors

Three amplitude-repeatability error mechanisms present in spectrum analyzers are step-gain error resulting from changes in reference level, repeatability error due to preselector mistuning, and amplitude jitter. Step-gain error is not considered because the reference level does not have to be changed if properly set during calibration.

The operator, though, has little control over error resulting from preselector mistuning. However, the measurement technique influences the impact that this will have on the overall error. The less-desirable technique requires stepping through the chosen frequency range twice during calibration and twice during measurement — one sweep made with the noise source on, the other with the noise source off. The four

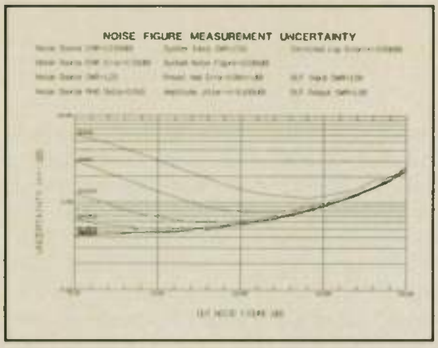

Figure 3. Noise figure measurement uncertainty. DUT input SWR = 1.50, output SWR=1.50 .

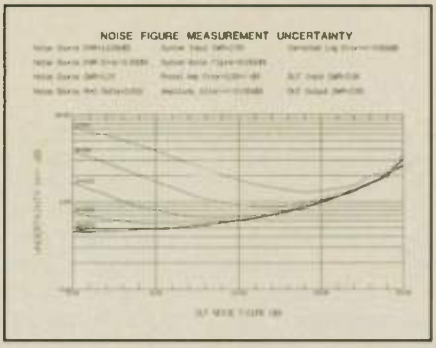

Figure 4. Noise figure measurement uncertainty. DUT input SWR = 2.00, output SWR=2.00.

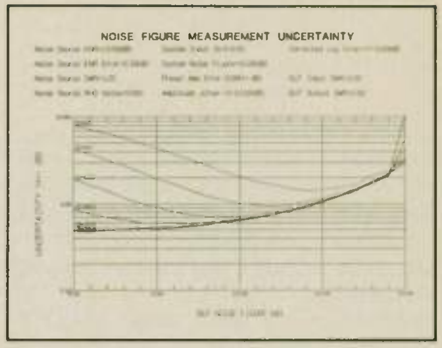

Figure 5. Noise figure measurement uncertainty. DUT input SWR = 2.50, output SWR=2.50 .

separate sweeps compound the problem of amplitude repeatability caused by preselector mistuning. The more desirable technique steps the analyzer through the frequency range of interest once for the calibration and once for the measurement. At each frequency, the noise source is turned on to measure the on-state noise power and then immediately turned off to measure the off-state noise power level. There should be little amplitude-repeatability error between the two measurements because the analyzer remains at the same frequency for the two measurements. Any error due to post-tuning drift of the preselector during the required time interval between the on/off state measurements is insignificant. The error model describes the errors generated by the latter measurement technique since it is more accurate.

Errors induced by amplitude jitter are present during each noise-power-level measurement. Measuring noise-power levels with a spectrum analyzer requires either a narrow video bandwidth, averaging, or a combination of both. Even though the analyzer setup is optimal, digitization errors and averaging errors induce amplitude jitter on the measurement. The typical amplitude-jitter error is small, ≤0.1 dB.

For an analyzer that corrects log-fidelity errors, the noise-power levels, including the preselector-amplitude-repeatability and jitter-error terms, may be described as follows:

$$N_{don} = N_{donmm} + E_{ampdut} + E_{jit1} \quad (29)$$

$$N_{doff} = N_{doffmm} + E_{logdut} + E_{ampdut} + E_{jit2} \quad (30)$$

$$N_{con} = N_{conmm} + E_{logdutcal} + E_{ampcal} + E_{jit3} \quad (31)$$

$$N_{coff} = N_{coffmm} + E_{logdutcal} + E_{logcal} + E_{ampcal} + E_{jit4} \quad (32)$$

E_{ampcal} is the random value of the magnitude of the preselector amplitude repeatability error, E_{amp}, and is the same for N_{con} and N_{coff}. The same is true for E_{ampdut} in N_{don} and N_{doff}. The jitter errors E_{jit1}, E_{jit2}, E_{jit3} and E_{jit4} are random values of the magnitude of the amplitude-jitter error.

Noise Source Error

The calibrated noise source also has an uncertainty with its published ENR values. In addition, the ENR may vary at frequencies between the calibration frequencies. This ENR uncertainty, $N_{s\Delta}$(±dB), is added to the nominal value, N_s. Therefore, N_s may be described as:

$$N_s = N_s + N_{s\Delta} \quad (33)$$

Uncertainty Results

To generate the error curves, all error terms except the mismatch terms are assumed to have a Gaussian probability distribution. The instrument specifications are presumed to be three standard deviations from typical performance. For the mismatch errors, the phases of the reflection coefficients are uniformly distributed between 0 and 2π. After the error terms are randomized as described above, the resulting noise-power levels are applied to the noise figure equation. This measurement simulation is then performed two-thousand times to generate a meaningful noise figure distribution. The displayed noise-figure-error curve represents the error at a point on the distribution that is two standard deviations from the mean.

As an example, the system parameters from the HP 71100A spectrum analyzer with an HP 70621A preamplifier module are used. This is a base-band analyzer, so no need exists for a preselector. This analyzer also has log-fidelity correction. Figures 2-5 show the relevant system and DUT parameters with the uncertainty plots. These graphs plot noise-figure error vs DUT noise figure and DUT gain. In addition, they describe measurement uncertainty for various DUT input and output SWRs.

A first impression of Figures 2-5 is that measuring low gain and noise figure DUTs will cause considerable measurement uncertainty. This makes intuitive sense because the amount of noise being measured during the measurement is similar to the noise measured during the calibration. Since the noise-level difference is small, the error terms have a greater impact on the uncertainty. To minimize the uncertainty, the difference between the noise-power levels should be as large as possible.

The DUT noise figure increases the uncertainty. The difference between noise-power levels N_{don} and N_{doff} decreases as the DUT noise figure increases because the noise power from the DUT becomes large enough that it overwhelms the noise power of the noise source. Therefore, turning the noise source on and off produces a small variation in the noise power at the output of the DUT. Again, as the variation in noise power level decreases, the uncertainty increases.

When using a spectrum analyzer to make a noise-figure measurement, there are several concerns that should be kept in mind in order to minimize measurement uncertainty. The most significant improvement is achieved by reducing the noise figure of the measurement system. Since noise figures of spectrum analyzers are usually poor, a low noise preamplifier with small input SWR should be connected to the analyzer input. Reducing the mismatch errors is also important. An isolator between the DUT and the input to the measurement system significantly improves the SWR of the measurement system and causes minimal degradation to the measurement-system noise figure.

When measuring noise-power levels, the analyzer should be set up to minimize averaging errors. This requires selecting the analyzer detector mode that produces the least display bandwidth, and setting the video bandwidth as narrow as time constraints will permit. In addition, the measurement should be made with the analyzer in zero span where the analyzer displays the noise level vs time. Therefore, a quick measurement of the noise-power level can be accomplished by averaging the points of the trace. Many analyzers require transferring the trace data to a computer to compute the average. However, the HP 70000 series spectrum analyzers have a helpful command, mean trace average, which returns the average value of the trace.

In order to minimize amplitude errors, the reference level and resolution bandwidth should not be changed between the calibration and measurement steps. To avoid changing the reference level, an educated guess of the DUT noise figure and gain should be made to determine the maximum noise-power level expected. The reference level should be set slightly higher than the maximum level. However, it is important not to set the reference level too high because the log fidelity in most analyzers degrades as the signal moves down the screen. The methodology used is also important. Again, it is preferable to cycle the noise source at each frequency during the calibration and measurement steps.

Minimizing Errors

Certain noise-source attributes should be considered. The noise source should have as high an ENR as possible to minimize noise-source-induced errors. If calibration data is available, the frequencies chosen for the measurement should coincide with the frequencies of the calibration data. Also, the output SWR and ΔSWR should be as small as possible. Often, a tradeoff between noise source ENR and output SWR must be made. A noise figure uncertainty analysis such as this can help determine which noise source will yield the most accurate measurements for a given DUT.

Conclusions

The measurement uncertainty of a spectrum-analyzer-based noise-figure measurement is greater than the uncertainty of the best noise-figure meters. The main contributor to the lower performance of the spectrum analyzer is the linearity of the spectrum analyzer's IF strip. The log amplifiers used in today's spectrum analyzers simply do not achieve the same linearity as a noise figure meter's IF detector. However, the measurement uncertainty, while not as good as that of a noise-figure meter, is acceptable for many applications, especially when DUT gain is greater than 15 dB. ***RF***

About the Author

Dave Massie works in the Signal Analysis Division at Hewlett-Packard Company. He may be reached at Hewlett-Packard Co., Signal Analysis Division, 1212 Valley House Drive, Rohnert Park, CA 94928. Tel: (707) 794-4425.

A Bi-Directional Amplifier for SSB Transceivers

By Mark W. Thompson
Harris Corporation,
RF Communications Group

Transceivers combine receivers and transmitters in a single unit, typically using the same conversion schemes for each function. Bi-directional amplifiers can be used to simplify circuity common to both receivers and transmitters, thus conserving space, components, and money. A design for such an amplifier, which eliminates many of these extra components by using one active device as an amplifier in both directions, is discussed in this paper.

The function of a single sideband transceiver is to translate an audio spectrum from RF frequencies down to audio and from audio up to RF frequencies. Receivers translate the signals down from RF and exciters translate the signals up from audio. This is essentially a reversible procedure and many receivers and exciters use the same frequency translation schemes, but in opposite directions. For this reason, in SSB transceivers the receiver and exciter are often one module sharing much common circuitry. Passive circuits, such as filters and mixers generally lend themselves to being used in both directions, whereas active circuits are not so easily adapted for this purpose. Amplifiers are common building blocks in both receiver and exciter design. Typically, two are used in the IF path of a receiver/exciter, one for receive and one for transmit, and are switched in when appropriate (Figure 1). It is desirable from a cost and component count standpoint to eliminate as much circuitry from these blocks as possible.

The JFET consists of a conducting channel between two pn-type junctions. In the fabrication process of small signal JFETs there is little difference between the drain junction and the source junction, and as long as the gate is properly biased, the direction of the current flow solely depends on the DC potential between the drain and the source terminals. Therefore, a JFET, with its inherent reversibility of drain and source can be used in a common gate configuration as a bi-directional amplifier. The direction of the amplification being only determined by the DC bias applied to the transistor.

In a common-gate amplifier the output current is the same as the input current, and the input impedance is low. Gain is achieved by providing a high impedance on the drain. This voltage is matched down in impedance to develop the desired power gain into the working load. An L-matching network is often used to convert the high drain impedance down to the load. The low input impedance of the JFET can either be directly connected to the source if it is close enough to provide a satisfactory input match, or matched using a low Q matching network. The operating power gain of this circuit is:

$G_P = g_m \times R_L$

Where: G_P is operating power gain
g_m is the forward transconductance of the device, and
R_L is the load resistance.

In order to make the circuit operable in both directions, it is necessary to design a symmetrical matching network which will provide a transformation from the load to a high impedance at the "output" terminal and couple the source directly to the low impedance at the "input."

A simple modification of the L-matching network will produce the desired result. An additional parallel capacitor is added across the resonating inductor. The inductor value is then modified to resonate with the additional capacitor and the series output capacitor when it is reflected across the inductor. The effect of the additional capacitor is to dominate the reflected capacitance of the series output capacitor and the output capacitance of the device. When the terminal is used as the input, the series capacitor is shorted out by a PIN diode. The source, therefore, is looking directly at the input impedance of the JFET. Since this impedance is low, it decreases the Q of the tank circuit such that the mis-alignment of the circuit due to the shorted capacitor is negligible (Figure 2).

The active device chosen for this design was a U310 JFET. The U310 has a nominal g_m of 12 millimhos, making the input impedance in the common gate configuration 83 ohms. A resistor was placed across the drain to provide a fixed output impedance for the JFET and a symmetrical matching network was designed by using commonly found formulas for the L-network. The value of the additional parallel capacitor was

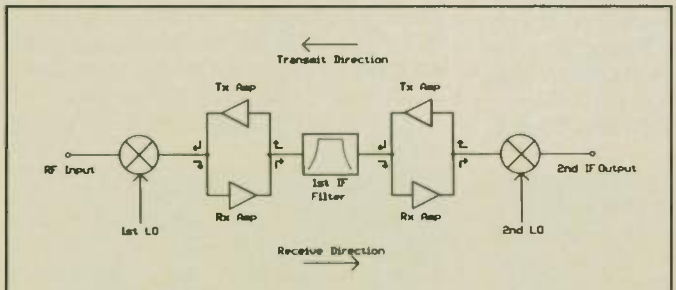

Figure 1. Simplified receiver block diagram showing transmit and receive signal paths.

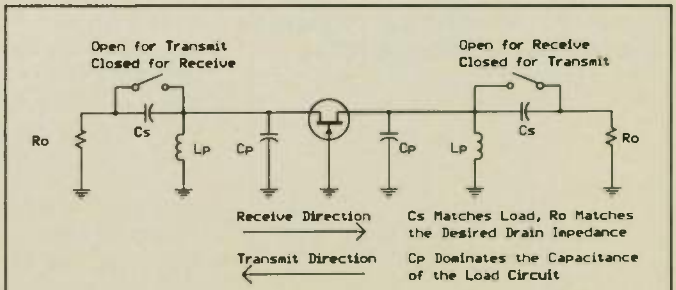

Figure 2. Simplified circuit diagram.

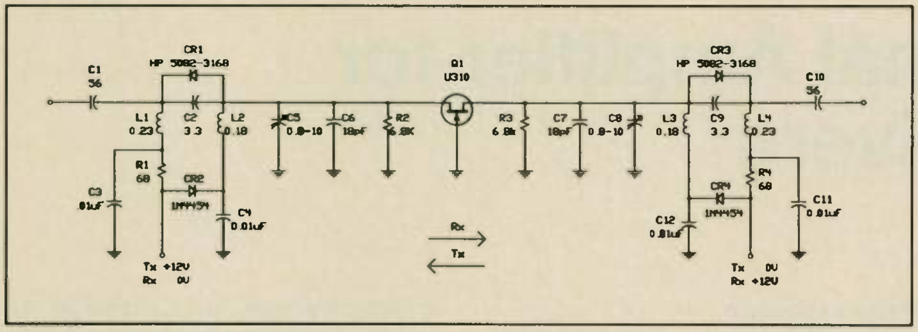

Figure 3. Final schematic.

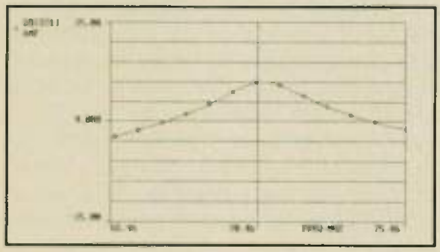

Figure 4. Theoretical forward transmission coefficient (S21).

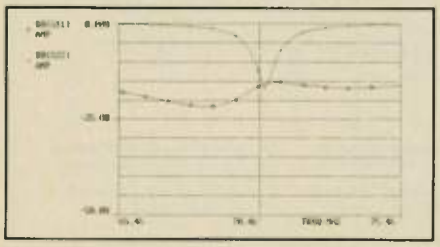

Figure 5. Theoretical input and output return loss.

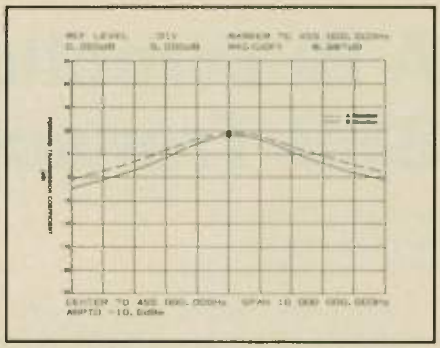

Figure 6. Forward transmission coefficient versus frequency.

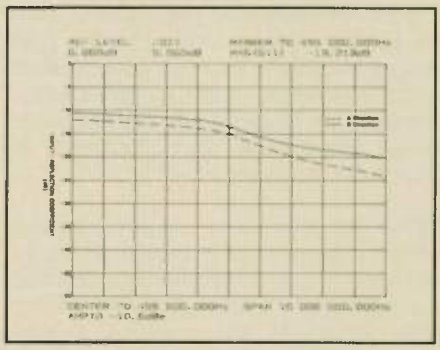

Figure 7. "Input" reflection coefficient versus frequency.

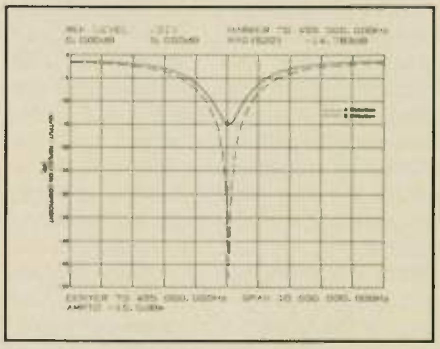

Figure 8. "Output" reflection coefficient versus frequency.

chosen to be approximately five times the value of the series output capacitor, and the inductor value was adjusted to resonate at the operating frequency of 70.455 MHz. The output tank tends to have a high enough Q where tuning becomes necessary, so the total parallel capacitance is actually made up of both a fixed and a variable component.

Driving the source directly into the JFET will give a reasonable return loss, but for this application a slightly better input match was desired so a low Q matching network was added to further transform the impedance down to 50 ohms. This is done on both the input and the output for symmetry and does not change the bi-directional nature of the circuit. The direction of amplification by the circuit is chosen by applying DC supply to the "output" terminal and taking the "input" terminal to ground through an appropriate resistor value. The PIN diode is also connected such that it will be forward biased when the input terminal is taken to ground. The DC supply is applied to the "output" terminal through the resonating inductor and a switching diode when it is not required to be on and to block DC when the terminal is used as an input. A complete schematic is shown in Figure 3.

The circuit was first modeled by computer using Touchstone to determine potential circuit performance and possible instabilities or other problems. These results are shown in Figures 4 and 5. Testing showed that the circuit performance was close to the modeled performance and that indeed the desired feature of bi-directionality could be achieved. It was noticed, however, that the circuit was not exactly symmetrical, having variations in gain and return loss. The measured results are still quite satisfactory for the application (Figures 6, 7, and 8). Tuning of the circuit is simply done by adjusting each output tank capacitor for best output return loss when that direction is selected. If careful attention is paid to layout to minimize the coupling between the output and the input, there is little interaction between the two tanks. This is due to the lowered Q of the input tank and the small reverse transconductance of the JFET. If there is excessive coupling between the tanks it becomes difficult to tune the circuits for the same operating frequency. This problem highlights an interesting characteristic of the circuit. The two output tanks can be independently tuned for frequency, with the frequency of operation in one direction is different than the frequency of operation in the other. This may be useful for some applications, but was not a feature which was considered during this design.

In summary, an amplifier incorporating a JFET which is used to provide gain in two directions has been described and built. The circuit is used in the IF strip of a receiver/exciter to eliminate the need for two amplifiers, one for each signal path. This reduces the component count which in turn lowers module cost and improves reliability.

I would like to acknowledge the assistance I received on this design both in the form of ideas and encouragement from Don Martz and George Helm both of whom are with Harris Corporation.

A patent for this circuit is being applied for. *RF*

About the Author

Mark Thompson is a lead engineer at Harris Corporation, 1680 University Ave. Rochester, NY 14610. His phone number is (716) 244-5830. He received his BSEE in 1982 from Rensselaer Polytechnic Institute.

Twisted-Wire Transmission Lines

John H. Broxon II and
Douglas K. Linkhart
MICON Incorporated

Twisted-wire transmission lines have been used in telecommunications for many years. RF transformers, power combiners and splitters, and hybrids are often constructed by winding these lines on ferrite cores. This article presents a method for calculating characteristic impedances of twisted-wire transmission lines, and includes a computer program to quickly and accurately perform the necessary computations. Experimental results are compared with computed values for program verification.

Any type of transmission line can be used in a transmission-line transformer (1), but twisted wire is convenient for several reasons. First, the twisting holds the wires in close proximity to each other. However, similar performance can be obtained if the wires are held in proximity by other means (2). Twisting has the advantage of minimizing coupling between the transmission line and other adjacent circuitry, especially where the transmission line is off the ferrite core.

Second, the raw materials used to make twisted-wire transmission lines are inexpensive and readily available. Figure 1 shows a typical twisted-wire transmission line constructed from film-coated copper wire (magnet wire).

Finally, a wide variety of characteristic impedances can be accommodated by varying wire diameter, film thickness, and film type.

Characteristic impedance is important because the upper frequency response of transmission-line transformers is dependent on this quantity and on the electrical length of the transmission line (3).

Empirical characteristic impedance data for parallel-wire windings has been presented graphically (2), but this data is difficult to use for computer aided transformer design and is of limited accuracy. A method of characteristic impedance calculation and a computer program have been developed to perform the computations.

Theory

A parallel-wire transmission line has the same equivalent circuit as a twisted-wire transmission line if the twist is not extreme. This circuit is shown in Figure 2. The series wire inductance and inter-wire capacitance are distributed along the length of the transmission line. To find the characteristic impedance of the transmission line, we need to know the series inductance and inter-wire capacitance.

Equations have been formulated for parallel-wire transmission line inductance and capacitance (4). The capacitance equations are valid when the wires are surrounded by a uniform dielectric material. However, two different dielectric materials are present in most twisted-wire transmission lines as shown in Figure 1.

The parallel-wire inductance equations are valid because the wire insulation has the same permeability as air. The inductance is given by (4)

$$L = \left(\frac{\mu_0}{\pi}\right)\cosh^{-1}\left(\frac{R}{r}\right) \tag{1}$$

where μ_0 is the permeability of free space ($4\pi \times 10^{-7}$ H/m) and R and r are the dimensions indicated in Figure 3.

The calculation of the inter-wire capacitance is more difficult. Electric field equations could be derived in order to perform this calculation, but if certain assumptions are made, the equations are simpler and easier to understand. The first assumption is that the electric flux lines in the region between the wires are straight because the inter-wire spacing is small. The electric field is perpendicular to a plane between the wires. The second assumption is that the wire insulation has little effect on the electric field in the area outside the region between the wires because the electric flux line length is much greater than the insulation thickness.

Applying these assumptions, the total inter-wire capacitance is given by

$$C_t = C_1 + C_2 - C_3 \tag{2}$$

where C_1 is the capacitance calculated considering only the region between the wires, C_2 is the capacitance calculated considering a uniform dielectric (air) surrounding the wires, and C_3 is a correction factor for C_2. This correction factor compensates for an overlap of the two regions considered in the calculation of C_1 and C_2.

Calculate C_2 using the general parallel-wire transmission line capacitance equation (4):

$$C_2 = \frac{\pi\varepsilon_0}{\cosh^{-1}(R/r)} \tag{3}$$

where ε_0 is the permittivity of free space (8.85×10^{-12} F/m).

To calculate C_1, make the assumption that the flux lines in the region between

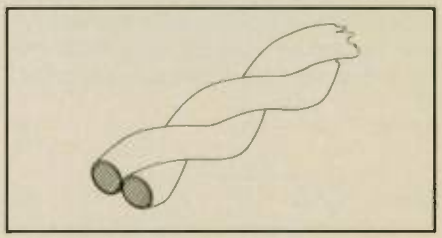

Figure 1. Typical twisted-wire transmission line.

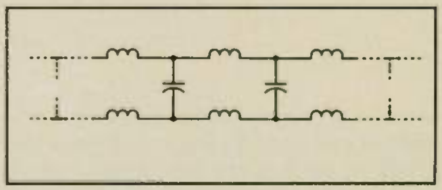

Figure 2. Twisted-wire transmission line equivalent circuit.

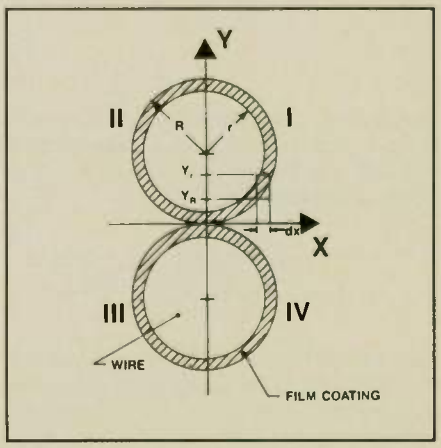

Figure 3. Integration scheme.

the wires are parallel to the y-axis in Figure 3. Then divide this region into infinitesimal parallel-plate capacitors with partial dielectric filling. An integration of these capacitors along the x-axis gives the value of C_1.

By symmetry, it is only necessary to integrate in one quadrant of the region between the wires in Figure 3. The limits of integration are x = 0 and x = r. The first-quadrant capacitance (C_I) is equal to the total capacitance of the region between the wires because the first-quadrant capacitance and second-quadrant capacitance (C_{II}) are considered to be in parallel, and this capacitance in turn is in series with the parallel combination of the third-quadrant capacitance (C_{III}) and the fourth-quadrant capacitance (C_{IV}):

$$C_1 = C_I = \frac{(C_I + C_{II})(C_{III} + C_{IV})}{(C_I + C_{II} + C_{III} + C_{IV})} \qquad (4)$$

To set up the integral, functions for the y displacement of the wire surface (y_r) and insulation surface (y_R) from the x-axis are needed. These functions are

$$y_r = R - \sqrt{r^2 - x^2} \qquad (5)$$

$$y_R = R - \sqrt{R^2 - x^2} \qquad (6)$$

The capacitance of each incremental area between the wire and the insulation is given by

$$C = \frac{\varepsilon_r \varepsilon_0 dx}{y_r - y_R} \qquad (7)$$

where ε_r is the relative dielectric constant of the wire insulation and dx is the width of each incremental area. The capacitance of each incremental area between the insulation and the x-axis is given by

$$C = \frac{\varepsilon_0 dx}{y_R} \qquad (8)$$

Combining the capacitances in equations 7 and 8 in series, substituting in equations 5 and 6, and simplifying, the integrand is derived:

$$C = \frac{\varepsilon_0 dx}{R + \left(\frac{1}{\varepsilon_r} - 1\right)\sqrt{R^2 - x^2} - \frac{\sqrt{r^2 - x^2}}{\varepsilon_r}} \qquad (9)$$

The integration of equation 9 gives us C_1. Calculate C_3 by performing the same integration with ε_r = 1 to find the corresponding capacitance without considering the wire insulation. Then combine C_1, C_2, and C_3 using equation 2 to find the total inter-wire capacitance.

After calculating the series inductance and inter-wire capacitance of the transmission line, calculate the characteristic impedance (Z_0) using

$$Z_0 = \sqrt{\frac{L}{C_t}} \qquad (10)$$

The first step in twisted-wire transmission line characteristic impedance calculation is to find C_1 by integrating equation 9. Then use equation 3 to calculate C_2. Next, set ε_r equal to unity and integrate equation 9 again to find C_3. Apply equation 2 to calculate the total capacitance, C_t. Next, compute the series inductance (L) using equation 1 and finally, compute the characteristic impedance using equation 10.

Computer Program and Verification

We present the characteristic impedance calculation algorithm in the form of a BASIC computer program listing in Figure 6. The program first prompts the user for the bare wire diameter, the wire diameter including the insulation, and the dielectric constant of the insulation. It then executes the algorithm previously described. The integration is performed using a Romberg numerical technique (5). The program then prints a report containing the input data and the characteristic impedance.

In order to verify the computer program, experimental data was taken for different sizes of film-coated copper wire (magnet wire) twisted 2 to 2-1/2 full turns per inch. The characteristic impedances were measured at relatively low frequencies (5 - 10 MHz) to avoid the effects of parasitic inductance and radiation. The impedance was measured looking into quarter-wavelength sections of transmission line terminated with various resistances at the far end. Then the characteristic impedances of the lines were calculated using

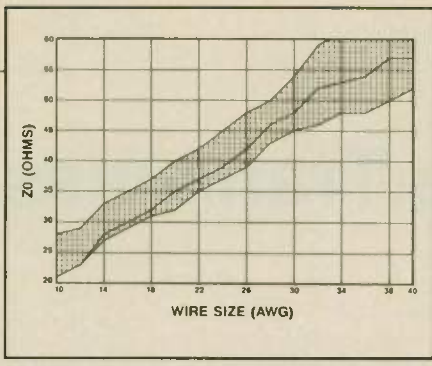

Figure 4. Measured and computed characteristic impedances of twisted-wire transmission lines.

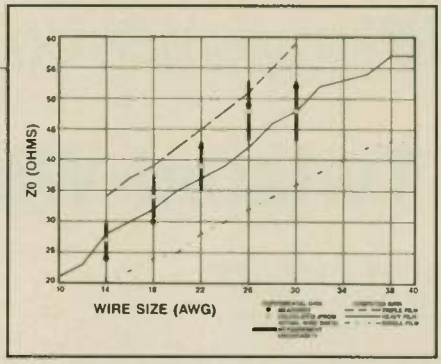

Figure 5. Effect of wire dimensional tolerances on characteristic impedances (heavy film).

$$Z_0 = \sqrt{ZR} \qquad (11)$$

where Z is the measured impedance and R is the terminating resistance.

The experimental data is presented in Figure 4 along with computed values for the particular wires used and computed values for nominal size single, heavy, and triple film wires having Phelps Dodge Poly-Thermaleze insulation (ε_r = 3.7). The measured data match the computed values within the range of experimental error. The computed values also compare favorably with other empirical values (2).

The primary sources of measurement error were the tolerances of the terminating resistor values and impedance measurement inaccuracy.

Small perturbations in wire diameter and insulating film thickness can have a large effect on the characteristic impedance. Figure 5 shows ranges of characteristic impedance for variations in wire diameter and film thickness within the tolerance range of various size Poly-Thermaleze heavy film wires. In order to accurately characterize a twisted-wire transmission line, the designer must know the precise dimensions of the wire to be used. Transmission line insertion loss and power handling capability depend strongly on the type of dielectric film on the wire (6). To verify this, we tested transmission lines made from two Phelps Dodge wires with different film coatings: Nyleze and Poly-Thermaleze. Poly-Thermaleze film has a lower dissipation factor than Nyleze. The insertion losses of 40-foot lengths of these two transmission lines differed by nearly 2 dB at 10 MHz.

These losses cause heating of the transmission lines in high-power applications, reducing power-handling capacity. The designer must choose wires coated with films having low dissipation factors to minimize losses.

Another consideration is the temperature dependence of the wire film dielec-

```
10 REM                    Program 'Twire'
20 REM        Twisted-wire transmission line design aid
30 REM
40 REM              Authors : Douglas K. Linkhart
50 REM                        John H. Broxon, II
60 REM
70 REM                    MICON Incorporated
80 REM                    A subsidiary of MPD Incorporated
90 REM                    316 East 9th Street
100 REM                   Owensboro, KY  42301
110 REM                   (502)-685-6200
120 REM
130 REM                   November 17, 1989
140 REM ***********************************************************
150 REM                              Initialization
160 REM
170 PI = 4 * ATN (1)                 'Archimedes constant
180 U0 = 4 * PI * .0000001           'Free-space permeability, H/m
190 C  = 2.997925E+08                'Velocity of light,       m/s
200 E0 = 1 / (U0 * C^2)              'Free-space permittivity, F/m
210 REM                              'Definition of capacitance function
220 DEF FN CAP (ER, R1, R2, X)
    = 1 / ( R2 + ( 1 / ER - 1) * SQR (R2^2 - X^2) - SQR (R1^2 - X^2) / ER)
230 REM ***********************************************************
240 CLS                              'Data input
250 REM
260 INPUT "WIRE DIAMETER (INCLUDING INSULATION), MILS "; D2
270 INPUT "BARE WIRE DIAMETER, MILS                   "; D1
280 INPUT "RELATIVE DIELECTRIC CONSTANT OF INSULATION "; ERD
290 R2 = D2 / 2000
300 R1 = D1 / 2000
310 ER = ERD
320 REM ***********************************************************
330 REM                              Calculate Z0
340 REM
350 GOSUB 570                        'Compute capacitance with dielectric
360 ACOSH = LOG ((R2 + SQR (R2^2 - R1^2)) / R1)
370 L     = U0 * ACOSH / PI          'Inductance of twin-wire line
380 CAPT  = E0 * PI / ACOSH          'Capacitance of twin-wire line
390 CAPT  = CAPT + CAPS (5,5)        'Sum capacitance
400 ER    = 1
410 GOSUB 570                        'Compute capacitance without dielectric
420 CAPT  = CAPT - CAPS (5,5)        'Subtract capacitance
430 Z0    = SQR (L / CAPT)           'Compute Z0
440 REM ***********************************************************
450 REM                              Print report
460 REM
470 LPRINT "*** TWISTED-WIRE TRANSMISSION LINE DESIGN DATA ***"
480 LPRINT
490 LPRINT USING "OUTER WIRE DIAMETER --------------- ###.# MILS"; D2
500 LPRINT USING "BARE WIRE DIAMETER ---------------- ###.# MILS"; D1
510 LPRINT USING "INSULATION DIELECTRIC CONSTANT ---    #.#";     ERD
520 LPRINT USING "CHARACTERISTIC IMPEDANCE --------- ### OHMS";   Z0
530 END                              'End main program
540 REM ***********************************************************
550 REM                              Integration subroutine
560 REM
570 FOR I = 1 TO 5                   'Trapezoidal integration
580    CAPS (I, 1) = 0               'Initialize capacitance
590    DX          = R1 / 2^(I - 1)  'dx
600    FOR X = DX TO R1 STEP DX      'Integrate
610       X1          = X - DX
620       CAPS (I, 1) = (FN CAP (ER, R1, R2, X1) + FN CAP (ER, R1, R2, X))
                        * DX * E0 / 2 + CAPS (I, 1)
630    NEXT X
640 NEXT I
650 FOR J = 2 TO 5                   'Romberg correction
660    FOR I = J TO 5
670       CAPS (I, J) = (4^(J - 1) * CAPS (I, J - 1) - CAPS (I - 1, J - 1))
                        / (4^(J - 1) - 1)
680    NEXT I
690 NEXT J
700 RETURN                           'End integration subroutine
```

Figure 6. Listing of computer program for twisted-wire transmission line design.

tric constant. Testing a film dielectric constant suspected of changing with temperature, we found that there was no significant change over the temperature range of −25 to +125 C.

The design of high-power twisted-wire transmission lines requires special care. The conductor circumference (or perimeter of a rectangular conductor) must be large to reduce resistive losses due to skin effect. When this dimension is increased, the insulation thickness must also be changed to maintain the same characteristic impedance. If wire with thicker insulation such as Teflon-insulated stranded wire is not available, uninsulated wire can be inserted into teflon tubing.

High-impedance transmission lines can be realized using small diameter wire. For high-power or low-loss applications, larger wires can be used in conjunction with thicker insulation as previously described.

To implement low-impedance transmission lines, either use large wire diameters with thin film coatings or rectangular conductors. The characteristic impedance of these rectangular strips can be determined using strip-line equations (7).

The preceding material and the accompanying computer program take much of the guesswork out of the design of twisted-wire transmission lines. The theory has been developed to support most of the empirical work done in this area. The characteristic impedance computation algorithm is useful for the design of RF transformers, power combiners and splitters, hybrids, and related devices. The algorithm can be readily incorporated into existing design procedures. *RF*

Acknowledgement

We would like to thank Andrew Owens for his help in the experimentation involved in the preparation of this article and MPD, Incorporated for the use of their facilities.

References

1. C.L. Ruthroff, "Some Broad-Band Transformers," *Proceedings of the IRE*, Aug. 1959, pp. 1337 - 1342.
2. J. Sevick, *Transmission Line Transformers*, Newington, CT: American Radio Relay League, 1987.
3. O. Pitzalis and T. P. M. Couse, "Practical Design Information for Broadband Transmission Line Transformers," *Proceedings of the IEEE*, Apr. 1968, pp. 738 - 739.
4. W. H. Hayt, *Engineering Electromagnetics*, New York: McGraw-Hill, 1981.
5. P. A. Stark, *Introduction to Numerical Methods*, New York: Macmillan, 1970.
6. H. O. Granberg, "Broadband Transformers and Power Combining Techniques for RF," AN-749, Phoenix: Motorola Semiconductor Products, Inc.
7. G. L. Matthaei, L. Young, and E. M. T. Jones, *Microwave Filters, Impedance-Matching Networks, and Coupling Structures*, Norwood, MA: Artech House, 1980.

About the Authors

Douglas K. Linkhart is a senior development engineer with Micon and John H. Broxon III is a development engineer with MPD Incorporated. They may be reached at Micon Incorporated, 316 East 9th Street, Owensboro, KY 42301. Tel: (502) 685-6337.

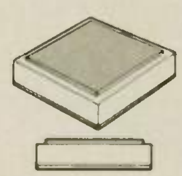

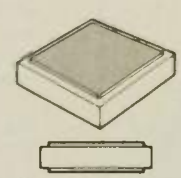

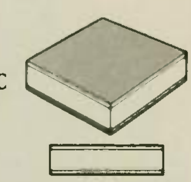

RF literature

Crystal Oscillators/Filters

Thomson announces a full line catalog of TCXO's, DTCXO's, OCXO's, and linear phase filters. Typical applications are radar, avionics, synthesizers/test equipment, and telecom equipment.
Thomson Electron Tubes and Devices
INFO/CARD #230

Instrumentation Catalog

The 1990 Test and Measurement Instrumentation Catalog has been published by Wavetek. Included are signal processing filters, function and arbitrary waveform generators, frequency synthesizers, wavetest software, and RF components.
Wavetek Corporation
INFO/CARD #229

Brochure Describes Aluminum Nitride

"Aluminum Nitride — The Choice for Thermal Management Applications," a brochure that describes the thermal management properties of aluminum nitride (AlN) for ICs, substrates, RF/microwave packages, and other applications, has been released by The Carborundum Company. Data is included on electric and corrosion properties, in addition to thermal characteristics.
The Carborundum Company
INFO/CARD #228

Quartz Crystal Products

Piezo Crystal announces its 1990 catalog covering quartz crystals and crystal oscillators for commercial, military, and spacecraft applications. The catalog includes technical information on the products and technical papers written by Piezo Crystal staff.
Piezo Crystal Company
INFO/CARD #227

Analog IC Data Book

PMI has released their Analog IC Data Book, Volume 10, which contains high performance linear and conversion ICs in CMOS, Bipolar, and BiCMOS technologies, operational amplifiers, and A/D and D/A converters. Included are data sheets covering operational and instrumentation amplifiers, matched transistors, switches, and high performance audio ICs.
Precision Monolithics Inc.
INFO/CARD #226

Microwave & RF Connectors

ROSENBERGER/MICRO-COAX has issued a summary of its products. Listed are coaxial connectors, high performance UTiFLEX^R flexible microwave cable assemblies, UT^R semi-rigid coaxial cable and cable assemblies, and miniaturized coaxial filters.
ROSENBERGER/MICRO-COAX
INFO/CARD #225

Frequency Control Products

This handbook, for the design and component engineer, gives specifications, graphs, diagrams, and applications for PTI's product line. Products include monolithic and discrete crystal filters, LC filters, crystal and non-crystal oscillators, and RF assemblies.
Piezo Technology, Inc.
INFO/CARD #224

Substrates for Frequency Dependant Applications

A brochure describing low loss substrates that perform at specified frequencies is available from Arlon. These substrates include woven glass/PTFE materials and bonding films, ceramic filled/PTFE materials, and non-woven glass/PTFE laminates.
Arlon, Microwave Materials Division
INFO/CARD #223

Microwave Flexible Cables

United Microwave Products Inc. introduces its flexible cables catalog which contains information on cables with up to 35 GHz performance with SMA, BNC, TNC, N or 7 mm connectors.
United Microwave Products, Inc.
INFO/CARD #222

VCO and Synthesizer Product Catalog

This catalog provides data sheets on VCO and synthesizer products covering frequency ranges from 20 MHz to 3 GHz. Z-COMMUNICATIONS also gives the reader application notes on how to solve layout, grounding and other related problems.
Z-COMMUNICATIONS, Inc.
INFO/CARD #221

RF Power Amplifiers and Generators

ENI introduces its RF Power Amplifiers and Generators brochure which contains information on amplifiers and generators in the 0.8 MHz to 1 GHz range and the 1.2 to 5000 W power range, including models for MRI, spectroscopy, communications, and laboratory applications.
ENI
INFO/CARD #220

Quartz Crystals and Oscillators Catalog

Low and high frequency quartz crystals and clock oscillators are available in this catalog from NEL Frequency Controls. It covers crystals from 1 kHz to 220 MHz and clock oscillators from 244 Hz to 220 MHz.
NEL Frequency Controls, Inc.
INFO/CARD #218

RF Iron Powder Cores

MICROMETALS, Inc. introduces its RF Cores catalog and applications guide. This issue contains new iron powder balun cores, information on broadband designs, and detailed application notes.
MICROMETALS, Inc.
INFO/CARD #217

Advertising Index

A.H. Systems 61
American Technical Ceramics Corp. 28
Amplifier Research 29
Apcom 17
Applied Engineering Products 43
ASM Software, Inc. 59
Avantek 30
Aydin-Vector 15
Bird Electronic Corp. 66
Bradford Electronics, Inc. 55
CADpoint 68
Cal Crystal Lab., Inc. 55
California Eastern Laboratories 14, 69
Cir-Q-Tel Microwave 66
Coilcraft 70
Communication Concepts, Inc. 75
Daico Industries, Inc. 4
DGS Associates, Inc. 38
Dielectric Laboratories Inc. 31
Eagleware 58
EEsof 2
The Electro-Mechanics Company 62
Henry Radio 68
Hewlett-Packard Co. 11-13, 36, 45-47
IFR Systems, Inc. 3
Instant Board Circuits 76
Instruments for Industry 59
Intusoft 64
Johanson Manufacturing 63
Kalmus Engineering International, Inc. 24-25
Kay Elemetrics Corp. 49
KVG 53
Lindgren RF Enclosures 83
M-A Com Semiconductor—Products Division 9
MCL, Inc. 8
Miteq 18
MTS Microelectronics, Inc. 63
Noise Com, Inc. 7
Oscillatek 37
Penstock Engineering, Inc. 78
Programmed Test Sources 32
QUALCOMM, INC. 37
Quartztek 21
Radiation Systems, Inc. 54
RF Monolithics 19
RHG Electronics Laboratory, Inc. 84
Sawtek Inc. 20
SCITEQ Electronics, Inc. 56-57
Siemens—Special Products Division 48
SGS Thompson Microelectronics 22
Sprague-Goodman Electronics, Inc. 51
Stanford Telecommunications 64, 65
STC Components 26
Surcom Associates, Inc. 65
Tecdia 75
Temex Electronics, Inc. 44
Tesoft 40
Trilithic, Inc. 44
Trim-Tronics Inc. 55
Trontech 35
TRW Electronics Systems Group 39
TTE, Inc. 54
Tusonix 21
Voltronics Corporation 79-80
Werlatone Inc. 6
Wide Band Engineering Company, Inc 76

LINDGREN - *For Every Shielding Application*

Lindgren RF Enclosures offer complete design, development and installation capabilities for all types of EMI/RFI shielding systems. Complete turnkey services can be supplied to meet your specific requirements.

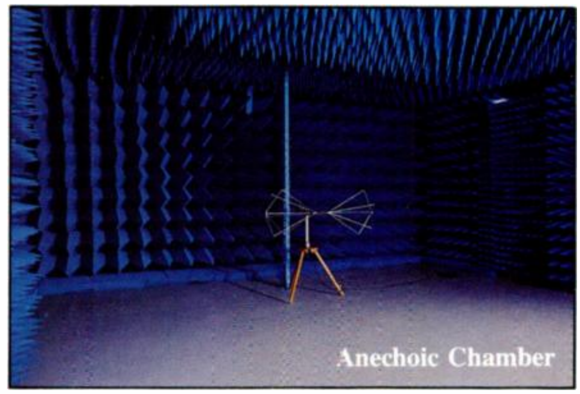

Anechoic Chamber

You can look to Lindgren for:
- Consistently high quality
- Unmatched service
- Total installation and testing capabilities
- Architectural and engineering assistance
- Over 35 years of shielding system experience

Tempest Computer Room

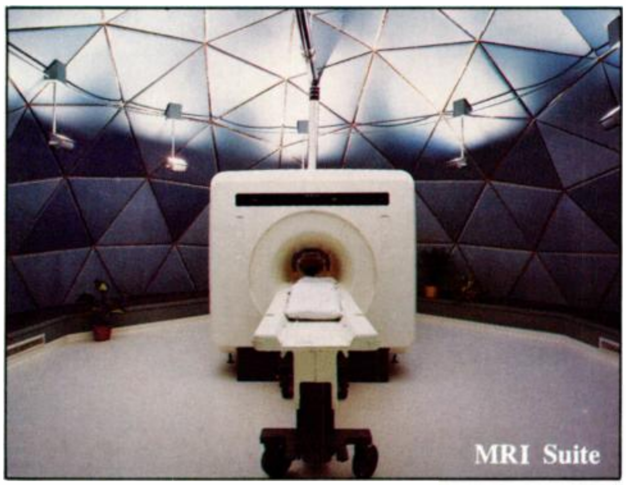

MRI Suite

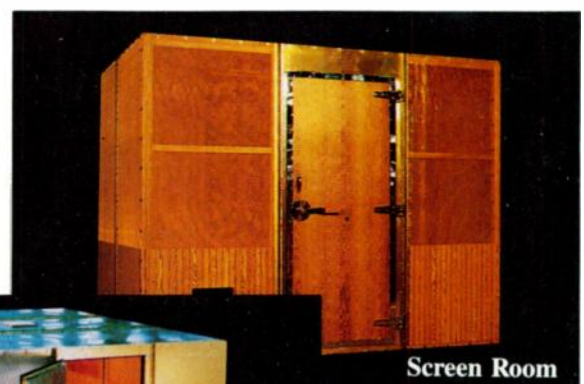

Screen Room

All Lindgren Enclosures have these features:
- Lightweight
- Fully demountable
- Ease of assembly
- High performance doors
- Complete line of accessories including various floor and penetration alternatives

Solid Room

Whatever your shielding requirements, Lindgren can provide the solution. Call us for more information and applications assistance.

LINDGREN
RF ENCLOSURES

400 High Grove Blvd.
Glendale Heights, IL 60139
708-307-7200 • FAX: 708-307-7571

INFO/CARD 73

1 + 1 = 1

State-Of-The-Art Breakthrough Combines Constant Phase Log Amp and Limiter In One Miniature Package

- Operating frequency: 30 ± 5, 60 ± 10, 160 ± 40, or 450 ± 50 MHz
- Simultaneous power & phase information
- Accurate amplitude & phase comparisons
- For monopulse and multi-channel systems
- Phase-tracked sets available

OPERATING SPECIFICATIONS, MODEL HLL160

Operating frequency (MHz)	160 ± 40
Input dynamic range (dBm)	0 to −70
DC power (mA)	140 @ −12 VDC; 75 @ +12 VDC

LOG VIDEO CHARACTERISTICS:

Slope, nom. (mV/dB)	20
Voltage out, nom. @ 0 dBm (mV)	1500
Linearity @25°C (dB)	±0.75
Video rise time (nsec)	≤15

IF OUTPUT CHARACTERISTICS:

Power, nom. (dBm)	+10
Insertion phase over temp. (deg)	±12
Phase variation @160 MHz, over dynamic range, @25°C (deg)	±3

ENVIRONMENTAL: Operating temperature −55°C to +85°C; hermetically sealed package; meets applicable requirements of MIL-E-5400

RHG ELECTRONICS LABORATORY, INC.

161 East Industry Court, Deer Park, NY 11729
(516) 242-1100, FAX: 516-242-1222, TWX: 510-227-6083

RHG
A M/A-COM COMPANY

INFO/CARD 74